LUDWIG MAXIMILIANS-UNIVERSITÄT MÜNCHEN
FAKULTÄT FÜR GEOWISSENSCHAFTEN

Wissenschaftliche Arbeit zur Erlangung des akademischen Grades Master of Science

Master Thesis

Comparison of airborne laser scanning and digital aerial photogrammetry for characterizing canopy openings in the boreal forest in Alberta, Canada

Vergleich von flugzeuggestütztem Laserscanning und digitaler Stereophotogrammetrie zur Charakterisierung von Waldflächen im borealen Nadelwald in Alberta, Kanada

Studiengang: Umweltsysteme und Nachhaltigkeit – Monitoring, Modellierung und Management

Erstgutachter: Prof. Dr. Ralf Ludwig
Verfasser: Annette Dietmaier
Matrikelnummer: 10739188
Anschrift: Emil-Riedel-Str. 6, 80538 München
E-Mail: annette.dietmaier@campus.lmu.de

Datum: 30.11.2018

Acknowledgements

I would first like to thank my thesis advisor Professor Dr. Ralf Ludwig of the Department of Geography at Ludwig-Maximilians-Universität. Thank you for providing me with the opportunity to work on this fascinating topic that combines ecology and remote sensing techniques into one captivating research project. Further, I am grateful for all your assistance in making my research stay in Canada possible and for making time to supervise my thesis in very constructive and helpful meetings.

I would also like to thank Professor Greg McDermid at the Department of Geography at the University of Calgary. Our weekly lab meetings helped me stay on track with my research progress and showed me what scientific ambitions I can aspire to. You made my research in Canada possible and provided me with this project. Thank you for always giving undivided attention to any problem I might run into, for your inspiring supervising style and your open-door policy.

My sincere thanks also goes to Mustafizur Rahman and Julia Linke. Without your technical assistance, the point clouds would not exist, and your ideas on opening definitions were invaluable to me. Thank you for going through the trouble of re-configurating software processes countless times until we were content with the point clouds' quality. Thank you for all your valuable input during lab meetings and showing me how to set up my RTK GPS.

I am grateful to all of those with whom I have had the pleasure to work and share office space. Thank you Dr. Philip Marzahn for setting up a workspace for me in your office and your insight in the German academic system, which helped me determine the best path for me going forward. On the Canadian side, I would like to thank Jennifer Hird for helping navigate Government of Canada websites, Kiran Basran, Fai Wu and especially Silvia Losada for helping me transition into Calgary.

A special mention should be made about Keifer Biddle, Alex Hamilton, Gus Lopes Queiroz and Jack Sugden. Field work was exhausting but with you, time flew by. I made memories for a life time in Conklin, mostly because of you. Thank you for taking a clueless German and introducing her to the Canadian wilderness.

This research was supported by a Natural Sciences and Engineering Research Council of Canada Collaborative Research and Development Grant (CRDPJ 469943-14) in conjunction with Alberta-Pacific Forest Industries, Cenovus Energy, ConocoPhillips Canada, Devon Canada Corporation, and the Regional Industry Caribou Collaboration. My stay in Alberta was further supported by a generous scholarship granted by PROSA$^{\text{LMU}}$. I am very honoured and grateful to be the recipient of this award.

By concluding my studies at the LMU with this thesis, I would like to use the opportunity to express my gratitude towards my parents, Dr. Med. Evi Dietmaier and Prof. Dr. Wolfgang Dietmaier, my sister Louisa and my partner Haley. Thank you for always supporting my scientific dreams and ambitions and for helping me chin up on those days when frustration takes over. Thank you for helping me become the scientist I am today.

Executive Summary

Openings in forest canopy cover play a crucial role in the rejuvenation of forest structure and the maintenance of biodiversity. However, if human disturbances affect the habitat of certain species, openings may have detrimental effects on the ecosystem. Airborne laser scanning (ALS) and digital aerial photogrammetry (DAP) are three-dimensional remote-sensing data sets that both have the potential to characterize canopy openings. While ALS is the more well-known data source of the two, DAP is less expensive to acquire.

The objective of this study was to examine the capacity of ALS and DAP to canopy openings in the boreal forest of northern Alberta. While previous authors have conducted similar studies, they have all taken place in dense-canopy tropical and temperate rainforests. The current area of interest (AoI) is a 1-km2 expanse of boreal forest situated in northern Alberta, characterized by highly variable vegetation cover, ranging from low vegetation density wet lands to densely forested, drier uplands. Thus, traditional definitions of opening, and approaches to opening detection must be reconsidered and were tested for their applicability in this study. In addition to natural openings, the study area also contains anthropogenic linear features that are the consequences of large-scale oil exploration.

A fixed-height approach and variable-height approach to detecting canopy openings were applied to three canopy height models (CHMs) extracted from the two data sets: CHMALS, CHMDAP, and CHMHybrid, which is a combination of both DAP and ALS data. Validation was conducted based on field measurements, supplemented by visual image interpretation.

Overall accuracies for CHM_{ALS} were 90% and 93% for fixed- and variable-height approaches, respectively, compared to 63% and 82% for CHM_{DAP}, and 64% and 82% for CHM_{Hybrid}. Large errors of omission were produced by both the DAP and Hybrid data sets (15% - 46%). We found that especially small openings (< 200 m^2) were incorrectly classified by DAP and Hybrid when using the fixed-height approach, and showed large errors of omission ($> 90\%$). Markedly better results were achieved in these smaller openings when using the variable-height approach. Accuracy only varied by 3% when using the variable-height approach with ALS data, and was distinctly higher for all opening-size classes. Number and average size of the openings detected varied clearly between the approaches, with ALS detecting more than twice the number of openings when using the fixed-height approach than the DAP/Hybrid data sets. The average opening size detected by the fixed-height approach was less than half the size of each model's corresponding variable-height approach results.

Lower overall accuracies and the omission of small openings are attributed to the method of data acquisition by DAP, which characterizes the top of canopy but doesn't penetrate to the forest floor reliably. Thus, this optical technology is more vulnerable to occlusions, shadows, and tree sway: optical effects which negatively affect the image matching process and thus the quality of a detailed CHM.

This study demonstrates that ALS is a more accurate means for monitoring canopy openings in the boreal forest, and that DAP data does not yet achieve the

accuracies produced by ALS data in the context of detecting and mapping openings in this setting. However, given the improvements that were achieved in this study compared to previous studies, it is possible that with further software development, DAP will soon be a cheaper and more easily accessible means to monitor forest structure dynamics.

Zusammenfassung

Lücken im Blätterdach eines Waldes spielen eine wichtige Rolle im Regenerierungsprozess und Erhalt seiner Biodiversität. Wenn menschliche Eingriffe aber das Habitat einer Spezies signifikant beeinträchtigen, können sich diese Lücken negativ auf das Ökosystem auswirken. Im Untersuchungsgebiet, einem 1 km^2 großen Bereich im borealen Wald in Nordalberta, Kanada, führten ausgedehnte Ölexplorationen zu einem Netzwerk aus Schneisen (sog. *Linear features* oder *seismic lines*). *Airborne Laser Scanning* (ALS) und *Digital Aerial Photogrammetry* (DAP) wurden bereits auf ihre Eignung zur Detektion, Abgrenzung und Kartierung von Lücken im Blätterdach untersucht. ALS zeigte in mehreren Studien weitaus bessere Ergebnisse als DAP, allerdings bearbeiteten diese Studien hauptsächlich tropische und temperierte Regenwälder. Da DAP günstiger und leichter durchzuführen ist als ALS, sollen in dieser Arbeit die Genauigkeiten, mit denen ALS und DAP Lücken im borealen Wald detektieren miteinander verglichen werden.

Das Untersuchungsgebiet weist eine außerordentlich hohe Variabilität der Vegetationsarten auf. Es sind sowohl sehr dünn bewachsene Gebiete in den niedriger gelegenen Feuchtgebieten, als auch sehr dicht bewachsene Stellen in den höher gelegenen Trockengebieten vorhanden. Aus diesem Grund mussten traditionelle Definitionen von Waldlücken und Herangehensweisen auf ihre Anwendungseignung in diesem Ökosystem überprüft werden. Zwei Lückenklassifizierungen wurden durchgeführt: 1) mittels festem maximalen Höhenwert (*fixed height approach; FIX*) und 2) mittels einem zur umgebenden Schirmhöhe relativen Höhenwert (*variable height approach; VAR*), und auf drei *Canopy Height Models* (CHM) angewandt: 1) CHM_{ALS}, 2) CHM_{DAP} und 3) CHM_{Hybrid}, einer Kombination der beiden Datenquellen. Die Validierung basiert auf in-situ Daten, welche um Daten aus visueller Bildanalyse ergänzt wurden.

Gesamtgenauigkeiten für durch ALS erkannte Lücken liegen bei 90% für den FIX-Ansatz und bei 93% für den VAR-Ansatz. Im Vergleich dazu liegen die Gesamtgenauigkeiten für von DAP erkannte Lücken bei 63% und 82%, und bei 64% und 82% für vom Hybrid-Modell erkannte Lücken. Große Auslassungfehler (15% - 46%) wurden sowohl für das DAP- als auch das Hybrid-Modell verzeichnet. Vor allem kleine Lücken (< 200 m^2) resultierten in den DAP_FIX und Hybrid_FIX Modellen in Auslassungsfehlern von $> 90\%$. Diese kleinen Lücken wurden von den DAP- und Hybrid-Modellen unter Anwendung des VAR-Ansatze deutlich besser detektiert. Die Genauigkeiten in den verschiedenen Größenklassen für das ALS_VAR Modell schwankten dagegen nur um 3% und waren insgesamt deutlich höher. Die Anzahl und durchschnittliche Größe der detektierten Lücken schwankte stark zwischen den verschiedenen Herangehensweisen; das ALS_FIX Modell erkannte mehr als doppelt so viele Lücken als die DAP- und Hybrid-Modelle. Die durchschnittliche Größe der von den FIX-Ansätzen erkannten Lücken war die Hälfte der entsprechenden Lücken, welche mit den VAR-Ansätzen erkannt worden waren.

Geringere Gesamtgenauigkeiten und das Auslassen kleinerer Lücken werden auf die Methodik der Datenakquisition von DAP zurückgeführt. Diese erkennt lediglich die *top of canopy*, und kann die Baumkronen nicht wie ALS durchdringen. Dadurch ist diese

optische Technik anfälliger für Störfaktoren wie Verdeckungen, Schattenwurf und Bewegung der Baumkronen zum Zeitpunkt der Bildaufnahme.

Diese Studie zeigt, dass ALS ein geeignetes Mittel darstellt, um menschliche Einflüsse auf Waldsysteme zu überwachen, und dass DAP im Kontext der Detektion und Kartierung von Waldlücken im Untersuchungsgebiet noch keine ebenbürtige Alternative zu ALS ist. Betrachtet man allerdings die Fortschritte, welche im Vergleich zu früheren Studien festgestellt werden konnten, ist davon auszugehen, dass eine Weiterentwicklung von Software und Kameraeigenschaften DAP bald zu einer günstigeren Alternative werden lässt.

Table of Contents

List of Figures

List of Tables

List of Acronyms

3D	3 dimensional
ALS	Airborne laser scanning
AoI	Area of interest
ASPRS	American Society for Photogrammetry and Remote Sensing
CHM	Canopy height model
CHM_{ALS}	Canopy height model (ALS data only)
CHM_{DAP}	Canopy height model (DAP data only)
CHM_{Hybrid}	Canopy height mode (combination of ALS and DAP data)
CRS	Coordinate reference system
CV	Coefficient of variation
DAP	Digital aerial photogrammetry
DSM	Digital surface model
DSM_{ALS}	Digital surface model (ALS data only)
DSM_{DAP}	Digital surface model (DAP data only)
DSM_{Hybrid}	Digital surface model (combination of ALS and DAP data)
FIX	Fixed height approach
GCP	Ground control points
GEDI	Global ecosystems dynamics investigation
GSD	Ground sampling distance
GPS	Global positioning system
LAI	Leaf area index
LiDAR	Light detection and ranging
LIS	Low impact seismic line
NDVI	Normalized difference vegetation index
NIR	Near infra-red
OTH	Overlap threshold
OvA	Overall accuracy
PAR	Photosynthetically active radiation

RADAR	Radio detection and ranging
RMSE	Root mean square error
RTK	Real-time kinetic
RP	Reference polygons
SAGD	Steam-assisted gravity drainage
SARA	Species-at-risk-Act
STH	Structural threshold
SRTM	Shuttle Radar Topography Mission
TIN	Triangular irregular network
TMP	Target map polygon
ToC	Top of canopy
UAV	Unmanned aerial vehicle
VAR	Variable height threshold

List of Equations

1 Introduction

Naturally caused canopy openings occur in every forest. They are an essential part of the natural mature forest stand development cycle and add to the health and upkeep of a forest ecosystem's biodiversity (Feldmann et al., 2018; Lawton & Putz, 1988; Nagel et al., 2010; Runkle, 1982; Whitmore, 1989). Depending on the size and duration of the canopy opening, a significant increase in nutrient and solar radiation supply facilitates regrowth of diverse vegetation and offers new niches for birds, insects, and other fauna (Vepakomma et al., 2012). In addition to naturally occurring openings that are usually caused by small scale disturbances, such as wind throw (Bonnet et al., 2015), tree or branch falls (Ferreira De Lima, 2005; Fox et al., 2000) and snow destruction (Caron et al., 2009), anthropogenically affected sites like clear cuts or road clearings are kept free of vegetation, which prevents an increase of diverse regrowth.

In addition to natural openings, the area of interest (AoI) for this research, a 1 x 1 km expanse of boreal forest south of Conklin in northern Alberta, Canada, is also affected by a variety of human disturbances; particularly seismic lines. Seismic lines are linear clear-cut corridors in the boreal forest which present in a grid-like fashion and are produced by heavy machinery to facilitate extensive seismic underground oil exploration (EMR, 2006). In addition to these corridors, roads, pipelines and bitumen extraction sites require large scale clear cuts (S. Chen et al., 2017; Downing & Pettapiece, 2006). These disturbances show cumulative effects on wildlife habitat and biodiversity (S. Chen et al., 2017).

One representative of a negatively affected species is *Rangifer tarandus caribou*, the boreal woodland caribou, whose populations have shown a decline linked to seismic-line disturbances (Athabasca Landscape Team, 2009; Hebblewhite, 2017). A federal recovery plan identifies the amount and location of critical habitat for each woodland caribou population and points out the critical need for aggressive habitat protection and restoration measurements. As a necessity for a federal recovery plan under the Canadian federal Species-at-Risk Act (SARA), Environment Canada identifies an approach for continued monitoring of natural disturbances, as well as habitat quality and quantity (Environment Canada, 2012).

Before three-dimensional (3D) opening detection was made possible by ALS using light detection and ranging (LiDAR) and specialized software was developed to compute large amounts of photogrammetry imagery, spectral remote-sensing approaches such as normalized difference ratios were a well-established way of assessing the state of a given area of vegetated land. The normalized difference vegetation index (NDVI) is the most commonly used spectral vegetation index (Coppin & Bauer, 1996; Jönsson et al., 2010; Senf et al., 2017; Zhirin et al., 2016). Using the difference between strong absorption in the visible red, and reflection in the near-infrared (NIR) wavelength (equation 1), the NDVI is an index for "greenness" (Jönsson et al., 2010).

$$NDVI = (NIR - R)/(NIR + R) \tag{1}$$

where

NIR = Near Infrared reflectance

R = Red reflectance

The NDVI assumes values between -1 and 1, -1 – 0 representing low to no vegetation cover, and 0 – 1 representing denser vegetation cover (Wulder, 1998). Chen & Cihlar (2000) assess the validity of NDVI values in forests in Saskatchewan and Manitoba using in-situ measurements for their validation. They found that these vegetation indices were useful for determining leaf area index (LAI) for boreal forests, however, they note that the understory's contribution can severely distort the calculated NDVI values. In addition, NDVI values change over the course of a year, with more reliable results being derived from satellite imagery acquired in the spring than in autumn. These limitations make spectral indices like the NDVI less reliable, but their easy usage and free access to data and software are their strong advantages.

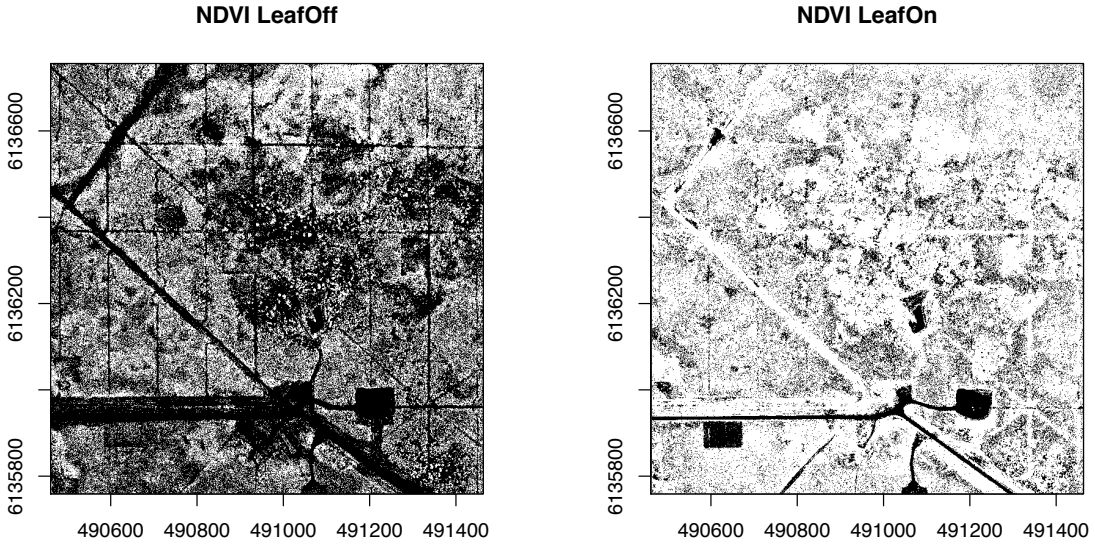

Figure 1 Two NDVI images derived for the study area: one in the early spring (leaf off, left) and another in mid summer (leaf on, right). Depicted are areas where NDVI < 0.1 are classified as opening (depicted in black) and areas where NDVI > 0.1 are classified as non-opening (depicted in white). It is apparent that there is little consistency between the two images and that they offer barely any reliability regarding the classification of opening vs. non-opening. This is mainly due to grassy seismic lines being classified as non-openings in the leaf-on imagery. The only disturbances which can be reliably classified as such are roads and clearings which are consistently completely free of any vegetation.

Two NDVI images (figure 1) were derived for the study area, which produced unsatisfactory results. A threshold of 0.1 was chosen for the binary classification to consider Their overall accuracies (OvA) in detecting openings (defined as areas where NDVI < 0.1) were found to be 50% when based on an orthophotos acquired in May (NDVI_LeafOff) and 71% for the LeafOn data set.

Aiming for higher reliability and accuracy, airborne laser scanning (ALS) and digital aerial photogrammetry (DAP) were tested for their applicability in mapping openings in forest canopy. ALS and DAP are two different technologies with the ability to produce 3D point clouds. Using vegetation height instead of the greenness of vegetation constitutes are radically different approach in opening detection compared to normalized difference ratios.

Various studies have examined the applicability of the ALS and DAP technologies in the detection and mapping of canopy openings, mainly in tropical and temperate rain forests, as well as temperate deciduous forests. In contrast to traditional field campaigns to gather in-situ measurements, which are time consuming and costly (Bonnet et al., 2015; White et al.,

2018), ALS and DAP have been used to efficiently examine canopy cover structure (S. Chen et al., 2017; Holopainen et al., 2015; Järnstedt et al., 2012; Lovitt et al., 2017). The opening detection accuracies were found to be 74.5% (Gaulton & Malthus, 2010), 82% (Bonnet et al., 2015), 96.5% (Vepakomma et al., 2008; White et al., 2018) for ALS and 78.2% (Gaulton & Malthus, 2010) and 50% and 59.5% for DAP (White et al., 2018).

ALS has experienced a surge of popularity in the last decade and was even rumored to eventually replace stereophotogrammetry (Leberl et al., 2010). LiDAR's ability to penetrate the canopy cover made it an ideal tool for forest-inventory assessment, and stereo imagery could not compete on price and output. However, the evolution of digital data acquisition, fully automated triangulation algorithms, dense matching, high density point clouds and unprecedented detail due to high geometric resolution made DAP affordable and easily accessible (S. Chen et al., 2017; White et al., 2018). In combination with lower costs and the emergence of efficient consumer grade unmanned aerial vehicles (UAVs), these developments. initiated a new enthusiasm for photogrammetry (Leberl et al., 2010). Especially in the domain of repeated multitemporal monitoring, as demanded by the Provincial Woodland Caribou Recovery plan (Alberta Government, 2017), lower costs and easier accessibility of DAP data would make stereophotogrammetry the data source of choice, if it can be shown to be of sufficient accuracy.

This study builds on the promising outcomes of studies from Gaulton & Malthus (2010), Bonnet et al. (2015) and White et al. (2018), which showed great potential of the use of LiDAR data for detecting canopy openings, and Chen et al. (2017), whose novel DAP standalone approach produced satisfying results for measuring vegetation height. Pioneering in comparing ALS and DAP and a combination of the two, and their applicability in the detection of canopy openings in the boreal forest of northern Alberta, Chen et al.'s study's results will be valuable input for quantifying the human impact for purposes like monitoring the success of governmental habitat protection plans. The Provincial Woodland Caribou Range Plan (PWCRP) specifically includes monitoring of landscape condition, characterized by

1) the area of anthropogenic disturbance features,
2) the area of disturbed and undisturbed habitat and
3) the amount and density of linear features (Alberta Government, 2017).

The new evaluation of the two technologies is necessary because this study's area of interest (AoI) is characterized by a higher diversity of tree phenology – especially height and density – than most regions of interest in previous studies. Tree height in temperate and rain forests is usually homogenous, whereas the boreal forest of northern Alberta exhibits a wide range of tree height, with small trees growing in the bogs and fens of the lowlands, and very tall pine and birch trees in the uplands (Lovitt et al., 2017).

The detailed comparison of canopy opening detection via ALS versus DAP technologies, as undertaken in this study, can be broken down into 3 technological and 1 ecological research questions:

1) What are the accuracies for detecting structural openings in the canopy cover of the boreal forest ecosystem using ALS and DAP technologies?
2) Is it possible to produce a reliable CHM using solely DAP data?

3) Are LiDAR and DAP appropriate technologies to quantify the human impact in the study area and naturally occurring canopy openings?

4) Are LiDAR and DAP appropriate means to help execute the Provincial Woodland Caribou Range Plan?

Chapter 2 identifies existing research projects and resources in the context of the ecological significance of openings in forests, the technological qualities of LiDAR and DAP, and point cloud based opening detection. The study area with its meteorological, biological and geological features, and the local disturbance regime, as well as relevant definitions are discussed in chapter 3. Data and methods used in this study are presented in chapters 4 and 5, respectively. The results and their critical discussion can be found in chapters 6 and 7. Chapter 8 offers an outlook in the future research of ecological and technical challenges identified in this study.

2 Literature Review

The literature on canopy openings is diverse and provides a variety of approaches to assessing canopy structure. There does not seem to be a uniform definition of what constitutes a "canopy gap", assuming every ecosystem is unique in its structure. This chapter sums up the most important approaches to provide an overview of existing solutions when deciding on the definition of canopy openings in this study's context.

2.1 Canopy Openings and Forest Dynamics

The ecological importance of canopy openings to the forest ecosystem has been well recognized and backed by extensive research conducted on the topic since the end of the 19th century (Mccarthy, 2001; Muscolo et al., 2014). Numerous studies have been published on canopy openings in tropical rain forests (Brokaw, 1985; Brokaw & Scheiner, 1989; Lawton & Putz, 1988; Schnitzer & Carson, 2001), coastal temperate rainforests (Lertzman et al., 1996; White et al., 2018), temperate hardwood forests (Busing & White, 1997; Canham et al., 1990; Poage & Peart, 1993; Runkle, 1982, 1992; Stewart et al., 1991; Zieli et al., 2018) and temperate coniferous forests (Coates, 2000; Gray & Spies, 1996, 1997; Stan & Daniels, 2018). Kneeshaw (1998) reported a lack of research conducted on boreal forests in North America which he concluded to be due to the domination of large scale disturbances such as extensive fires. McCarthy (2001) adds insects and wind disturbances as reasons for the lack of attention concerning openings in boreal forests.

While some studies have recently focused on the boreal ecosystem of the northern United States and Canada (Cumming et al., 2000; Kneeshaw & Bergeron, 1998; Vepakomma et al., 2010, 2011, 2012) as well as of Europe (Caron et al., 2009; Dai, 1996; Hörnberg et al., 2011; Leemans, 1991) and Japan (Kubota, 1995), the examination of canopy openings in the boreal forest ecosystem is still underrepresented in comparison to the aforementioned ecosystems (Mccarthy, 2001).

2.1.1 Definitions of Canopy Openings

It is crucial to consider the different aspects that characterize the tropical, the temperate and the boreal forest ecosystems when defining a canopy opening. However, the literature at hand focusing on the tropical and the temperate zone, though not representing the ecosystem of this study, aids at acquiring a first overview of definitions, causes and effects of canopy openings.

Runkle defined canopy openings in temperate hardwood forests in 1982. He differentiated between two types, the first being the canopy opening itself, defined as the *"land surface directly under the canopy opening"* and the second being the expanded opening which he defined as *"the canopy opening and plus the adjacent area extending to the bases of canopy trees surrounding the canopy opening"* (Runkle 1982, p. 1534). The concept of the expanded opening (fig. 2) was useful when considering indirect effects of openings in the forest canopy, such as changes in the supply of solar radiation reaching the ground in the northern adjacent areas located under closed canopy (Runkle, 1982).

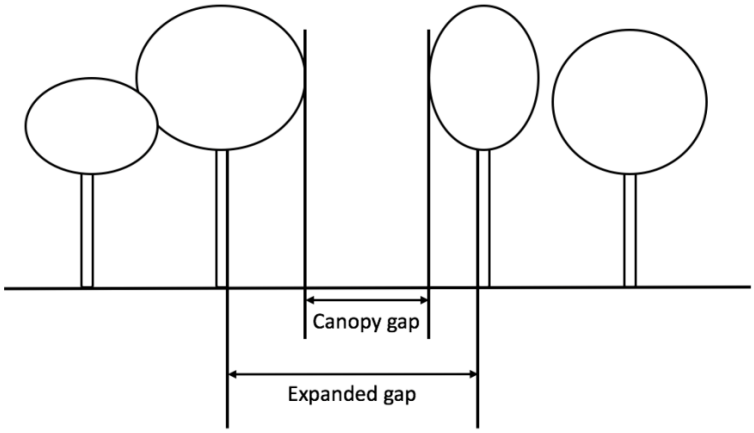

Figure 2 Opening definitions for canopy and extended openings (Runkle, 1992).

A definition for treefall openings in the tropical forest was offered by Brokaw (1982): a *"gap is a "hole" in the forest extending through all levels down to an average height of two m above ground"* (Brokaw 1982, p. 159). He defines the walls of the opening as irregular in profile but, simplifying reality for a more workable definition, he makes the assumption that they are vertical, and accepts singular, isolated small trees and branches as part of an opening (Brokaw, 1982). While this definition seems quite logical, there are different opinions regarding some of the central opening characteristics, the most prominent ones being minimum and maximum size.

The minimum size of a disturbance to be identified in the literature as an opening ranges from 4 m^2 (Lawton & Putz, 1988) to 25 m^2 (Fox et al., 2000; Runkle, 1992; Schnitzer & Carson, 2001) or can be set indirectly, e.g. as one half canopy tree (Christensen & Franklin, 1987; Runkle, 1992). Openings are, by definition, localized and discrete and *"are not part of an "open-ended" system such as a wetland or a large burned area"* (White et al. 2018, p. 1). One attempt to identify the maximum size of an opening in the forest to qualify as a canopy opening was undertaken by Christensen & Franklin (1987). Here, the maximum size is the spatial extend of the area affected by ten dead trees. Fox et al. (2000) and Stewart et al. (1991) state that an opening can reach a size of 0.1 ha, Schnitzer and Carson (2001) defined their openings with a maximum size of 75 m^2. Finally, Runkle (1992) defines the maximum size as the opening created by the death of ten canopy trees, or when the canopy height to opening diameter ratio reaches 1.0, *"whichever is larger for the forest studied"* (Runkle 1992, p. 16).

Openings can be rapidly closed by advance regeneration, adjacent vegetation in the initial growth stages or radial expansion of the edge tree crowns (Vepakomma et al., 2012). Thus, it is important to identify, besides minimum and maximum horizontal extent on the ground, a height limit of regrowth vegetation within an opening after the disturbance (regrowth vegetation). Studies agree that openings are areas within the forest that are either devoid of trees or *"where the canopy (leaf height of tallest stems) is noticeably lower than in adjacent areas"* (Runkle 1992, p. 2), and that an opening is a site that is lacking a competitively dominant canopy tree (Runkle, 1992). While there are various-fixed value approaches to identifying openings, e.g. 15 m in a beech forest in Japan (Nakashizuka, 1987) or 15-20 m in a temperate coastal rain forest in Chile (Veblen, 1985), Runkle (1992) suggests the use of a variable approach: the canopy opening still qualifies as an opening if the regrowth vegetation is low enough to *"expose to the sky the crowns of stems that otherwise would be in the understory. Gaps close when replacement stems reach a height indistinguishable from that of*

the surrounding closed forest" (Runkle 1992, p. 16). Schnitzer and Carson (2001, p. 914) consider the temporal consistency in their approach: an opening is an area that had a *"sustained canopy height of at least 20 m for two consecutive years and then dropped to a height of 5 m or less during the following year"* (Lawton and Putz (1988) accepted areas with trees with an opening canopy height of no more than 50% of the surrounding canopy height. The last three approaches illustrate the importance of keeping the site-specific characteristics of the AoI in mind when defining a vertical limit for the regrowth vegetation.

2.1.2 Opening Formation

Canopy opening openings can be the effects of various disturbances. In general, two types of disturbances can be distinguished based on their source:

1) ephemeral openings: caused by exogenous disturbances (both natural and anthropogenic)
2) persistent openings: caused by edaphic or topographic conditions, such as streams or rock outcroppings (Lertzman et al., 1996).

In the tropical forests, while there are occasional severe disturbances such as earth quakes, mud slides, volcanic eruptions or hurricanes, chronic treefall and limb fall are the most common forms of natural disturbances (Lawton & Putz, 1988; Veblen, 1985). In boreal forest ecosystems, large scale disturbances do exist, such as fires (Burton et al., 2008; Caron et al., 2009; Vepakomma et al., 2010), hurricanes and windstorms (Poage & Peart, 1993; Runkle, 1982; Stewart et al., 1991), droughts (Stewart et al., 1991), and large scale insect infestation (Barrette et al., 2017; Safranyik et al., 2010; Vepakomma et al., 2010). However, small scale disturbances, such as wind throw, (Bonnet et al., 2015), tree or branch falls (Ferreira De Lima, 2005; Fox et al., 2000) and snow destruction (Caron et al., 2009), natural mortality and heart rot (Caron et al., 2009), are the most common causes for canopy openings in boreal forests (Feldmann et al., 2018).

In addition to natural opening formation, evidence of anthropogenic disturbances is omnipresent and affect forests in every ecosystem. Silvicultural practices and wildlife management practices (Fox et al., 2000), like thinning (Bonnet et al., 2015), harvestings and other logging activities (Vehmas et al., 2011), as well as clear cuts for roads and other infrastructure (Fox et al., 2000) can be found in almost every forest in the world, all of which create openings in the forest canopy an thereby contribute to opening formation. A particular form of anthropogenic disturbance in the study site are seismic lines, pipelines, and gas wells (Hebblewhite, 2017; Lovitt et al., 2018; Rahman et al., 2017) and shall be discussed further in chapter 2.3.1.

2.1.3 Forest Dynamics and Opening Recovery

Given that most forests will produce regrowth in openings when left long enough, canopy openings created by small scale disturbances like branch or treefall play a vital factor

1) enabling the process of regenerating forest vegetation and
2) maintaining a meaningful biodiversity within the forest ecosystem (Feldmann et al., 2018; Lawton & Putz, 1988; Nagel et al., 2010; Runkle, 1982; Whitmore, 1989).

Openings in the canopy are thus a crucial factor in the natural forest recovery cycle (fig. 3) (Bartels et al., 2016). Whitmore (1989) calls them the most important part of this cyclic successional pathway. Canopy openings assume this role mainly by influencing and changing the amount of solar radiation and thereby the supply of photosynthetically active radiation (PAR) which reaches the ground and understory vegetation (Canham et al., 1990; Dai, 1996; Nagel et al., 2010; Whitmore, 1989). For example, in a study in 1996, 9% of above canopy PAR reached the ground under the closed canopy cover, while 25% of above canopy PAR reached the ground within the examined openings. In addition, the growth rate was 23.9% higher within openings compared to areas beneath the canopy cover (Dai, 1996).

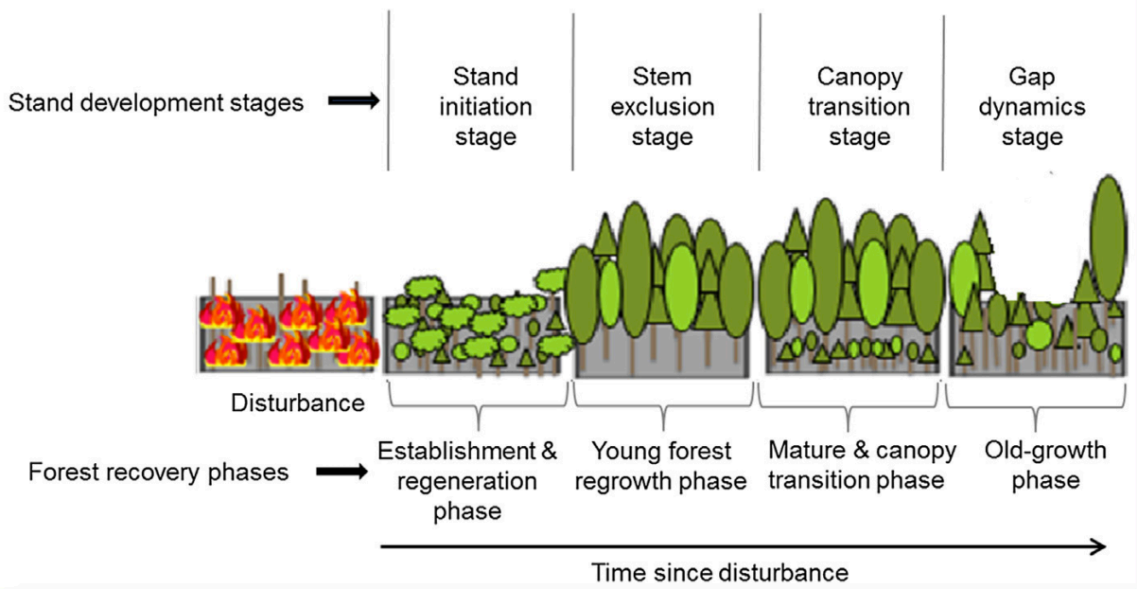

Figure 3 Schematic stages of early to mature forest stand development following major disturbances (adopted from Oliver and Larson, 1996). The species composition, height structure and time elapsed since the disturbance at each stage vary with type of disturbance, dominant species an site conditions (Bartels et al., 2016).

The species composition of regrowth vegetation within openings depends, for a large part, on the size of the disturbance (Lawton & Putz, 1988; Nagel et al., 2010; Stewart et al., 1991). Small openings are usually characterized by a continuously limited supply of PAR. This is especially true in high latitude forest stands where low sun angles throughout the day lead to little PAR reaching the ground (Barrette et al., 2017; Coates, 2000). Not only receive very small openings little light, but they are also usually filled quickly by the lateral expansion and ingrowth of adjacent canopy trees. Even slightly larger openings tend to stay shady. Here, regrowth consists mostly of shade tolerant advance vegetation, seedlings that were germinated under the closed forest canopy before the formation of the opening and commence their height growth when a canopy opening occurs (Whitmore, 1989).

In openings, large enough to allow for a significant increase in the supply of PAR, more light-demanding species can germinate after an opening has been formed (stand initiation phase, fig. 3). Those seedlings cannot be recruited prior to a canopy opening and fully depend on the formation of a large canopy opening (Whitmore, 1989). Whitmore (1989) therefore developed the autecological differentiation of opening regrowth vegetation into pioneer and non-pioneer (climax) vegetation. While pioneer vegetation requires direct sunlight at least part of the day and can only be germinated after the formation of a large canopy opening, climax or non-pioneer vegetation is able to germinate under a closed canopy cover and its juveniles

can survive in a shady environment (such as created by pioneer vegetation) for some years (Whitmore, 1989).

While radial expansion of existing trees plays a limited role in the closure of larger openings, the recruitment of new seedlings is the primary process of opening closure (Leemans, 1991; Poage & Peart, 1993; Runkle, 1982). By facilitating the regrowth and recruitment of young seedlings and saplings into the existing, possibly quite old or mature forest stand, openings facilitate for rejuvenation, adding to the heterogeneity and modifying the structure of the average forest ecosystem (Feldmann et al., 2018; Stan & Daniels, 2018; Stewart et al., 1991). And while openings are not essential for the recruitment of shade-tolerant tree species, they are necessary for the formation of secondary canopy layers, which is one criterion for the transformation from mature forests to old-growth forests (Gray & Spies, 1996).

There are several lines of evidence indicating that opening size is one of the most important factors influencing regrowth, leading some researchers to making out opening size to be the sole factor. (Brokaw & Scheiner, 1989; Lawton & Putz, 1988). However, while the concept of opening size influencing sunlight supply and thereby determining the species composition by allowing light-demanding species to grow in larger openings and shadow-tolerant plants in smaller openings, seems to be clear and intuitively correct, there are more factors than solely the spatial extent of the canopy opening that influence the composition and spatial distribution of regrowth species. Staying close to the topic of changes in the supply of solar radiation in openings, it should be stated that instead of opening size, one should consider opening geometry. Opening aperture and ratio of opening diameter to height result in an increase in sunlight with increasing vertical distance from the center of the opening and significant variations in the horizontal distribution of sunlight within the opening (Poage & Peart, 1993). Depending on the geographical location (and thereby sun path and the incidence angle of solar radiation), opening geometry might have more consequential impacts on opening regrowth than opening size (Canham et al., 1990; Coates, 2000; Gray & Spies, 1996). Opening geometry is especially important in the boreal forest ecosystem. Given the low sun path, openings are often too small for sunlight to reach the ground in the opening (Leemans, 1991). This results in modifications in the regeneration process: in northern boreal forests, the regeneration process is dominated by growth of advance vegetation of shade tolerant species. To a much lesser extent, light demanding individuals are established (Barrette et al., 2017). Besides opening size and opening geometry, there are, however, multiple other factors that affect the temporal and spatial variability in seedling recruitment. Given that openings do not show laboratory conditions for colonization, regrowth is affected by the presence or absence of woody debris, existing vegetation, nurse logs and disturbed mineral soil (Lawton & Putz, 1988), environmental heterogeneity, understory plants (Stewart et al., 1991), management history (Feldmann et al., 2018), resilience to shadow in different life stages (Nagel et al., 2010), presence of seed consumers and dispersers, (micro)climatic variability (Coates, 2000), the length of the growing season (Gray & Spies, 1996), disturbance history (Stan & Daniels, 2018), existing vegetation influencing the quality of radiation penetrating the canopy (Dai, 1996), and substrate composition (Duncan et al., 1998).

2.1.4 Enhanced Biodiversity within Openings

Several studies found significantly elevated species density and richness/biodiversity within openings, compared to the closed-canopy forest stand (Busing & White, 1997; Schnitzer &

Carson, 2001). Openings, offering ideal conditions for plant regrowth (Muscolo et al., 2014), change the physical makeup of existing forest stands and thereby create and alter plant and wildlife habitats (Abdullah et al., 2018), increasing biodiversity (Fox et al., 2000). However, some studies suggest that the greater biodiversity found within openings might simply be due to a higher density of trees and other species growing within an opening in the initial stages of regrowth. This higher biodiversity is thus only a temporary effect of increased seedling recruitment and tree establishment, which can lead to higher species richness, depending on the pool of propagules of the species (Busing & White, 1997). This is then subject to the natural following thinning progress, caused, for example, by dry spells, competition and overgrowth by herbs, mosses and grasses, destruction by falling debris of disease (Canham et al., 1990; Leemans, 1991; Nagel et al., 2010; Schnitzer & Carson, 2001). Leemans (1991) found a high mortality rate during the first one to three years of regeneration. After an observation period of four years, only 0.6% of the initial regrowth individuals were still alive.

Openings can only regenerate the forest and maintain its ecosystem's biodiversity if the disturbances are small in scale and if the openings have enough time to produce regrowth without any renewed disturbance. Various studies in Fennoscandia have shown that disturbances, that are too numerous or not left alone for long enough, result in a decline in biodiversity and an increase in the number of endangered species (Caron et al., 2009). The only way to counteract such developments are the restriction of anthropogenic disturbances or the governmental protection of ecosystems and active treatment of disturbed sites to facilitate plant regrowth (Caron et al., 2009; Hebblewhite, 2017).

2.2 Technologies

The two main technologies compared in this study are ALS, applying one form of LiDAR, and photogrammetry. The following section provides insight into both technologies. Shortcomings and advantages will be presented.

2.2.1 LiDAR

LiDAR has received scientific attention for more than 15 years (Kukkonen et al., 2017). It is an active remote sensing technology, which can be mounted on handheld devices, drones and airplanes (Lefsky et al., 2002) or satellites, e.g. the Global Ecosystems Dynamics Investigation (GEDI) (Blumberg, 2018).

The sensor, which emits wavelengths of 900 nm – 1064 nm, records the return time of the emitted short-duration laser light pulse after reflecting off an object. The precise timing of the round-trip return time allows to calculate the distance (range) between the sensor and the detected object (Lefsky et al., 2001; Zolkos et al., 2013). In addition, LiDAR pulses can penetrate certain media, such as leaves in forest canopies. LiDAR can thus be used to digitize either a discrete combination of first, last and intermediate returns (fig. 4) (Næsset, 2015), or to present the returned energy in a quasi-continuous waveform, referred to as full-waveform LiDAR (Zolkos et al., 2013).

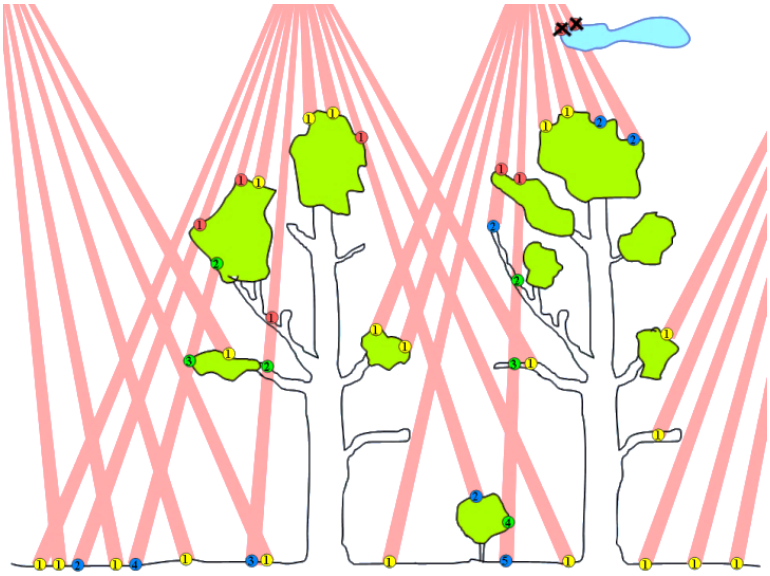

Figure 4 Laser pulses and discrete returns (Isenburg, 2016).

These abilities are utilized to produce high-resolution (sub-metre accuracy) measurements of surface elevations, which include vegetation, sea surface, bare soil and anthropogenic structures such as buildings and roads, based on x, y, z coordinated measurements (Bartels et al., 2016; Van Rensen et al., 2015; White et al., 2018). Previous studies have shown that LiDAR is the primary source of remotely sensed information for the use of deriving terrestrial topography (Næsset, 2015) and an excellent tool to measure forest structure characteristics accurately in a variety of forest ecosystems (Asner et al., 2013; Erdody & Moskal, 2010; Van Rensen et al., 2015; Vehmas et al., 2011; Vepakomma et al., 2008; White et al., 2018; Zhang, 2008). CHM derivation is facilitated by LiDAR providing both data for the digital surface model (DSM) as well as the digital terrain model (DTM). By subtracting the DTM from the DSM, a normalized CHM is produced.

2.2.2 DAP

In contrast to the active remote sensing technology LiDAR, DAP is a passive remote-sensing technology. First used in the 1940s with manual matching techniques, it has since developed into a well-established technology used to examine forest structure, mainly due to the straight forward fashion in which 3D images can be derived from stereo photogrammetry (Holopainen et al., 2015; White et al., 2013). Photogrammetry is based on the principle of parallax (fig. 5), which describes the apparent change in position of an object resulting from a change in viewing perspective (Lillesand et al. 2015, 177). If an object is viewed or imaged from two different positions, stereophotogrammetry enables the computation of the object's position relative to a reference datum (e.g. sea level, geoid, ellipsoid...) depending on the parallax (Holopainen et al., 2015; White et al., 2013).

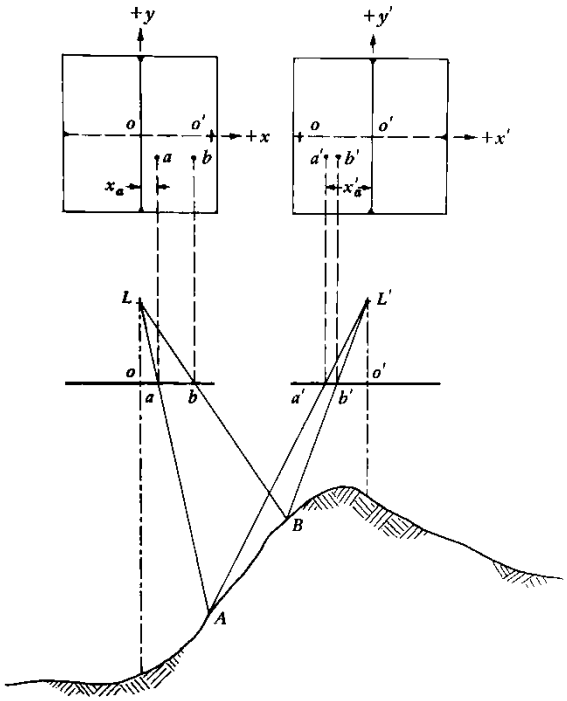

Figure 5 Parallax displacements on overlapping vertical photographs. A viewing line is constructed from the camera at each position to the common point in the image used for the image matching process. Triangulating the intersection of the two rays produces the 3D position of the point (Lillesand et al. 2015, p. 178)

Stereophotogrammetry uses two images for the matching process, but multi- image matching is required to produce the accuracies and details needed for reliable DSMs. Since the density of the point cloud increases with the amount of match points found in the matching process, an enormous improvement in the production of photogrammetry point clouds has been achieved by the development of affordable UAV and digital aerial cameras, which enable an easy acquisition of a large amount of high-resolution images needed for automated multi-view matching rather than manual stereo-matching (Holopainen et al., 2015). While the digital image resolution is defined as the ground sampling distance (GSD), which depends mainly on the flying height and technical specifications of the camera (Holopainen et al., 2015), the evolution of computing technology has led to more complex image matching algorithms, which further improve overall point-cloud quality (Remondino et al., 2014; White et al., 2013). The lack of ground returns under a canopy cover must be considered in the derivation of the CHM from DAP data (e.g. by using a pre-existing DTM).

3 Study Area

The area of interest (AoI) Kirby South is located in northeastern Alberta, Canada (fig. 6). In the following chapter, the AoI's physical makeup shall be described, as well as its disturbance regime. Further, definitions specifically applicable for this study and AoI will be presented.

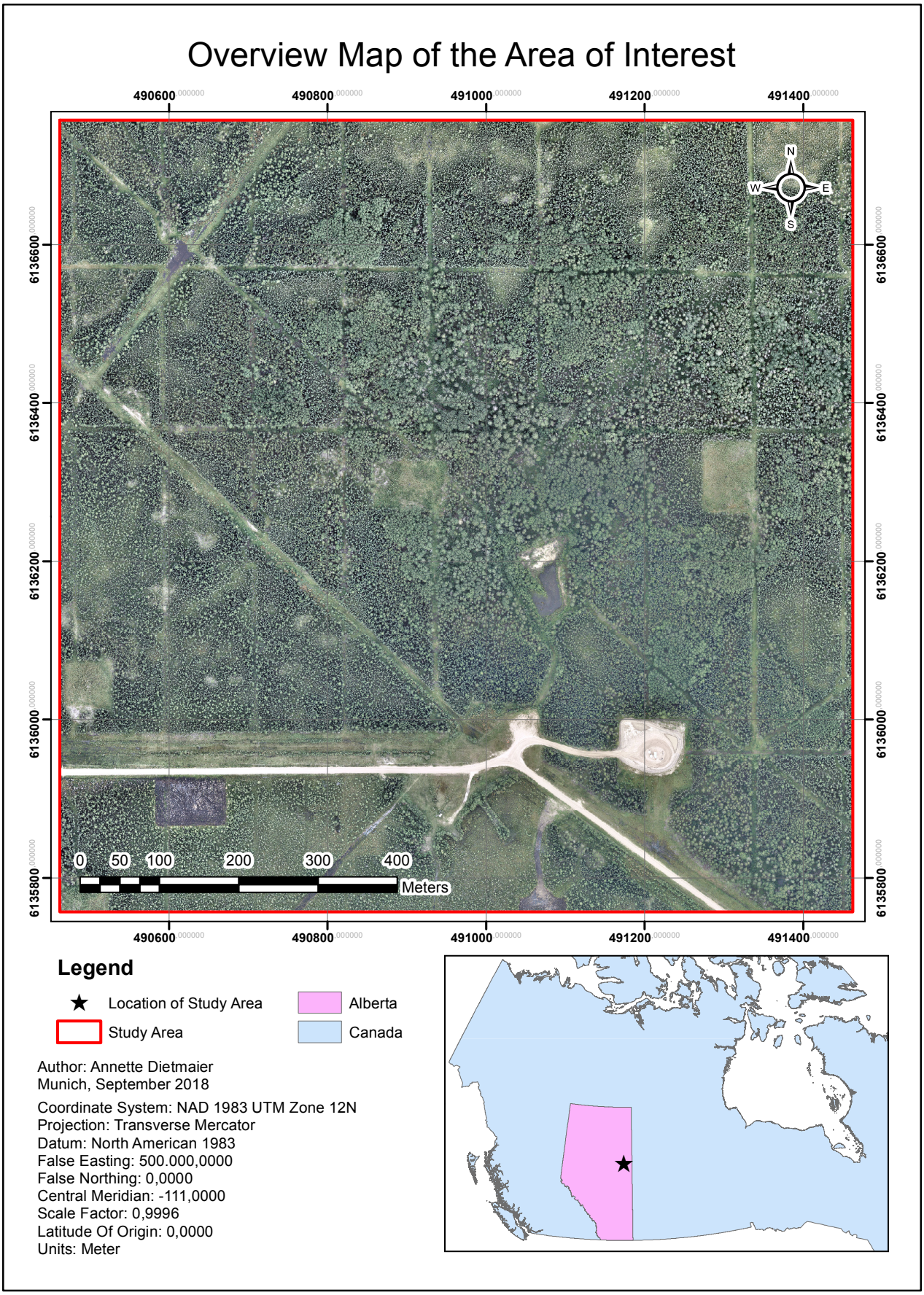

Figure 6 Overview map of the Area of Interest.

3.1 Climate

According to the effective climate system classification by Köppen, the climate in the AoI can be characterized by the class Dfb (Hendl & Liedtke 1997, 404). This class describes the Boreal Snow Climate, fully humid, with lower changes in the annual precipitation than warm temperate climates. The average temperature of the coldest month is below -3°C and the average temperature of the warmest month is above 10°C (Kottek et al., 2006). The climograph for Cold Lake, which hosts the closest weather station with publicly available data (118 km SSE of Kirby Lake), shows these criteria (fig. 7). With mean summer temperatures exceeding 15°C in July and August, mean winter temperatures dropping below -10°C in December, January and February, and an annual precipitation amplitude of less than 70 mm, Cold Lake is a good example of the fully humid Boreal Snow Climate. This subarctic climate is the largest of all Canadian climate zones and is characterized by cold extremes in the winter with temperatures below -40°- -50°C, caused and influenced by cold, dry Arctic air. The higher precipitation occurring during the summer months can is attributed to humid Pacific air dominating the weather patterns (Bone 2011, 56).

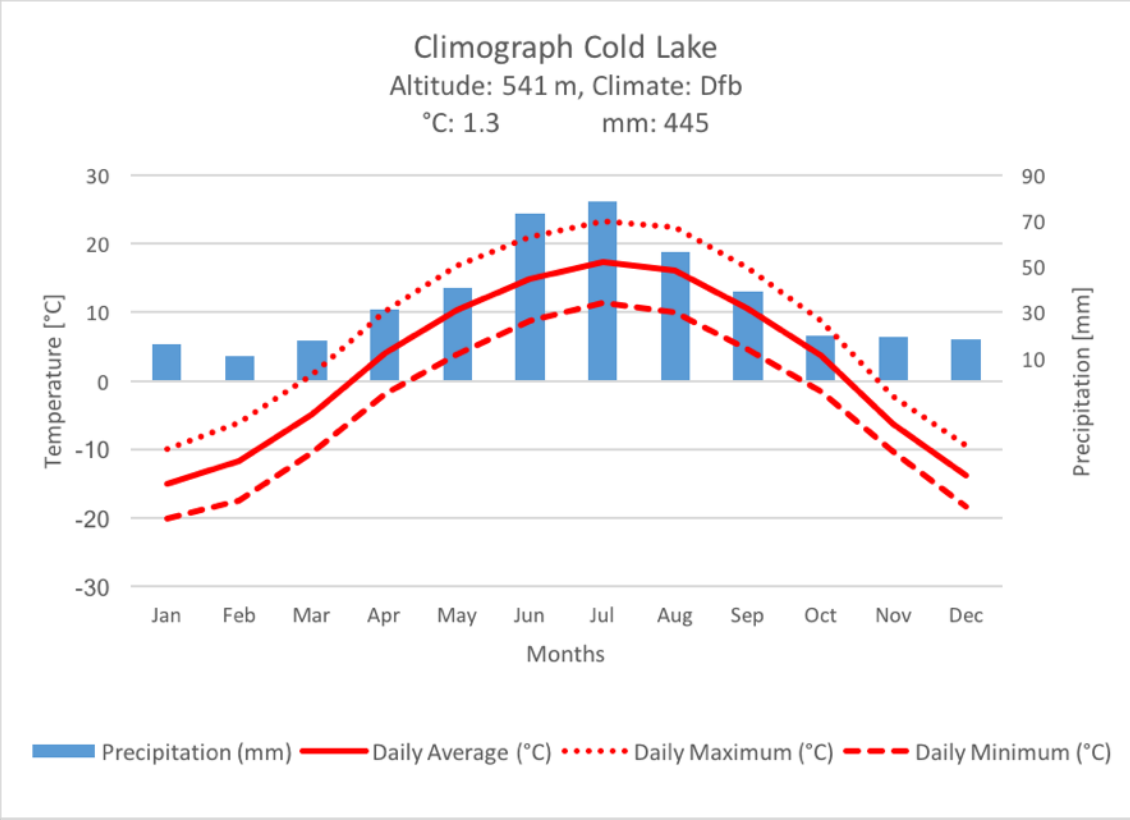

Figure 7 Climograph of Cold Lake, AB (Government of Canada, 2018), showing patterns typical of the humid boreal snow climate: cold extremes in the winter (-40 – -50°C) and higher precipitation during the summer months.

3.2 Flora and Fauna

The increase in temperatures and precipitation during the summer months provide adequate growing conditions for coniferous and mixedwood forest stands (Downing & Pettapiece, 2006). Given the relatively cool climate with summer temperatures around 15°C, the evaporation rate is kept relatively low, which promotes tree growth despite low precipitation, making black and white spruce (*Picea*), firs (*Abies*), aspen (*Populus*), and pines (*Pinus*) the dominating species

in the Canadian boreal forest. However, deciduous trees like birch, poplar, tamarack, aspen and larch can be found as well, especially along the southern edge of the boreal forest and as seral vegetation following a forest fire (Bone 2011, 56; Hess & Tasa, 2014, 364).

Due to adaption strategies, vegetation in the boreal coniferous forest can withstand minimum temperatures of -60°C. The coniferous trees tend to be tall, to receive more sunlight, and thin to avoid breakage under large amounts of snow (Hardy, 1967). In addition, the study area presents a remarkable amount of coarse woody debris within tree stands (fig. 8).

Figure 8 Coarse woody debris in the study area's forest.

Due to the tall growth structure and insufficient light availability, undergrowth is generally not pronounced underneath the closed canopy, except for a patchy layer of deciduous shrubs growing in profusion (Hess & Tasa, 2014), and a variety of herbaceous species or feathermosses and horsetails under deciduous and mixedwood stands (Downing & Pettapiece, 2006). More commonly, the ground is covered with mosses and lichens, and a decaying layer of needles overall (Hardy, 1967; Hess & Tasa, 2014). Over half of the Central Mixedwood Natural Subregion is characterized by low-lying wet, poorly drained fens and bogs, which affect large patches of the study area. The high moisture content makes mosses the dominant understory vegetation in these areas. Where tall growth trees are missing due to natural or anthropogenic disturbance or excessive soil moisture content, bearberry, blueberry, green alder, prickly rose, cloud berry, raspberry and Labrador tea occur and form a thick understory vegetation (fig. 9). These forms of understory are usually associated with coarse glacio-fluval or eolian deposits facilitating rapid drainage. The most common wetland type are species-poor black spruce fens with Labrador tea, peat moss and feathermosses (Downing & Pettapiece, 2006).

Figure 9 From left to right: raspberries, blueberries and red currants as found in the study area.

Due to slow plant growth, a relatively homogenous, species poor vegetation cover and harsh winter temperatures, the fauna's biodiversity is limited in the boreal forest and typically represented by mammals previously hunted for fur, like wolves and beavers, birds, and an abundancy of insects during the summer months (Hess & Tasa, 2014). During in-situ sampling, the study site proved to be home to black bears, caribou and wolverines.

3.3 Geology and Soils

The study site, positioned centrally in the interior plains, represents the Central Mixedwood Natural Subregion by comprising both undulating plains and some hummocky uplands. The most common underlying bedrock consists of Cretaceous shales and includes some sandstones and siltstones. In the well-drained hummocky areas of the uplands, one third of the surficial material is made of fine textured glaciolacustrine materials, one third by coarse glacio-fluvial and eolian sands, and another third by coarse to fine textured till. The wetlands are underlain by organic deposits (Downing & Pettapiece, 2006).

The Canadian boreal forest grows mainly on podzolic soils (Bone, 2011; Hess & Tasa, 2014). This soil requires acidic plant litter and a nutrient poor vegetation cover. It is thus commonly tied to the circumpolar boreal forest, where the needle litter leads to an abundance of acids and an adequate supply of precipitation makes for very effective leaching (Hardy, 1967; Hess & Tasa, 2014). Another favoring condition is the previous glacial detraction which distributed an abundance of broken rock debris on the surface. These rocks are of crystalline nature, rich in quartz and aluminum silicates and poor in alkaline mineral cations which would counteract the acidity and supply nutrients to the vegetation cover (Hardy, 1967; Hess & Tasa, 2014). Humus production is retarded due to a lack of productive microorganisms, which allows for effective leaching of cations, iron oxides, aluminum oxides and colloidal clays during the summer months (Hess & Tasa, 2014).

The resulting soils are shallow and acidic. They are characterized by an A horizon that is of a silty or sandy texture and leached to an ashy, light gray color, while the B horizon receives the leached iron oxides and clay minerals which give him a darker color (fig. 10). Podzols are characterized by low fertility and a crumbly structure susceptible to erosion (Hess & Tasa, 2014).

Figure 10 Outcrop found in the study area, depicting a shallow, silty and grey A horizon, followed by a darker B horizon.

Due to pronounced winters freezing the subsoil temporarily or permanently (Bone, 2011) and glacial derangement during the recent Pleistocene ice age, the boreal forest shows poor deep drainage. Thus, bogs and fens are frequent and the ground very moist to spongy in the summer months after precipitation events (Hess & Tasa, 2014). The most common soils underlying bogs and fens are organic soils, in varying stages of decomposition and with different amounts of resistant fibres in percent by volume (Downing & Pettapiece, 2006).

3.4 Disturbance Regime

Disturbance regimes determine the structure of forests in multiple ways. The following sections explain the distinct disturbance regime in the AoI. Anthropogenic disturbance in the AoI is of special importance.

3.4.1 Anthropogenic Disturbance

Oil exploration in northern Alberta dates back to the 19th century. The most decisive oil discovery, however, took place in February of 1947, when Imperial Oil discovered a large reservoir of oil in Leduc, just south of Edmonton. The drilling of the first Leduc oil well, called Imperial Leduc Number One, arguably turned Alberta into the oil province it is known as today. Within just one year, large-scale exploration for petroleum picked up, with 131 more oil wells taking up operation in Leduc and 888 wells in Redwater. The Pembina field supplied more than one thousand wells (Hardy, 1967). Once exploration showed that much of the province's ground was underlain by vast petroleum deposits, it was only a matter of time until oil was exploited in the study area. Cenovus Energy started the Christina Lake project in 2000, located 35 km from the study area. Using steam-assisted gravity drainage (SAGD) technology to extract bitumen *in situ* from 375 m underground. Christina Lake currently produces 210,000

barrels of oil per day and further expansions have been approved, which will add another 50,000 barrels of oil per day starting in the second half of 2019 (Cenovus 2018).

Seismic lines are a result of systematic scanning for oil (Downing & Pettapiece, 2006). To detect underground bitumen, corridors are cut into the forest in a grid-like pattern, creating so called "cut lines". Depending on the depth of the underground oil layer, seismic lines are typically between 100 and 1000 m apart, with larger distances if the oil is located deeper underground. The width of the lines usually depends on the machinery used for the drilling of shot holes. In treed areas such as the study area, cut lines are typically created by heavy bulldozers. They present a width of up to eight metres and follow a meandering course (Severson-Baker, 2004). The so-called "low impact seismic lines" (LIS), which are as little as ca. 2 m wide (EMR, 2006), are the minority of the seismic lines found in the study area. Most lines (except wide transportation lines) in the study area are approximately 5 m wide. Once the seismic line is completed, geophones are laid out along the line to record the sound waves. These are created in two ways:

1) Explosives placed in holes drilled in the ground or

2) Vibrations created by heavy plates on the ground.

Before explosives can be used, holes (so called shot holes) up to 20 m deep must be drilled in the ground until the surveyors find a layer of wet shale or mud which transports the sound waves better than sand or silt. These holes are created between 20 and 120 m apart. The explosives are then placed at the bottom of the holes and detonated. Alternatively, and especially on flat terrain, truck mounted surface vibrators can be used ("vibroseis"). The soundwaves then propagate through the soil, passing through various soil compositions and rock formations at different speeds, until they are reflected by a formation. This reflection is then recorded by geophones, receivers strategically placed along the seismic lines. The signals are transmitted to a computer which transforms them into information on the depth and type of the rock formations (Severson-Baker, 2004).

Usually, a 2-dimensional seismic assessment is conducted first. Should this initial exploration produce promising results, the receiver lines (consisting of geophones connected to each other) and shot lines may be laid out in a perpendicular fashion, resulting in a 3-dimensional image of the underground soil formations (Riva et al., 2018; Severson-Baker, 2004).

In recent years, some of these lines have been treated to facilitate regrowth of vegetation by planting seedlings, for example by erecting mounds of roughly 1 m^3 on which to plant trees to avoid their roots to grow in the high ground water. However, if left untreated, seismic lines in the study area present mostly grass as the dominant regrowth vegetation, mixed with an assortment of berries, Labrador tea and grasses (fig. 11, lower left).

Figure 11 Stages of regrowth vegetation on seismic lines in the study area. Upper left: grass as the sole regrowth vegetation. Lower left: medium density regrowth vegetation with shrubs, a thick layer or Labrador tea, and young trees. Right: Very dense regrowth vegetation.

Dirt roads, camps for oil workers, and well sites are not treated with the purpose of enhancing regrowth vegetation and thereby do not show any vegetation growth at all. Given that the emphasis of this study is the examination of the human impact on the boreal ecosystem, these disturbances were included in the definition of openings (fig. 12).

Figure 12 Left: Clearing of a well site. Right: Dirt road and adjacent clearing with small regrowth vegetation (grasses and flowers).

3.4.2 Natural Disturbance

Out of all natural disturbances able to cause the opening of a canopy opening, forest fires and insect infestations are among the most prolific (Timoney, 2003). Forest fires are an

important part of the natural forest stand development cycle (fig. 3). Further, insect infestations and limb fall can cause openings in the canopy cover. Increases in frequency, duration and/or severity of drought during the summer months and climate change associated heat stress puts the vegetation of the boreal forest under immense added physiological pressure and raises vulnerability for disturbances like insect infestations. Altered structure could also lead to more frequent natural tree death and snow destruction (Allen et al., 2010).

Due to the high moisture content in soil and vegetation, many, especially deciduous trees like birches and poplars, were discovered to be rotten inside even when they were showing a seemingly healthy canopy crown. On more than one occasion on a windy day during the field work, birch trees of 30 m in height broke in half, leaving a new opening in the canopy cover. Figure 13 illustrates the heart rot that had befallen a large birch tree in the AoI. Mature trees could be felled by the force of one person due to the weak physiological structure of the trees.

Figure 13 Mature birch trees could be broken easily by the force of one person. This demonstrates the heart rot and thus vulnerability for natural canopy openings at some of the tree stands AoI.

3.5 Definitions of Forest and Openings

Forests consist of trees growing close together so that their individual canopies generally overlap and create one interlaced closed canopy cover. The woodlands found in the bogs and fens of the AoI, while tree dominated, constitute plant associations without a closed canopy. Consequently, their undergrowth is not characterized by a lack of sunlight (Hess & Tasa, 2014). Given the diverse nature of the study site, which includes coniferous and deciduous trees as well as upland and wetland vegetation differing significantly in height and tree density, this study's definition of forest includes both low tree density wetlands characterized by small and sparse vegetation growth, as well as high tree density uplands with their typical dense birch, poplar and spruce tree stands. Further, there will be no differentiation made between single-

trunk trees and multiple-stem shrubs. The sole determining factor of forest classification will be vegetation height.

Chapter 2.1.1 presents the various definitions presented by scientific literature of *functional* openings, i.e. openings with the described ecological impacts on the local ecosystem and including vegetation forms like saplings up to 2 m. In contrast, this study aims at assessing the accuracies with which six different approaches detect *structural* openings in the AoI.

Runkle (1992) acknowledges the existence of areas that are permanently free of trees due to edaphic factors such as soil, bedrock or biological conditions. These areas may resemble openings in their attributes like species composition, structure and biological function, but not in their generation or their ecological dynamics. For example, the lowlands' understory, due to their low tree density, is not deprived of sunlight. One of the most prominent changes taking place after the opening of an opening, however, is the sudden increase in light supply on the ground. Given that the low-lying wetlands do not experience a stark, sudden change in light supply. In this study, they will be regarded as *structural* openings, which are detectable by means of remote sensing. The definition of structural openings in this study considers the space between stems of a forest's trees. *Functional openings* are considered as the ecological effects any form of opening in a forest canopy has on the local ecosystem and correspond roughly with Runkle's (1992) concept of expanded opening. However, it is to be noted that even functional openings should not be defined by their size, shape or setting, but rather be viewed through the lens of the species that are affected by them.

To identify openings in-situ, the following definition of opening was formed: structural openings in the canopy cover, which may vary in height and density, with no defined minimum or maximum extent, and a maximum height of regrowth vegetation that is 1.3 m or 25% of the surrounding maximum canopy height. The lack of a definition of minimum extent allows for the examination of ALS' and DAP's abilities to detect even very small openings in the canopy cover, though significant ecological impact such as tree regrowth is only to be expected in larger openings, starting at 50 m^2 (Bonnet et al., 2015). No upper limit was determined for the spatial extent to include large-scale anthropogenic disturbances such as networks of seismic lines, roads and pipeline clearings, which are part of the AoI's disturbance regime. The 1.30 m/25 % height limit was chosen to include even small-growth established tree vegetation in the wetlands and will be further discussed in chapter 6.1.1.4.2.

4 Data

Orthoshop Geomatics Ltd provided both the ALS and DAP data used in the study. The data was acquired by sensors mounted on a Cessna 210T during leaf-on (early May) and leaf-off (early August) seasons in 2017. Flying altitudes were approximately 850 m above ground and acquisition was timed in a fashion that aimed at minimizing negative effects of shadows and occlusions.

4.1 Airborne Laser Scanning Data

The ALS data used in this study was acquired in August 2017 using a Leica ALS70-CM sensor at a flying height of approximately 850 m above ground (table 1). The total amount of point records is 43,657,212. Average point density is 40 points/m^2 and point spacing was 0.15 m.

Table 1 ALS data acquisition parameters.

Parameter	Description
Sensor	Leica ALS70-CM
Aircraft speed	130 knots
Swath Width	550 m
Maximum Scanning Angle	35°
Beam divergence	0.2 mrad
Wavelength	1064
Flying altitude	850 m a.g.l.
Pulse Repetition rate	Max. 500 kHz
Overlap	60 %
Scan frequency	158 Hz
Number of returns per pulse	2
Point density	40 points/m^2

4.2 Photogrammetry Data and Multispectral Orthomosaics

DAP data were acquired using a Leica RCD30 digital camera with forward motion compensation and an 83 mm lens. Maximum pixel resolution was 0.055 m. More than 5000 photographs were generated on each of the two acquisition periods. The acquisition was conducted during diffuse light conditions to limit shadows in the area of interest to <20% (table 2). The data was subsequently processed into photogrammetric point clouds using Pix4D software and applying a minimum number of matches of 3, with a point density of > 270 points/m^2 and point spacing of 0.06 m. Additionally, multispectral (RGB+NIR) orthomosaics with a spatial resolution of 0.05 m were derived.

Table 2 DAP acquisition parameters.

Parameter	Description
Sensor	Leica RCD30 digital camera, 83 mm lens
Flying altitude	850 m a.g.l.
Spectral resolution	R, G, B, NIR
Maximum pixel resolution	0.055 m
Along track overlap	80%
Across track overlap	60%
Image acquisition Leaf Off	May 2017
Image acquisition Lead On	August 2017
Point density	270 points/m^2

5 Methods

The following chapter provides an overview of the methods applied in this chapter. This includes the processing steps of 3D data, the field campaign and validation data design, as well as gap classification.

5.1 Opening Detection

This study aims at classifying structural openings. Openings are defined based on the vegetation height at a given point, rather than optical signals. The steps of this process are described in the following sections.

5.1.1 3D Data Opening Detection

For opening detection based on 3D data, as provided in the form of ALS and DAP point clouds, a CHM must be generated. CHMs are traditionally produced by simply subtracting the DTM from the DSM of a given area (White et al., 2018; fig. 14), which results in the normalization of the DTM.

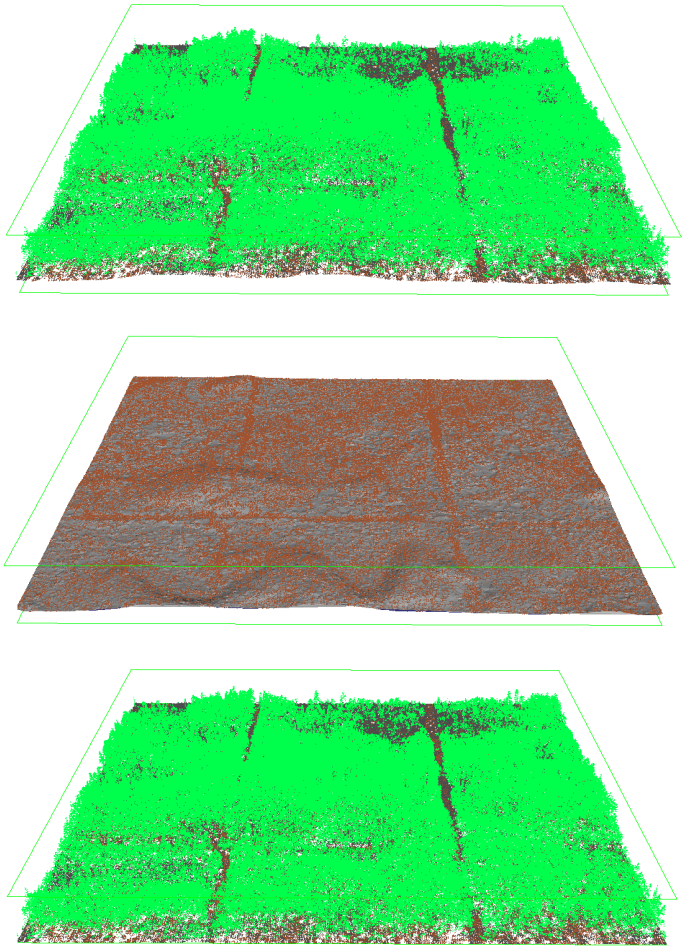

Figure 14 The three components required for the traditional derivation of a CHM (bottom) via subtraction of the DTM (middle) from the DSM (top).

In previous studies, the DTM used in combination with a DAP derived DSM (DSM_{DAP}) was either generated from an ALS dataset (White et al., 2018) or from the Shuttle Radar Topography Mission (SRTM). Both technologies possess the ability to penetrate layers of foliage and classify ground returns reliably (Jet Propulsion Laboratory, 2018). On the other hand, DAP point clouds are based on aerial optical imagery and can only reach the ground, and classify it as such, where the ground is openly visible from the position of the sensor (Holopainen et al., 2015). Thus, applying an ALS derived DTM (DTM_{ALS}) when using a DAP derived DSM (DSM_{DAP}) is appropriate (White et al., 2018).

In this study, an exceptionally high density point cloud was generated from the DAP data. To test if a CHM derived from DAP data only (CHM_{DAP}), e.g. by subtracting a DAP derived DTM (DTM_{DAP}) can produce reliable outcomes regarding opening classification, CHM_{DAP} was produced (DSM_{DAP} – DTM_{DAP}) in addition to the traditional (White et al., 2018) CHM_{ALS} and CHM_{hybrid} (fig. 15). As will be explained in chapter 6.1.1.2, a different approach regarding the derivation of CHM_{ALS} will make the step of manually producing a DSM_{ALS} superfluous. The grey visualization in figure 15 displays the traditional generation of a CHM_{ALS}, whereas the solid lines represent the process chain applied in this study.

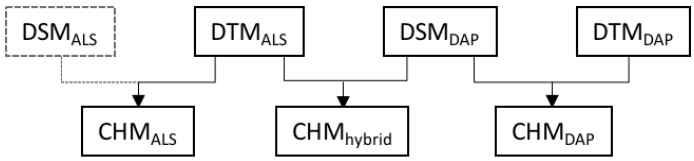

Figure 15 The derivation processes of the three CHMs produced in this study.

It is important to note that the DSM_{DAP} was derived from a DAP data set acquired in August 2017, representing the study site with a full canopy cover. This allowed for a high-density point cloud showing the top of the canopy (LeafOn). The DTM_{DAP}, on the other hand, was derived from a DAP point cloud acquired in May 2017, representing the forest after the deciduous trees had lost their leaves (LeafOff; Appendix A). This allowed for a better ground classification as the ground can be seen in more areas that would otherwise be covered by foliage.

5.1.1.1 LAStools

All three products (DTM, DSM and CHM) were derived from each data set (ALS and DAP) by a workflow using the LAStools tool set. LAStools is a collection of batchable, multicore command line tools developed by rapidlasso GmbH. Each tool was developed to execute one processing step (Isenburg, 2018). The steps in the processing chain were altered for the individual data sets to accommodate for the differences between ALS and DAP data (fig. 17 and 20). The batch scripts can be found in Appendix B.

5.1.1.2 Processing of ALS Data

Before starting the processing chain, lasinfo determines if the ALS data set conforms to the LiDAR (LAS) 1.0 and 1.4 specifications (e.g. Coordinate Reference System (CRS) Representation, Offset to point data, point data record format, number of points per return) issued by the American Society for Photogrammetry and Remote Sensing (ASPRS). If the automatically generated validation report results in “PASS” (as opposed to “WARNING” or “FAIL”), the processing of the files can begin.

Various parameters must be set in the initial stage. They will be discussed in the context of the tools in which they are applied.

1) Lastile: produces manageable tiles from the raw data set
    a. *tile_ size*: 250 m.
    b. *buffer*: avoids fringe artifacts such as sliver triangles when triangulating between points (set to 10 m).
2) lasnoise: classifies isolated points as noise
    a. *step_ xy* and *step_ y* were kept at default values. This step is complemented by manual classification later in the chain.
3) Lasground_new: classifies ground points
    a. *spike*: threshold in meters vertically from the triangulated ground area at which spikes get removed (set to 0.3).
    b. *wilderness*: results in a step size of 3 meters to include smaller features on the ground.
4) lasclassify: classifies vegetation, buildings etc.
    a. *small_ trees*: recognizes overly small trees.
    b. *small_ buildings*: recognizes overly small buildings (such as well site buildings and pipelines).
5) lasheight: produces a normalized point cloud (height above ground)
6) las2dem: produces DTM tiles
    a. *keep_ classification*: triangulates points classified as ground (class 2) for DTM.
    b. *first_ only*: keeps first returns only for DSM.
    c. *use_ tile_ bb*: eliminates buffer points.
    d. *elevation*: rasters the elevation of each pixel.
7) lasthing: places uniform grid over data set and thins the data set for a given criterion
    a. *highest*: keeps highest value in each 0.2 x 0.2 m cell
    b. *subcirc*: thickens data set by replicating each point 8 times in a discrete circle with a radius of 0.1 around every original input point to simulate the laser beam width
8) blast2dem: reads large ALS datasets, triangulates seamlessly and projects triangulation onto DEM.
    a. *Drop_ z_ below*: drops elevation value below (or above) a certain value (0)

The result of the preprocessing batch depicted in the grey box in figure 17 are classified 3D point clouds (fig. 16). Their classifications include vegetation, ground, power lines and buildings. Noise (outliers in extreme heights) was not flagged as such but deleted from the data set.

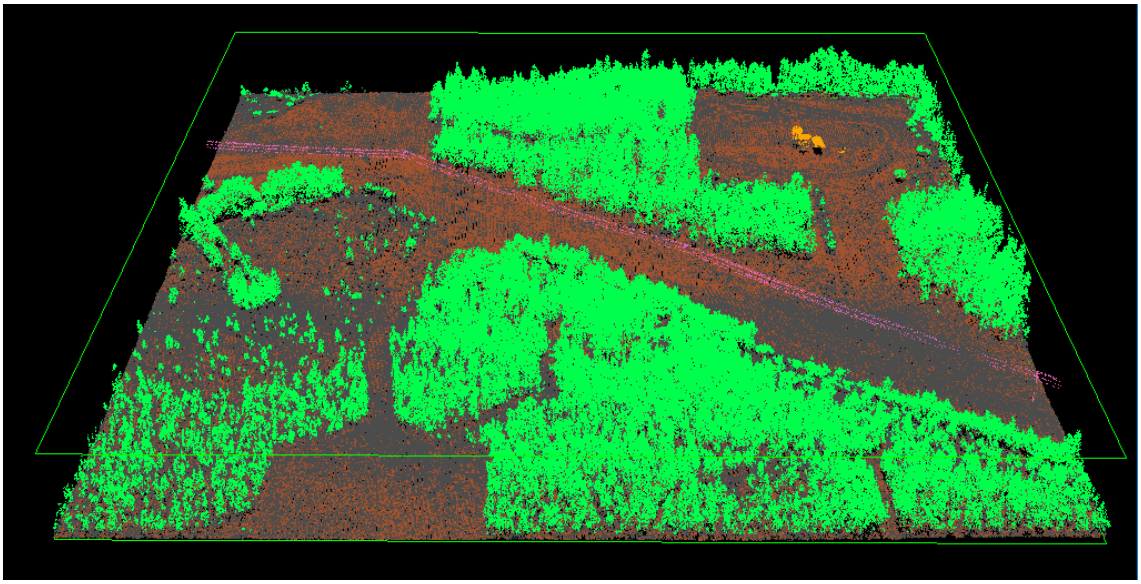

Figure 16 Classified ALS point cloud from the AoI, depicting ground points (brown), ground triangulation (grey), vegetation (green), power lines (pink) and buildings (orange).

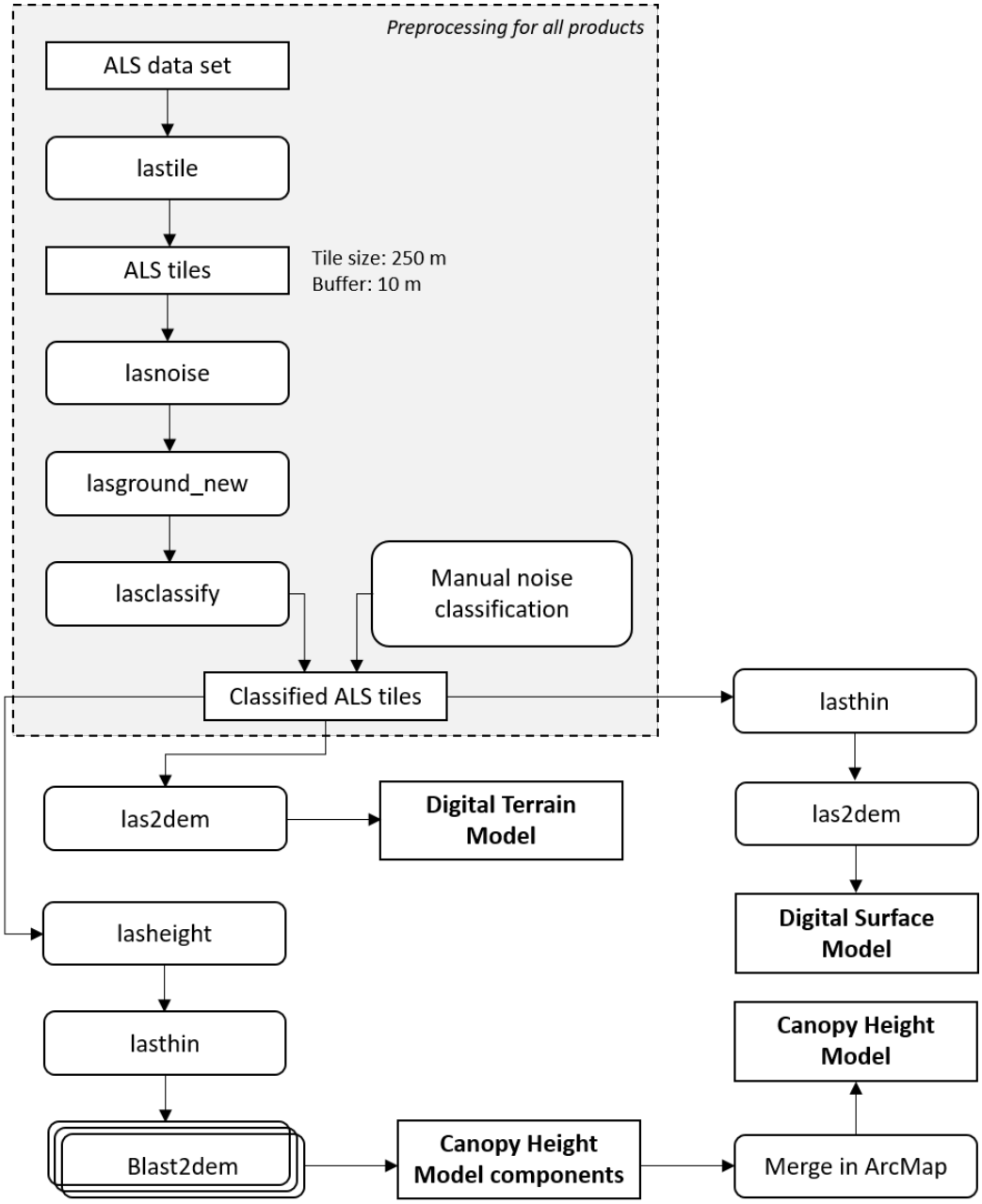

Figure 17 The processing chain for the ALS data set. The first batch of tools is applied to generate all three models (DTM, DSM and CHM). The DTM is the first product, which can be derive immediately after this first batch. The generation of the DSM requires a thinning of the point cloud prior to triangulating the first returns. The CHM is generated by producing several DSMs using points above five different minimal height above ground values (0m, 5 m, 10 m, 15 m and 20 m). This way, needle shaped triangles to the ground and the omission of canopy cover points will be avoided in the triangulation process. The resulting components are subsequently merged in a different GIS software, e.g. ArcMAP.

Traditionally, CHMs have been generated as shown in figure 14. To derive a DSM, first returns only are usually used to interpolate the surface of a DSM. This procedure is based on the assumption that first returns reflect the highest return point. Using a 2D Delaunay triangulation, the interpolating surface and the resulting Triangular Irregular Network (TIN) is rasterized onto a grid and stored as a DSM (Isenburg, 2016). However, Isenburg (2016) notes two critical drawbacks of the first return interpolation for DSM generation.

1) Important details are missing when using first return information only (fig. 18). This especially affects off-nadir scan angles in traditional airborne surveys, where the laser

beam is interrupted by foliage and cannot reach lower lying, laterally offset points. These points would warrant a first return when hit from straight above, but off-nadir scan angles and clouds can hinder the laser beam propagation and lead to misclassifications (Isenburg, 2016).

2) Needle shaped triangles (fig. 18) will result when every first return is considered in the triangulation. Some first returns might be situated underneath a layer of foliage that was not detected due to an off-nadir scan angle or through very small openings in the canopy surface.

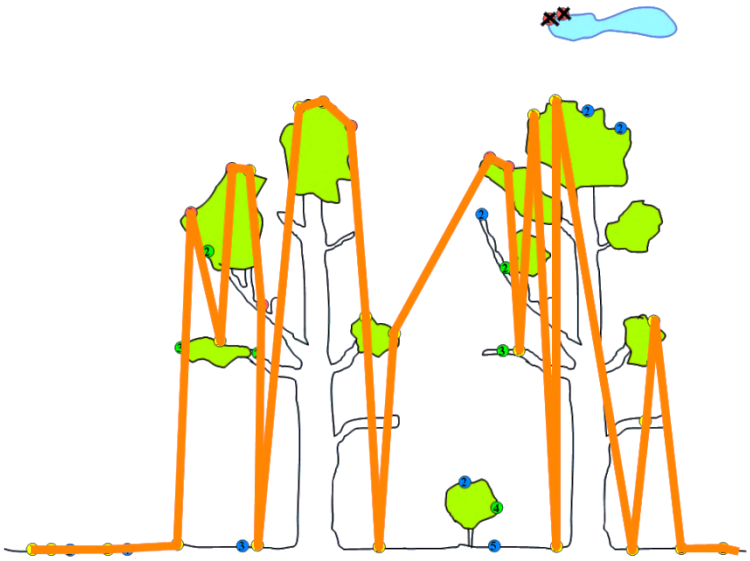

Figure 18 Needle shaped triangles resulting from interpolating all first returns. In addition, some parts of the canopy are missing because they were not recorded as first returns. The different colored dots identify first, intermediate and last returns (Isenburg, 2016).

These drawbacks can be mitigated in the following way. After thinning the data set so that it only contains the highest point in each 0.2 x 0.2 m grid cell and adding several points around each input point to simulate the laser beam width using lasthin, five iterations of blast2dem were applied. The first one considering every return after the thinning step, the second one containing every point above a height of 5 m above the ground, the third one containing every point above a height of 10 m, then 15 m, and finally 20 m. This way, all the highest returns were considered and omissions of detail can be minimalized, and first returns which are situated underneath the canopy were not considered to be part of the canopy surface (Isenburg, 2016). The resulting DSMs or CHMs are expected to represent the canopy height as shown in fig. 19.

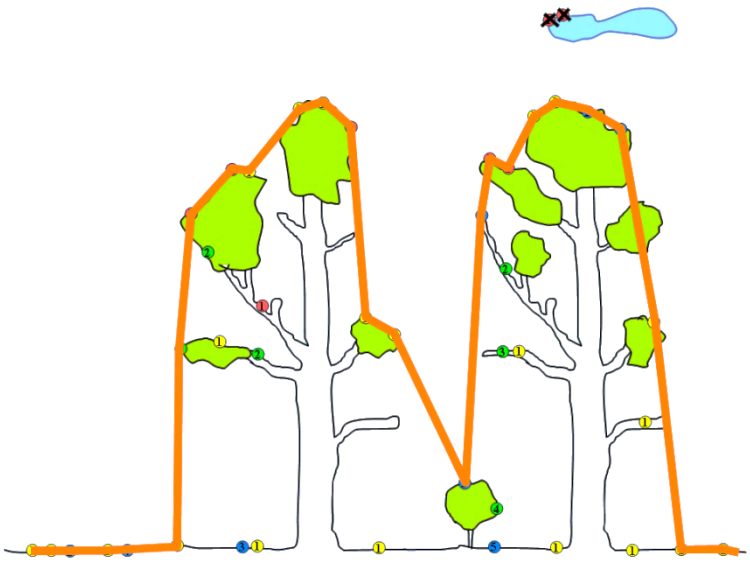

Figure 19 Spike free DSM. Expected result after assembling partial DSMs for different minimal heights, thus each considering the highest possible points in the DSM generation process (Isenburg, 2016).

5.1.1.3 Processing of DAP Data

Due to the nature of DAP data collection, which differs from the penetrating active remote sensing technique that is LiDAR, some steps in the processing chain had to be altered to fit the features of photogrammetric data.

As can be seen in figure 20, which shows the general workflow for a DAP data set, two alterations had to be implemented in the ground classification. Since DAP data does not possess the ability to penetrate layers of biomass, and can thus only triangulate the points where the ground is bare and openly visible from above, two changes were made:

1) lasthin was added before classifying the ground to thin the data set to only include the lowest points:
    a. *step*: set grid cell size to 0.5 x 0.5 m.
    b. *lowest*: thin dataset to include the lowest point in each grid cell.
2) lasground_new:
    a. *step*: set to 10 m to allow for a coarse triangulation and interpolation over longer distances between the ground points.
    b. *spike*: threshold at which spikes get removed, set to 0.1.
    c. *offset*: maximal offset in meters up to which points above the current ground estimate get included, set to 0.1.
    d. *bulge*: specifies how far the current ground estimate may bulge upwards or downwards in order to include points above or below the current ground estimate, set to 0.1.
    e. *extra_coarse*: setting for very flat terrains.

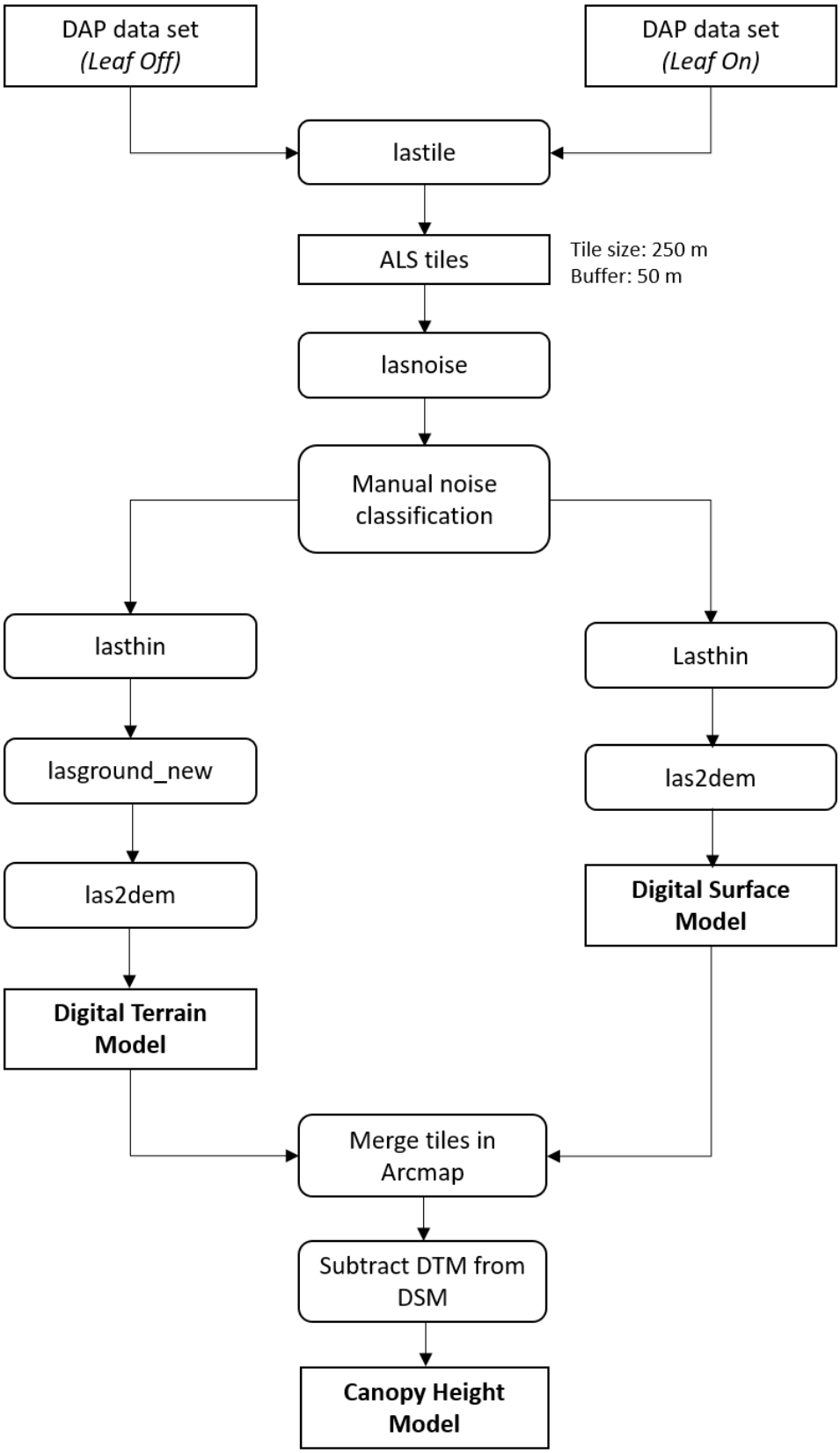

Figure 20 Processing chain for DAP data.

Another alteration should be implemented in the generation of the DSM_{DAP}. A different set of challenges presents itself with DAP data. DAP technology is not able to penetrate the canopy cover and thus cannot produce first, intermediate and last returns, which would be used in the derivation of DSMs and DTMs. For the derivation of DSM_{DAP}, which characterizes

the forest canopy and vegetation structure, the LeafOn data set is thinned to only contain the highest points in each 0.2 x 0.2 m grid cell and these points are consequently broadened into discs with a radius of 0.2 m. Subsequently, the data set is rasterized into a DSM.

As noted earlier, another difference to the ALS process chain is the differentiation between two data sets (LeafOn and LeafOff) for the purposes of deriving the DSM_{DAP} and the DTM_{DAP}, respectively. By deriving the ground classification from the LeafOff data set, and the canopy classification from the LeafOn data set, the two will have to be combined later as shown in figure 15. By subtracting the DTM from the DSM, the CHM_{DAP} is generated. This process is naturally based on meticulous georeferencing of both point clouds.

5.1.1.4 Opening detection using Canopy Height Models

Once the CHMs are retrieved from the data sets, further processing continues without differentiations made between the data sets and the different models. The two most common approaches for deriving openings in CHMs (Gaulton & Malthus, 2010; White et al., 2018) are the Fixed Height Approach (FIX) and the Variable Height Approach (VAR). Both approaches depend heavily upon the structure and features of the ecosystem at hand and should be adjusted by the user as needed. Both the FIX approach as well as the VAR approach were conducted for each of the three CHMs for comparison of outcomes between the data sets and the two opening detection approaches.

5.1.1.4.1 Fixed Height Approach

For the fixed height approach, the minimum height of a given piece of vegetation, above which it is not considered regrowth vegetation but rather established vegetation, must be determined. Given the presence of large boggy, swampy patches in the study area, which result in small plant growth, this threshold had to be small enough to include short yet mature and established coniferous vegetation growing under these adverse conditions. It was determined that a pixel of the CHM should be considered an opening if the value was less than 1.30 m. Thus, vegetation below a height of 1.30 cm was considered regrowth vegetation or structural opening, whereas vegetation above this threshold was considered established vegetation, as it is mostly safe from ungulates (Downing & Pettapiece, 2006). This includes small growth established vegetation in the wetlands, as well as vegetation in the early stages of maturity in the drier uplands. No differentiation between trees and other forms of vegetation, such as shrubs, was made. The resulting map shows “opening” where height of vegetation is ≤ 1.30 m and “no opening” where height of vegetation is > 1.30 m.

5.1.1.4.2 Variable Height Approach

The variable threshold considers the surrounding area and classifies each pixel as “opening” or “no opening” depending on the average canopy height surrounding it. The method applied here is based on the technique presented by Gaulton and Malthus (2010). Here, two values must be determined. The first is the variable height threshold. This value indicates the height which a given piece of vegetation must have in comparison to the surrounding canopy cover height for it to be considered regrowth vegetation or no vegetation (opening) or established vegetation and thus part of the canopy cover (no opening). Gaulton and Malthus (2010) use the ratio of canopy drip line to canopy height to derive this threshold. The relative height of the canopy drip line is applicable in the ecosystem of Sitka spruce plantations in the UK as examined by Gaulton and Malthus (2010), however, most vegetation at the study site in question is

characterized by black spruce rather than other coniferous trees. In contrast to pine trees, for example, black spruces depict a very different growth structure, which is characterized by their branches growing vertically distributed along the trunk rather than branches forming a distinct bulk of foliage at the upper half of the tree. This makes it difficult to determine a relative height of canopy drip line (fig. 21).

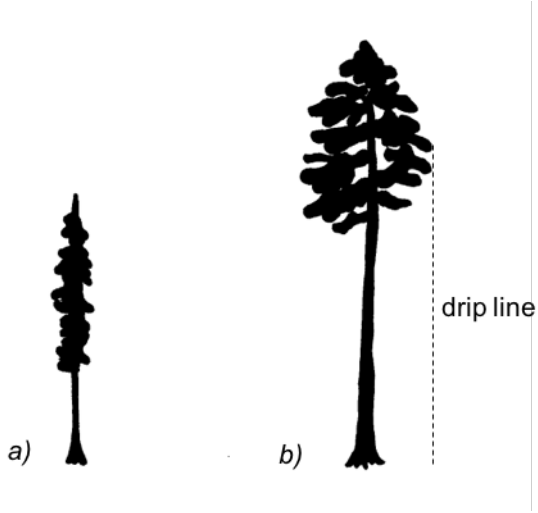

Figure 21 Schematic depiction of silhouette of the majority of trees found at the study (a) vs silhouette of mature pine trees (b).

Given the distinct vegetation structure of the boreal forest and the great heterogeneity within the vegetation, a different approach of determining the variable height threshold was used. Coming back to the issue about taking even very small growth established vegetation into consideration, a threshold of 25% was chosen for the variable height approach. This is a much lower value than used by Gaulton and Malthus (2010) and White et al. (2018), however, after an in-situ assessment of the vegetation structure in the study area, it became clear that the forest is too heterogeneous in height and structure to apply a higher threshold and still classify small trees as tree vegetation.

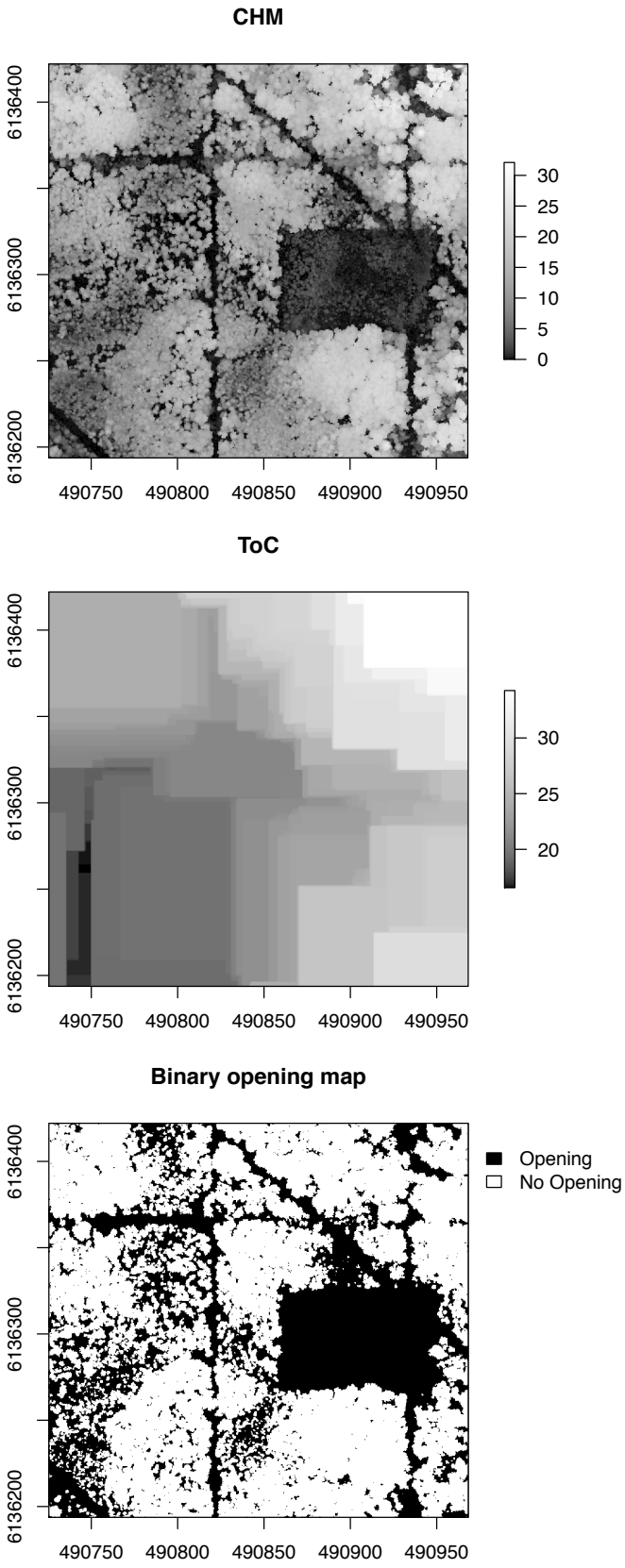

*Figure 22 Process of deriving a binary map of openings using the variable height approach. Left: The original CHM. Middle: Top of Canopy Layer, depicting the maximum values of the CHM in a 100 x 100 m moving window. Right: The resulting binary map of openings in the canopy, showing openings in white and canopy in black. Openings are areas where ToC * 0.25 < CHM.*

In order to take the surrounding area into account, a new layer was created, representing the Top of Canopy (ToC). This was achieved by applying a moving maximum filter in a 100 x 100 m (500 x 500 pixel) window to the CHM. The window size had to be slightly larger than the largest clear cut area (95 m across) so that the ToC would not dip within these areas characterized by a low average vegetation height and make them undiscernible in the subsequent analysis. At the same time, the window size had to be small enough to consider the height variations between the various tree stands. For example, upland spruce stands in the study area are characterized by a higher vertical vegetation growth than wetland conifers and a smaller height than birch tree stands. In the next step, each pixel in the CHM was classified as "opening", if the CHM value was ≤ 25 % of the corresponding pixel in the new ToC layer. Conversely, if the CHM pixel value was > 25%, the pixel was classified as "non-opening" (fig. 22).

5.2 Validation of Opening Detection

Validation data was derived from in situ sampling during a field campaign in July of 2018 (fig. 26). The process of stratification and determining the appropriate amount and location of the sample points shall be discussed in the following sections. The details of the in-situ sampling are presented in the field plan which can be found in the field plan (Appendix C).

5.2.1 Sampling Design

This study focusses on the impact of anthropogenic disturbances on the boreal forest ecosystem. Canopy opening patterns differ vastly between areas that were previously disturbed by human interference versus area that have been untouched by human. To make sure that these differences are considered and adequately sampled, the first stratification step had to include the differentiation between a) areas that were impacted by human disturbances, and b) areas that were left at their natural state. Another emphasis of this study is the comparison of accuracy of various approaches regarding different size openings. It is to be expected that the accuracy of opening detection will vary especially between very small and very large openings. To find out the relative accuracies for different opening sizes, a second level was introduced, referred to as Opening class. Thus, the study area was stratified into two levels:

1) Disturbed vs. undisturbed areas in the study area
    a. Altered areas are defined as altered by human influence such as clear cuts, seismic lines, roads etc.
    b. Natural areas are defined as the inverse areas of the altered areas stratum
2) Opening (size) class
    a. Opening class 0: No Opening
    b. Opening class 1: 0 – 4 m^2
    c. Opening class 2: 4 – 20 m^2
    d. Opening class 3: 20 – 200 m^2
    e. Opening class 4: > 200 m^2

For the first stratification level, disturbed areas were identified based on visual interpretation of the LeafOn Orthomosaic and the CHM_{ALS} (fig. 23). Based on literature review (White et al., 2018), the fixed height approach on CHM_{ALS} (ALS_FIX) was expected to deliver the highest accuracy of opening classification and therefore offered the best base for validation data stratification.

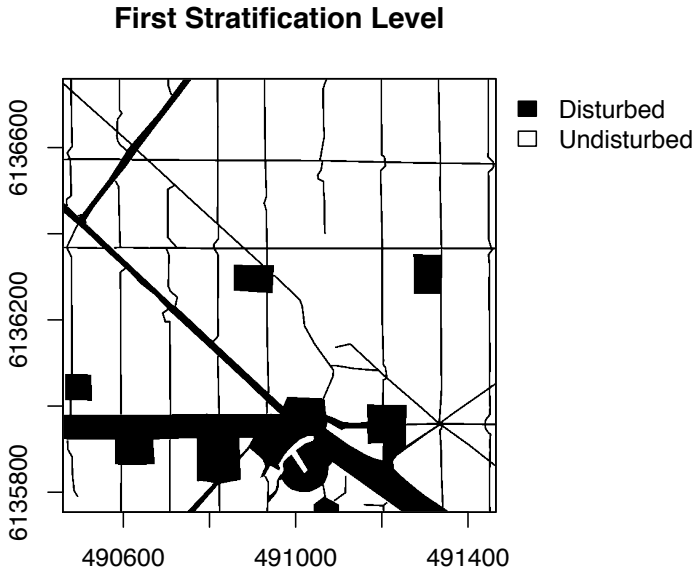

Figure 23 Mask of disturbed and undisturbed areas in the study area.

While the spatial accumulation of all edges should be included to determine the total effect of the human influence on the study area, they were not considered in this step. Edge effects can magnify the influences of human disturbance on physical and chemical conditions, plant growth, plant community composition, wildlife behaviour and the interactions between these factors on a much greater scale than the actual disturbance itself (Dabros et al., 2018). However, since edge effects have different ranges in which they influence a given site, and these ranges cannot be determined in the framework of this thesis, edge influences are neglected in the delineation of anthropogenically disturbed areas.

Within these areas (altered vs. natural), the second stratification level was determined by size class. Class 1 represents openings that are not included in common definitions of functional openings due to their small size limiting a significant increase of PAR on the ground. It was nonetheless included in this study to examine LiDAR's and photogrammetry's ability to detect even very small structural openings in the canopy cover. Size classes 2, 3 and 4 were chosen on the criterion to be easily distinguishable by the surveyor in the field. Traditionally, very large openings like seismic lines, which are part of a bigger opening system, would not be included in the traditional definition of functional opening, however, in this ecosystem, seismic lines and clear cuts are a critical part of the disturbance regime and thus had to be included in the definition of structural opening.

In the opening map derived from ALS_FIX, within each size class stratum, the appropriate number of sample points was determined based on the opening size variability, using equation 2 (Kershaw et al. 2016).

$$n = \frac{t^2 CV^2}{E^2} \quad (2)$$

where

n = number of points required for desired precision E, with the probability level implied by the value of t

t = Student's t (in this case Z-test)

CV = coefficient of variation (in percent) for the opening size sampled

E = allowable error or desired precision (in percent) for the average area.

To apply this equation, first, the variation in size of the openings in each size class was calculated to determine CV. Next, we applied a confidence level of 80%, which resulted in 1.3 for the Z Value (Student's t) and 20% for the corresponding allowable error (E). n depended on the variability of opening sizes within each size class. As was to be expected, non-opening areas (class 0) showed a very high CV in size which resulted in a high number of samples. However, given that the focus on this study is the detection of openings rather than non-openings, the sample size was reduced to 100 for non-openings in altered areas and to 300 for non-openings in natural areas. These sample sizes reflect the ratio of 1:3 of the proposed sample sizes derived from equation 2. Furthermore, to strengthen statistical reliability, sample size for size class 2 in the natural areas was raised from 26 to 30. This resulted in a total of 1835 sample points (table 3).

Most sample sites were measured in-situ. Where access to a sample site was impossible due to safety concerns, or where the surveyor had low confidence in the correctness of the classification, visual image interpretation based on the LeafOn orthomosaic was conducted to fulfill the required sample size and confidence of the validation data set. The distribution of the sample sites in the AoI is presented in figures 24 and 25.

Table 3 Sample sizes of each stratum. Originally derived sample sizes that had to be changed are given in parenthesis.

			N for each Size Class in Stratum "Altered"					N for each Size Class in Stratum "Natural"				
Conf. Level	Z	E	0	1	2	3	4	0	1	2	3	4
80%	1,3	20	100 (2940)	116	36	69	396	300 (8399)	102	30 (26)	104	582

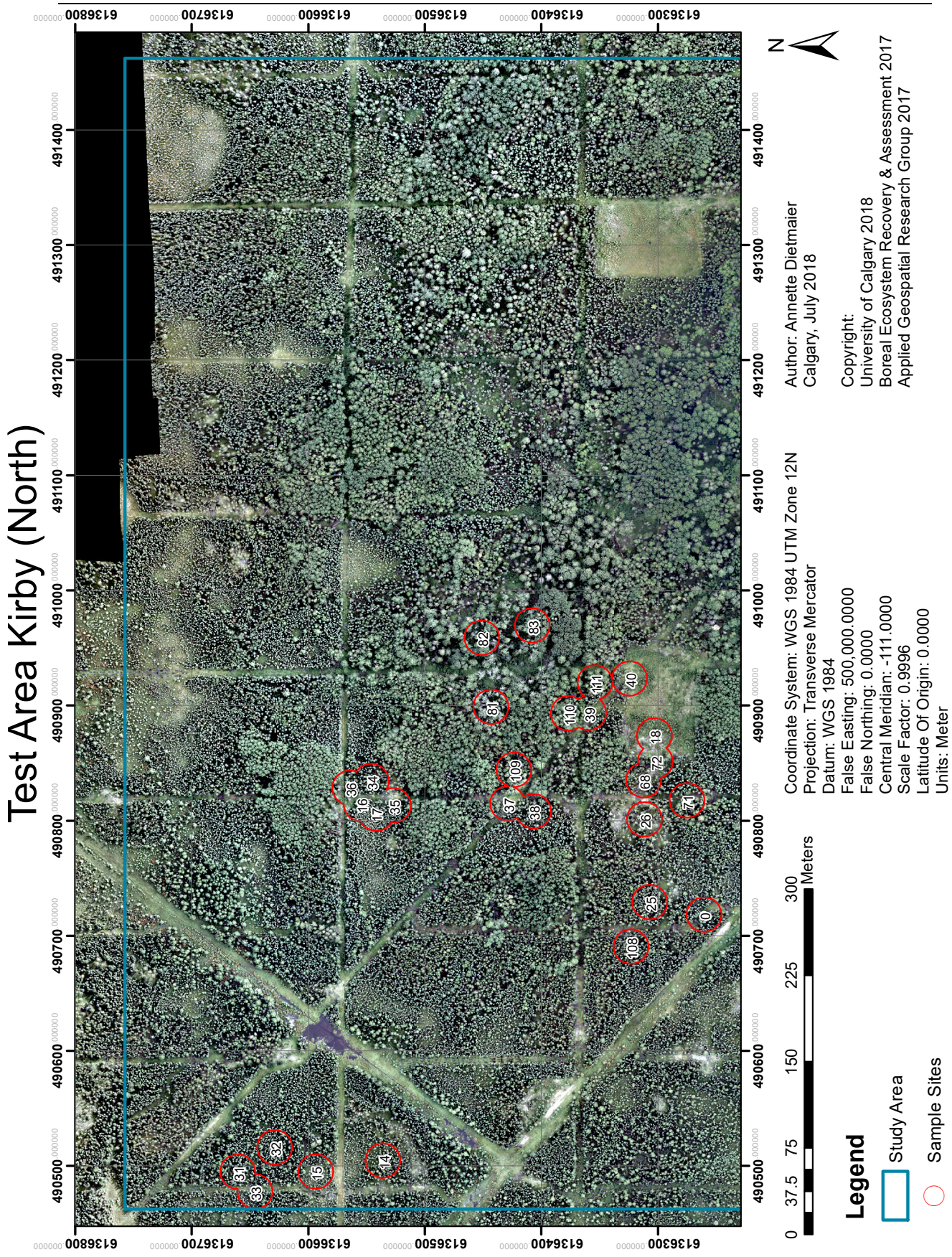

Figure 24 *Field map of the AoI Kirbe (northern part) with the sample site which contained the sample points visited during the field campaign. The individual sample points are not depicted.*

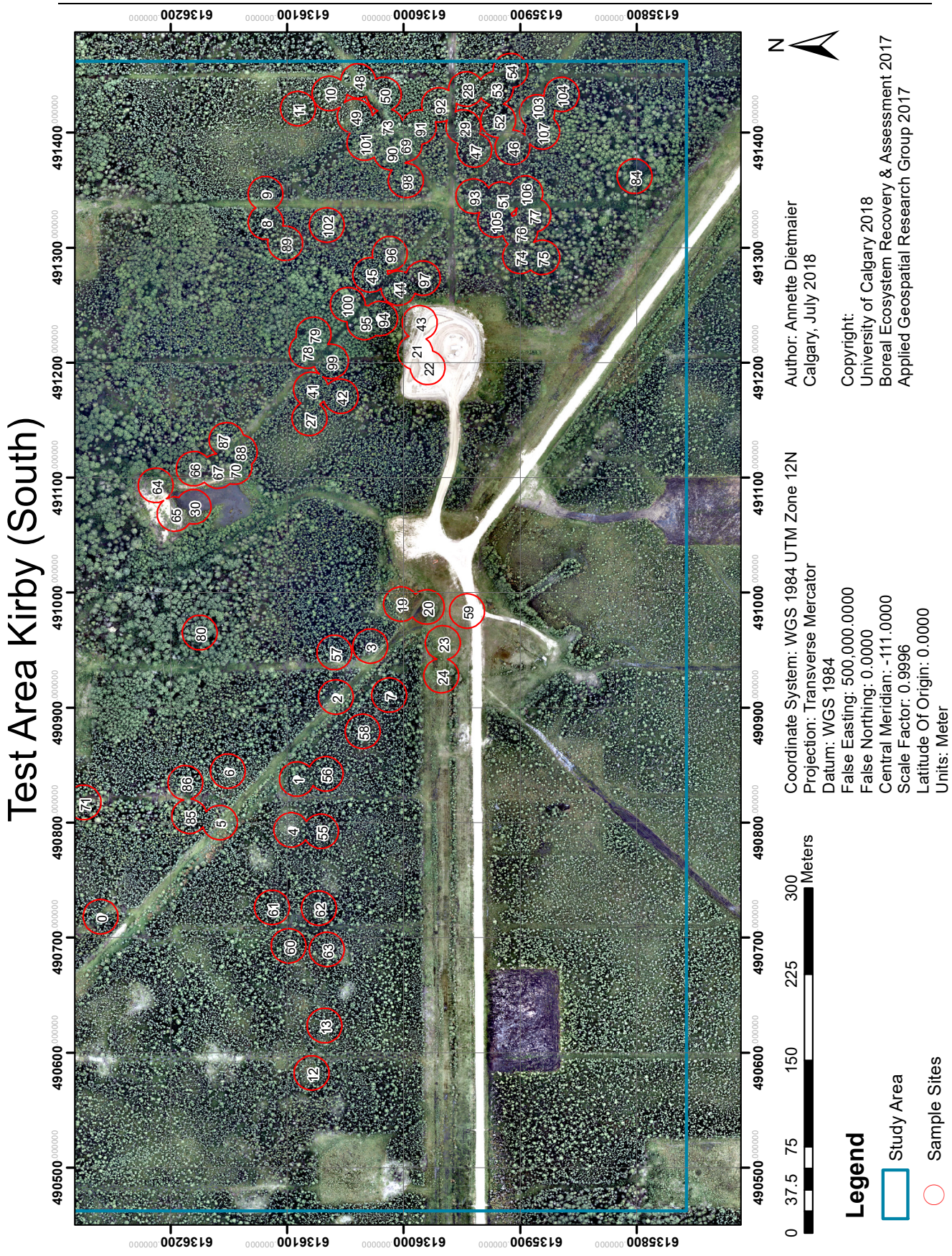

Figure 25 Field map of the AoI Kirby (southern part) with the sample sites which contained the sample points visited during the field campaign. The individual sample points are not depicted.

5.2.2 In Situ Sampling

A precise account of how the in-situ sampling took place is given in the field plan (Appendix C). The list of points selected as appropriate random stratified sample, including their UTM coordinates, was printed out prior to the field campaign. Each morning, a list of coordinates that could realistically be visited that day, considering weather conditions, was decided upon. The location of each sample point was found and determined by a Real Time Kinematic Global Positioning System (RTK GPS), consisting of a base station, which was set up in the morning, and a mobile rover, on to which a hand-held device was attached. Using a method of carrier-phase differential GPS positioning, the current position was obtained in centimeter-level accuracies in real time.

Upon approaching a sample site, a picture was taken with the camera facing straight up, being held at breast height (1.3 m). If the sky was visible at the centre of the image, that point was classified as one of the opening classes (fig. 27). The size class had to be determined to the best of the surveyor's judgement and knowledge of the opening structure. If no sky was visible, the sample point was classified as no opening (class 0; fig. 27). In addition to the opening class, vertical vegetation structure and classification confidence was also noted, ranging from 1 (very confident) to 3 (not confident at all). Sample point classifications with confidence levels of 3 were manually verified via visual image analysis upon finishing the field campaign.

Figure 26 The field crew on our last day of work in the AoI (from left: Jack Sugden, Annette Dietmaier, Keifer Biddle). A typical seismic line is visible as a deep cut in the forest canopy on the right.

Figure 27 Photographs taken during the in-situ sampling of a) class 1 opening, b) class 2 opening, c) class 3 opening, d) class 4 opening and e) no opening (class 0). The classification is based on whether sky is visible in the centre of the photograph taken.

5.3 Comparison of Opening Detection Accuracies and Opening Characteristics

Before opening characteristics were examined, the CHMs produced were compared to CHM_{ALS}. Differential images were produced to visualize divergence patterns and the Root Mean Square Error (RMSE) was calculated for CHM_{DAP} and CHM_{Hybrid} compared to CHM_{ALS} (equation 3; Sachs & Hedderich, 2009).

$$RMSE = \sqrt{\frac{\sum_{i=1}^{n}(P_i - O_i)^2}{n}} \quad (3)$$

where

P = predicted value

O = observed value

n = sample size.

Overall accuracies, patterns of omission and the performance of all six approaches relative to opening size was evaluated. The number and size, as well as opening fraction was determined. Proportions of openings detected relative to size class gives a sense of whether an approach tends to classify openings as larger openings than they were found to be in the field.

Various opening characterization metrics were applied to all openings larger than 4 m^2 derived from all three data sources and using both approaches. These examinations aim at characterizing the geometric features of the openings detected and compare them to each other. Opening size distribution was examined using the Zeta distribution (also referred to as the discrete Pareto distribution) power-law probability density. This distribution is appropriate for characterizing opening size distribution because of its ability to properly depict both a very small number of large openings as well as a disproportionally large number of small openings (Kellner & Asner, 2009). When plotting on a log-log scale, the negative relation between opening frequency and opening size can be described with the parameter λ. The steeper the slope of this relation, the higher the value of λ. The values are expected to range between 1.0 and 3.0 for forested areas. A threshold of 2.0 is generally used to distinguish areas dominated by small openings ($\lambda > 2.0$) or large openings ($\lambda < 2.0$) (Asner et al., 2013). The values of λ were derived using a maximum likelihood estimator, following the method as presented by Hanel et al. (2017).

Size itself was examined in average (mean) values, as well as its variability (standard deviation) and its median. In addition, a shape index (McGarigal & Marks, 1995) was applied to the openings. This shape index (equation 4) characterizes the similarity of an opening to a perfectly round circle.

$$shape\ index = \frac{perimeter}{2 * (\pi * area)^{0.5}} \quad (4)$$

As a normalized ratio, this shape index characterizes the complexity of the boundary of an opening. The shape index is 1 for a perfectly round circle, and increases with the complexity of the opening boundary. Furthermore, the average height and standard deviation of height within openings was calculated applying the opening delineations of each approach to each CHM.

Spatial overlap of the detected openings was evaluated in two parts. The first step was to produce a raster of agreement, which shows the sum of all opening maps (where opening = 1, no opening = 0) and thereby the number of opening maps agreeing on the classification of

a specific pixel as opening. Raster of agreement pixel values of 5 for example indicate that this pixel was classified as an opening by five of the six approaches. In the second step, the opening maps were converted into shapefiles, assigning the value 1 to openings and No Value to non-opening areas. Using ArcGIS for this step and the following calculations, a decision tree was applied to these polygons as presented by Linke et al. (2017). This decision tree does not result in a binary layer of overlap and no overlap, but classifies the kind of overlap into four cases (fig. 28). For this approach, the reference polygons were the binary opening map that showed the highest overall accuracy, and the four overlap cases were computed for each of the remaining five maps. The structural overlap threshold (STH), which defines the total minimum area of overlap between a given target-map polygon (TMP) and one or more reference polygons (RP) was set to 20%. This is the threshold that determines whether an RP was detected (true positive). As Linke et al. (2017) state, bot STH and spatial overlap threshold (OTH) must be determined based on the research question on hand. Considering that the maps to be compared will vary in number, shape and size of the openings detected, an OTH of 50% was chosen. These openings do not depict thematic polygons, but rather differences in vegetation structure detected by different technologies. Thus, a lower OTH is appropriate.

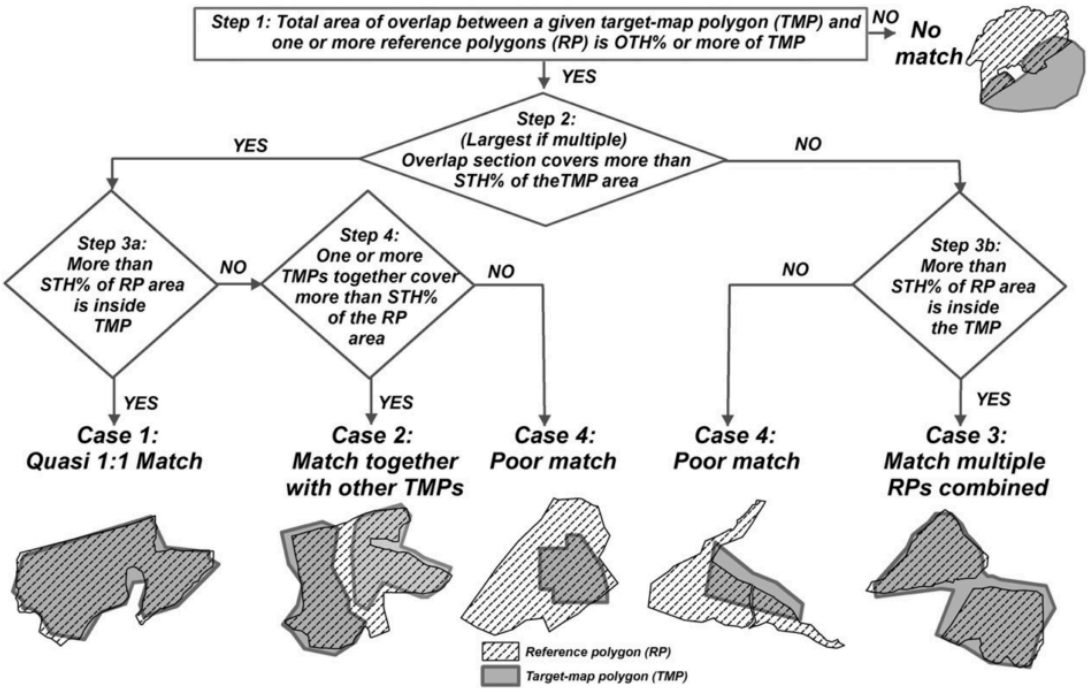

Figure 28 Decision-tree to assess the polygon-based structural accuracy of a given target map relative to a reference map. In this example, both OTH and STH were set to 50%.

To detect these four cases, first, the two maps to be analyzed had to be intersected. The resulting shapefile had to be expanded to include columns for the size of each original polygon (A_RP and A_TMP), the size of the intersection and the percentage of the intersect compared to the size of the original polygons (P_RP and P_TMP). Then, this layer was "dissolved" twice, once with the FID_RP and once with FID_TMP as dissolving factor. In this step, the sums of P and A were calculated for each polygon (TMP_diss.SUM_P_TMP, RP_diss.SUM_P_RP, TMP_diss.SUM_A_TMP and RP_diss.SUM_A_RP). The next step was the selection and export of the cases by attributes:

Case 1
```
TMP_diss.SUM_P_TMP >= 0.2 AND
intersect.P_TMP >= 0.5 AND
intersect.P_RP >= 0.5
```

Case 2
```
TMP_diss.SUM_P_TMP >= 0.2 AND
intersect.P_TMP >= 0.5 AND
intersect.P_RP < 0.5 AND
RP_diss.SUM_P_RP >= 0.5
```

Case 4.1
```
TMP_diss.SUM_P_TMP >= 0.2 AND
intersect.P_TMP >= 0.5 AND
intersect.P_RP < 0.5 AND
RP_diss.SUM_P_RP < 0.5
```

Case 3
```
TMP_diss.SUM_P_TMP >= 0.2 AND
intersect.P_TMP < 0.5 AND
intersect.P_RP >= 0.5
```

Case 4.2
```
TMP_diss.SUM_P_TMP >= 0.2 AND
intersect.P_TMP < 0.5 AND
intersect.P_RP < 0.5
```

6 Results

The methods described in Chapter 5 led to six different binary opening/non-opening maps (fig. 32). First, the derived CHMs shall be compared and their accuracy in relation to CHM_{ALS} examined. Second, the overall accuracies of each opening detection method will be presented, using validation via ground truth sampling. Third, their relative abilities in comparison to CHM_{ALS} in describing opening characteristics, such as opening size, shape, regrowth height and overlap are presented.

6.1 Comparison of CHMs

Figure 29 shows the three CHMs produced with normalized vegetation height above ground. Differences between the three CHMs, which are due to the fashion the data were acquired, were compared using a differential image approach. The results from this examination can be seen in figure 30 and provide information on the relative quality of CHM_{DAP} and CHM_{Hybrid}.

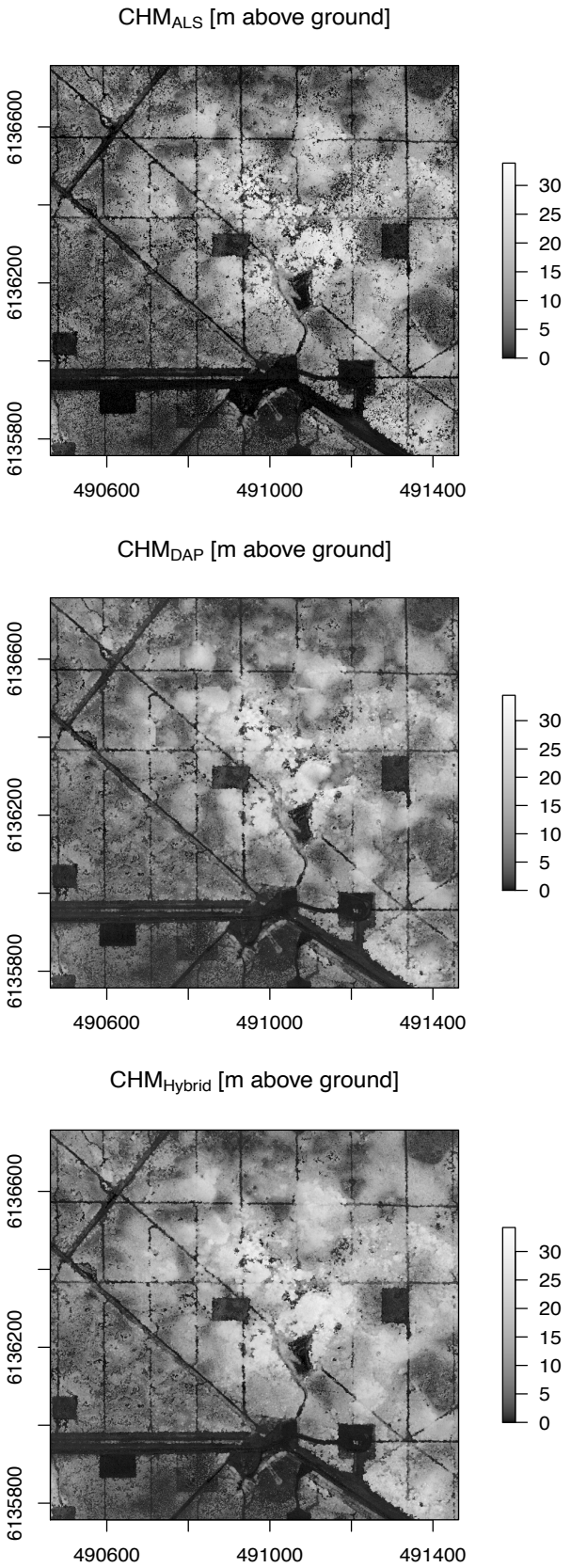

Figure 29 Canopy Height Models for from LiDAR data, photogrammetry data and a combination of both. Values are height above ground (h.a.g.). It is apparent that there are differences in detail between CHMs that contain DAP data and CHM_{ALS}. CHM_{DAP} further displays some linear artefacts where the ground was not visible for proper ground classification.

Figure 30 shows the differential images depicting the similarity of CHM_{DAP} and CHM_{Hybrid} with CHM_{ALS}. For this purpose, CHM_{DAP} and CHM_{Hybrid} were each subtracted from CHM_{ALS}. Positive values indicate higher values in the LiDAR based CHM, whereas negative values describe locations in which photogrammetry based data produces higher values. As figure 30 shows, there are stark differences in the divergences between the CHM_{DAP} and CHM_{Hybrid}, and CHM_{ALS}. The differential image with CHM_{DAP} shows large, solid patches of high divergence (illustrated in blue and pink), whereas the differential image with CHM_{Hybrid} is missing these conglomerations of high divergence pixels. Here, areas showing high values and thereby a large difference in comparison to the CHM_{ALS}, are more spaced out and considerably smaller in size.

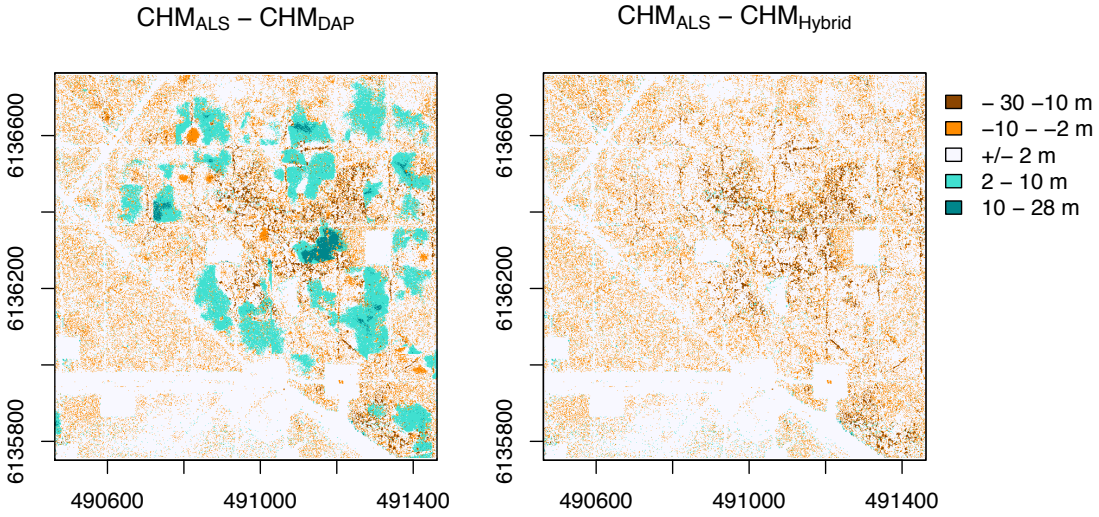

Figure 30 Differential images of CHM_{DAP} and CHM_{Hybrid} compared to CHM_{ALS}.

Figure 30 further shows that most of the divergence between CHM_{ALS} and CHM_{DAP} takes place in the positive value range, which indicates that CHM_{DAP} values tended to be lower than the corresponding CHM_{ALS} pixels. This is a result of overestimating DTM values (fig. 31), which in turn can be traced back to the limitations of photogrammetry ground classification in areas where the ground is not visible from above, such as in high density areas. It is apparent from table 4 that CHM_{Hybrid} matched with CHM_{ALS} within an acceptable allowance of +/-2 m across 81% of the study area. The total ranges of divergence from CHM_{ALS} did not differ considerably (57.3 m for CHM_{Hybrid} and 57.2 m for CHM_{DAP}). While the proportion of pixels classified within a +/ 10 m value range in the two differential images was quite similar for both CHMs (97% for CHM_{DAP} and 98% for CHM_{Hybrid}), CHM_{Hybrid} had 11% more pixels in the +/- 2 m range of the CHM_{ALS} than CHM_{DAP}. Surprisingly, the mean divergence from CHM_{ALS} was larger for CHM_{Hybrid} (-1.2 m) than for CHM_{DAP} (0.4 m). Interestingly, the RMSE of both images were quite similar, and only slightly better for CHM_{Hybrid}.

Table 4 Quantitative comparison of CHM_{DAP} and CHM_{Hybrid} compared to CHM_{ALS}.

	Min [m]	Max [m]	Mean [m]	Proportion of pixels within -10 and 10 m	Proportion of pixels within -2 and 2 m	RMSE [m]
ALS – DAP	-30.0	27.2	0.4	97%	70%	3.6
ALS – Hybrid	-29.6	27.7	-1.2	98%	81%	3.1

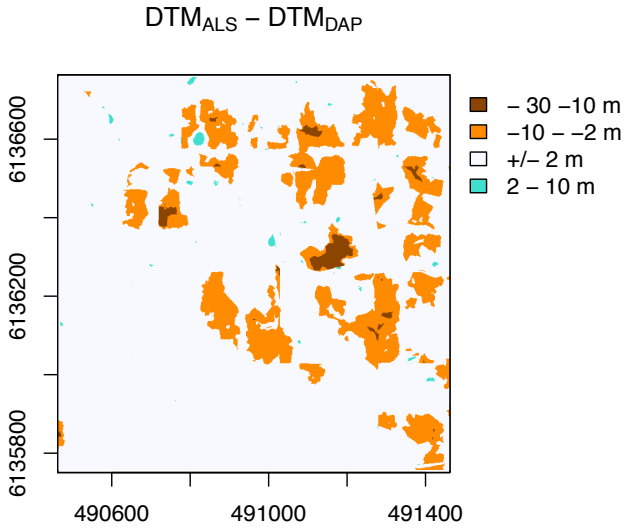

Figure 31 Differential Image of DTM_{ALS} and DTM_{DAP}. Large patches of overestimation of ground values are due to photogrammetry's inability to reliably classify point cloud elements as ground points when the ground was not visible from the sensor's perspective. This leads to the divergence patterns depicted in figure 30.

Figure 31 shows patches of overestimated ground values in DTM_{DAP}. These are a result of limited visibility of the ground in densely forested areas, which leads to match points, located in the canopy cover, being classified as ground points. These ground points naturally assume the value of the top of canopy, which produces the conglomerations of high overestimation depicted in orange and red in figure 31.

6.2 Comparison of opening detection accuracies

Figure 32 presents the six derived maps delineating structural openings using each approach. It is apparent that there are differences between the maps, especially in terms of number of openings, total area classified as opening and average opening size. These differences will be discussed in the following sections.

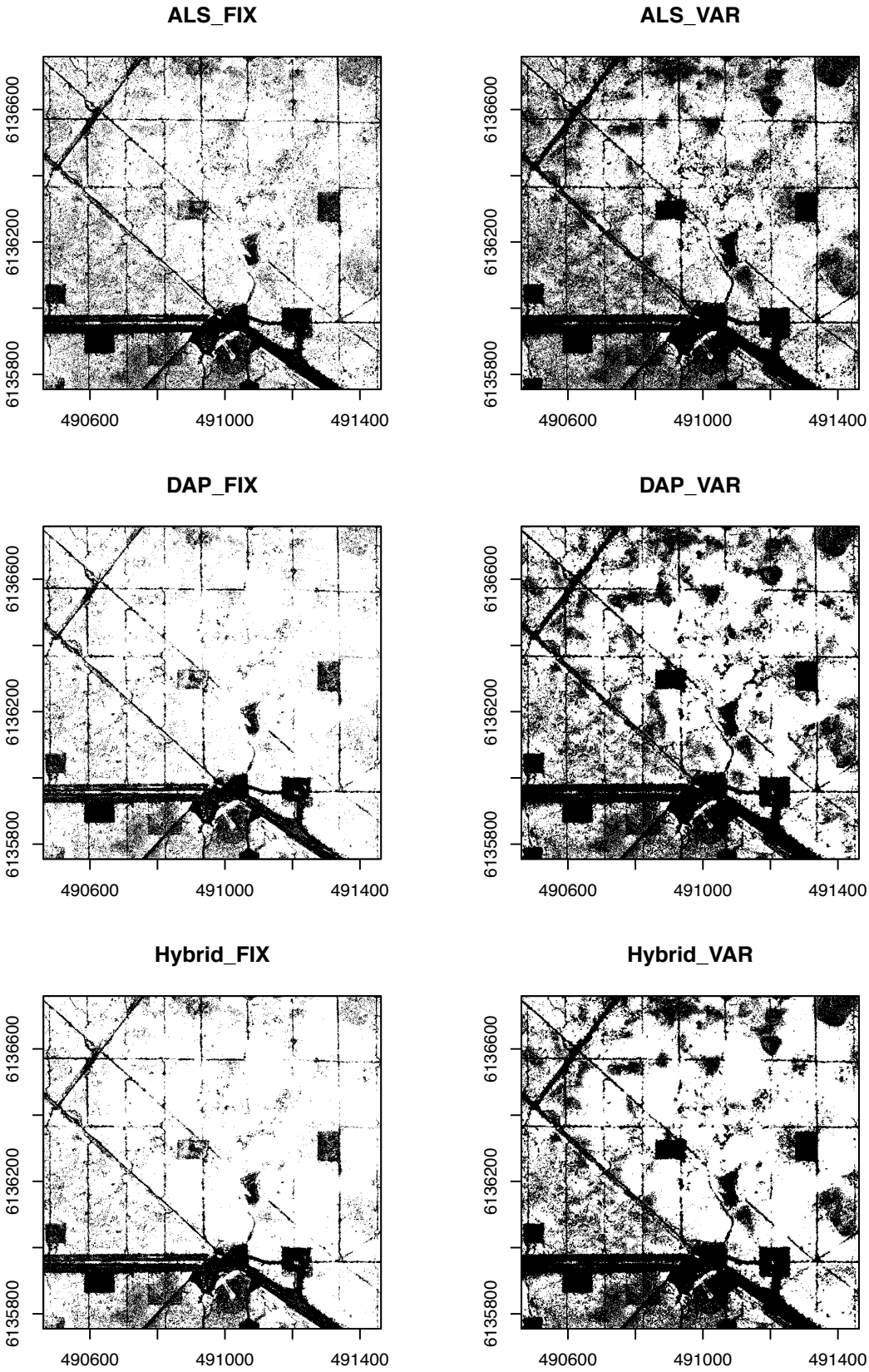

Figure 32 Maps showing opening delineations for each approach. Openings are depicted in black, areas classified as non-opening are depicted in white. There are visible differences in total area classified as opening, average opening sizes and number of openings, all of which will be discussed in the following chapters.

Overall accuracies ranged between 63% and 93%, with DAP_FIX showing the lowest and ALS_VAR the highest overall accuracy (table 5). The DAP and Hybrid datasets produced similar results within each approach. Using the fixed height approach, they both were 82%. When applying the variable height approach, the difference in overall accuracy lies at 1%. DAP and Hybrid show lower overall accuracies than ALS data in both approaches, however, the difference is larger when using the fixed height approach (26%) than when using the variable height approach (11%).

Table 5 further shows errors of omission and commission, which can be translated into underestimation and overestimation of openings. Between the data sets within each approach, there are stark differences in errors. When using the fixed height approach, ALS shows an omission error of 10% and a high commission error for non-openings at 30%. The range of errors for this approach using DAP and Hybrid datasets is much larger. At almost no commission error for openings (openings are overestimated by only 1%) and a corresponding low (2%) error of omission for non-opening, these data sources have a high commission error for areas that are classified as non-opening. Their omission error for openings is also high (46%). When applying the variable height approach, table 5 shows that the errors of omission in areas that are non-opening are relatively similar for all three datasets (24% - 29%). In those same areas, DAP and Hybrid data present commission errors of 47%, whereas this this error is only 8% when using ALS data. Commission errors for areas that are openings are balanced among the data sets (7%). The lowest omission error for openings is produced by ALS_VAR (2%), compared to 16% by DAP_VAR and 17% by Hybrid_VAR. The individual confusion matrices can be found in Appendix D.

Table 5 Summary of opening detection confusion matrices: Overall accuracies, errors of omission and commission [%].

	Overall Accuracy	Opening		Not Opening	
		Omission error	Commission error	Omission error	Commission error
Fixed Height Approach					
ALS	90	10	2	8	30
DAP	63	46	1	2	66
Hybrid	64	46	1	2	65
Variable Height Approach					
ALS	93	2	7	29	8
DAP	82	16	7	27	47
Hybrid	82	17	7	24	47

Figure 33 presents relative opening detection accuracy within the different opening size classes. It shows the proportion of openings correctly detected in each class. While there is a clear trend of the variable height approach producing the best results for opening detection, ALS_FIX produces much better results than the fixed height approach applied on the DAP or Hybrid data sets. When classifying non-opening areas, the fixed height approaches show much better accuracies. The fixed height approach improves strongly when classifying larger openings. In size class 4, accuracies for DAP_FIX and Hybrid_FIX were 75% and 77%,

respectively, whereas their accuracies in size class 1 are 7%. The larger an opening, the more reliably it can be detected by all methods. It is apparent from figure 33 that approaches applied on ALS datasets continuously produces the highest accuracies, which is corroborated by the results presented in table 6.

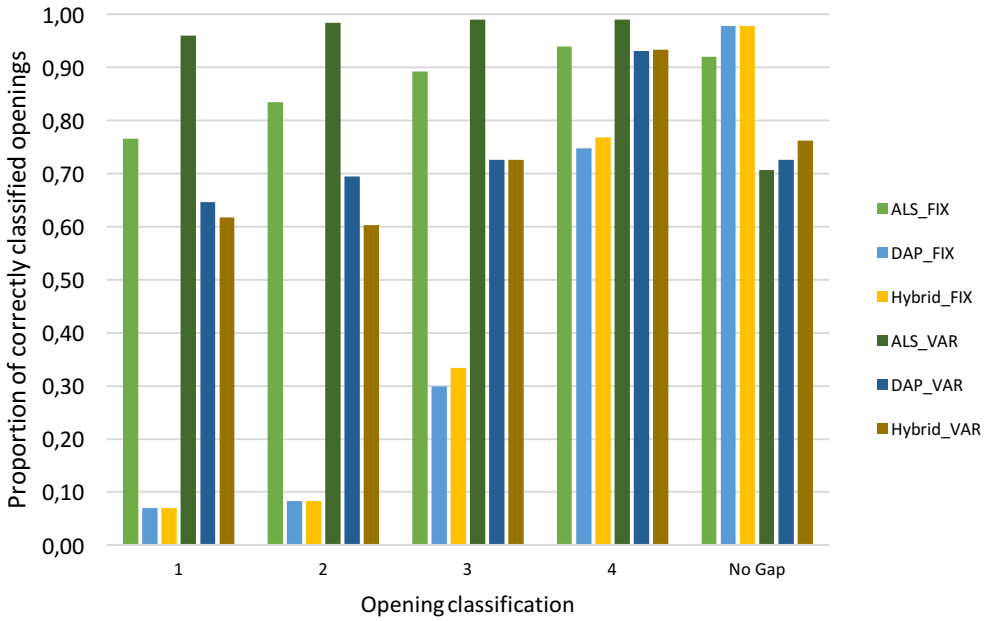

Figure 33 Results of canopy opening detection using fixed and variable height approaches by opening size classification.

Table 6 shows the complimentary errors of omission in each opening class, which are the negatives of figure 33. They are highest for all approaches in opening class 1 with decreasing values for the bigger opening classes. The fixed height approach, as seen above, provides smaller errors of omission of no opening areas.

Table 6 Proportion of incorrectly classified openings/non-openings (errors of omission) relative to opening size classes 1 - 4 and non-openings in [%].

	Opening size class				
	1	2	3	4	No Opening
Fixed height approach					
ALS	23	17	11	6	8
DAP	93	92	70	25	2
Hybrid	93	92	67	23	2
Variable height approach					
ALS	4	2	1	1	29
DAP	35	31	28	7	27
Hybrid	38	40	28	7	24

Total number of openings detected varied both between data sets and opening detection approaches. To characterize canopy opening detection of very small openings, size class one

was assessed individually. It is apparent from table 7 that ALS data produced a greater number of detected canopy openings, both in size class 1, as well as openings larger than 4 m^2. Using the fixed height approach, the number of openings detected with ALS data was almost always at least twice the number of openings detected by DAP. When applying the variable height approach, this trend stays true, however, it is less pronounced. Here, ALS produces 1.3 to 1.5 times the number of openings detected by DAP and the Hybrid approach, respectively.

Table 7 further shows that there are marked differences in the proportion of opening to non-opening in the AoI. Values range from 19% opening in the canopy cover (DAP_FIX) to 75% (ALS_VAR). ALS data produced the highest proportion in each approach. Interestingly, the values derived using the fixed height (19% – 33%) approach are much smaller than those produced with the variable height approach (53% - 75%), with each FIX value more than twice the size of the corresponding VAR value. This same trend can be discovered in the total area of openings. The total area of openings produced from ALS was 1.1 to 1.5 times more than that derived from DAP_VAR or DAP_FIX, respectively. Here, too, the total area of openings is around twice the size when using the variable height approach, compared to using the fixed height approach.

Table 7 Number, proportion and total area of openings detected.

	Number of openings $< 4m^2$	Number of openings $> 4\ m^2$	Proportion of opening to non-opening in AoI [%]	Total area of openings [m^2]
Fixed height approach				
ALS	48,465	3450	33	245,92
DAP	20,969	1731	19	162,37
Hybrid	18,041	1638	21	172,67
Variable height approach				
ALS	27,075	2171	75	428,18
DAP	21,258	1736	62	382,03
Hybrid	18,558	1478	53	346,01

Distribution of detected openings relative to opening size was examined. Table 8 shows that the largest proportion of openings detected was size class 2 (4 – 20 m^2) when excluding openings $< 4m^2$, which are, by far, the most numerous (table 7). Overall, the fixed height approach detects more smaller openings and less larger openings. Depending on the approach used, between 70% and 89% of all openings detected were classified to be in this size range, with ALS_FIX detecting the highest number of size 2 openings and Hybrid_VAR the lowest. The fixed height approach detected a smaller proportion of size class 3 openings (20 m – 200 m^2; 19% – 20%) than the variable height approach (21% – 26%). The same trend is true for size class 4 openings. Here, ALS produced smaller proportions in each approach, while the proportions produced by DAP and Hybrid are relatively similar (2% and 3%, and 4% and 4%).

Table 8 Distribution of detected openings relative to size class in percent.

Data Source	Proportion of openings Size Class 2 [%]	Proportion of openings Size Class 3 [%]	Proportion of openings Size Class 4 [%]
Fixed height approach			
ALS	79	19	1
DAP	79	19	2
Hybrid	77	20	3
Variable height approach			
ALS	78	21	1
DAP	70	26	4
Hybrid	70	27	4

6.3 Comparison of Opening Characteristics

In the following section, metrics for characterizing size, shape, within-opening vegetation height and overlap are applied to all openings $> 4m^2$, derived from all three data sources and using both approaches. Size class 1 was excluded to prevent a distortion of the values, since they are detected very differently among approaches, and, by their sheer number, would lead to misguiding results.

6.3.1 Average opening size, shape and opening size distribution

Average opening size based on ALS data was smaller than corresponding values based on DAP or Hybrid data sets (table 9). Hybrid_VAR produced the largest mean opening size, which is 3 times the value of ALS_FIX. While median opening sizes were quite similar among the different approaches and data sets, table 9 shows that variability in opening size depended more on the approach than the data set used. Within the fixed height threshold, results varied slightly around 2500 m^2, whereas the variable height approach produced values that were up at least twice as high. ALS_VAR showed the highest variability in opening size (7155 m^2).

Table 9 Opening size characteristics for openings sized $> 4m^2$.

	Mean opening size [m^2]	Median opening size [m^2]	SD opening size [m^2]	Shape Index Mean
Fixed height approach				
ALS	71,3	8,64	2525	2,87
DAP	93,8	8,4	2429	2,71
Hybrid	105,4	8,84	2656	2,71
Variable height approach				
ALS	197,2	8,8	7155	2,54
DAP	220,1	11,16	5625	2,72
Hybrid	234,1	11,46	5713	2,69

The shape index was quite similar among approaches and data sets used. The mean values varied slightly between 2.54 (ALS_VAR) and 2.87 (ALS_FIX). The distribution of the shape indices for all results is depicted in figure 34.

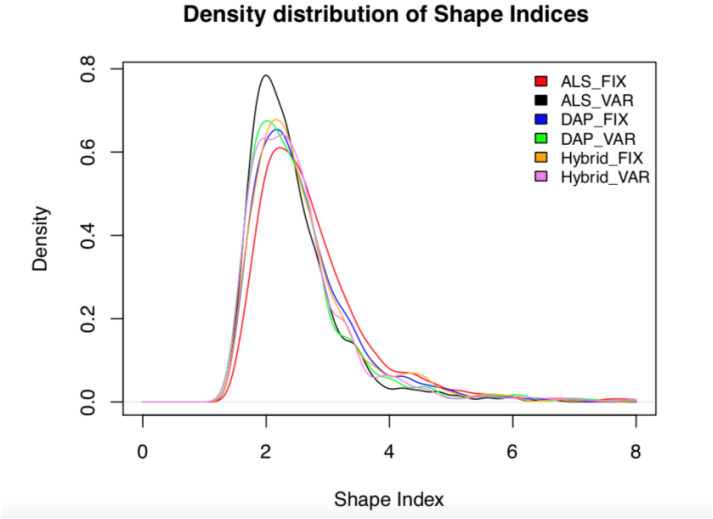

Figure 34 Density histogram for shape indices of the six approaches, showing a clear peak at values between 2.6 and 2.9.

T-tests for opening size and shape index were conducted (confidence level = 95%, p = 0.05). Because the population was not normally distributed, results were confirmed with the Wilcoxon Rank Sum W test (Sachs & Hedderich, 2009). Average opening sizes varied significantly from each other, whereas the shape index did not show any significant differences between the six approaches.

The distribution of opening size was assessed further using a Zeta distribution. This power law distribution is the appropriate means for depicting the negative slope between opening size and the frequency of that opening size. As described in table 7, a disproportionate number of openings are very small, and only a few openings are classified as large openings. This relation is depicted in figure 35. The steepness of the slope is described by the λ value. The higher this value of λ, the greater the proportion of small openings. The fixed height approach produced a constant λ of 1.8, with a slightly smaller value when applied to the Hybrid data set (1.71). The variable height approach produces the highest λ value when used on the ALS data set (1.77) and slightly lower when used on the DAP or Hybrid data set (1.55 for DAP_VAR and 1.52 for HYB_VAR). Figure 35 shows these findings in the form of Zeta distribution graphs. They demonstrate that the fixed height approach continuously produced a higher proportion of smaller openings, regardless the data set at hand. Especially when applying the variable height approach to the DAP and the Hybrid data sets, small openings seem to be lost and merged into bigger openings. This explains a lower λ value for the variable height approach and is reflected in the larger mean opening size value presented in table 9 for DAP_VAR and Hybrid_VAR.

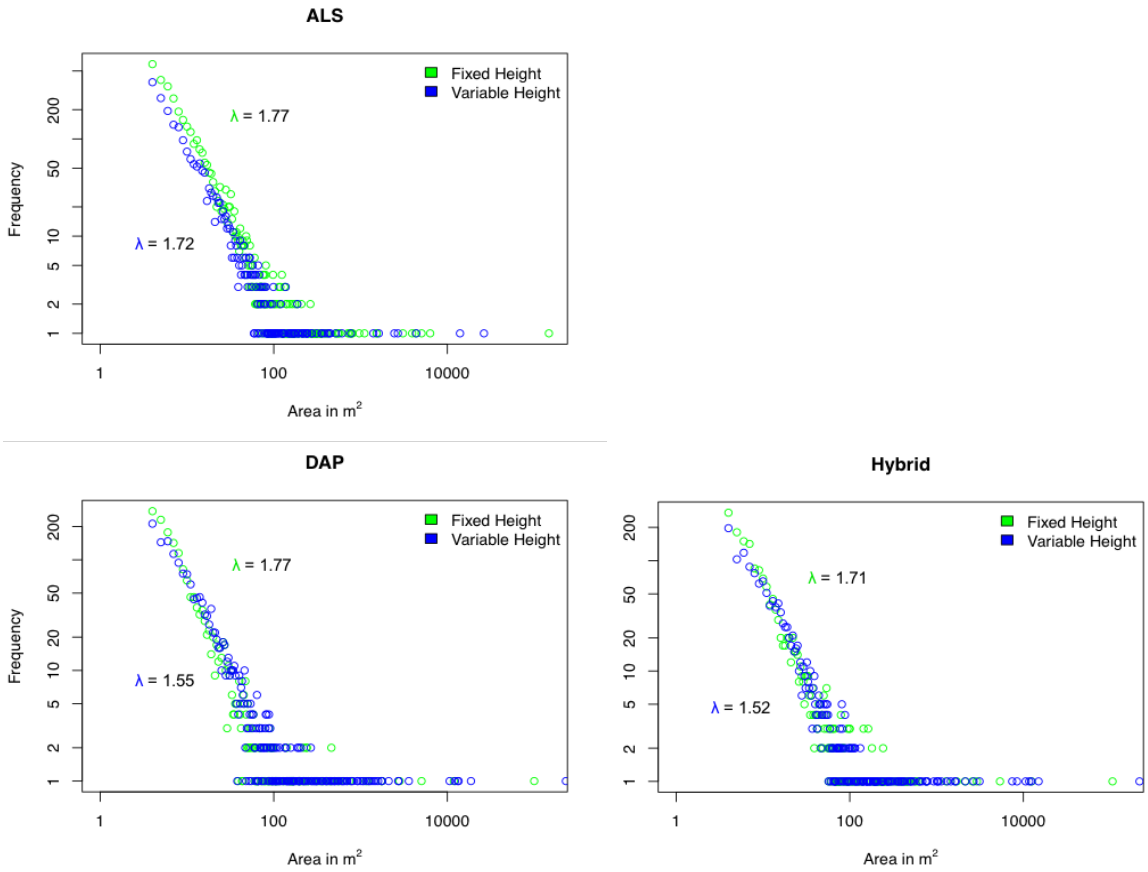

Figure 35 Zeta opening size distributions for each approach.

6.3.2 Regrowth vegetation height within openings

Differences in height within openings as suggested by the three CHMs was analyzed for significant difference based on the approach used for the opening delineation (table 10). Using the Wilcoxon Rank Sum W test (p = 0.5), it was determined that the height within each set of delineated openings varied significantly between the CHMs, while regrowth vegetation height might seem relatively similar, comparing the three different opening delineations on the same CHM. Using the fixed height approach, vegetation height in CHM_{ALS} in openings detected by all three data sets varied between 0.27 and 0.30 m. In contrast, table 10 shows that vegetation height provided by CHM_{DAP} and CHM_{Hybrid} is higher in openings detected by ALS than by DAP or the Hybrid approach. Here, values range between 1.96 m and 0.67 m, and 1.90 m and 0.56 m respectively. The vegetation height is thus more than twice as high, on average, in openings detected by ALS in CHM_{DAP} or CHM_{Hybrid} than in those detected by DAP or the Hybrid approach. When applying the variable height approach, vegetation height is greater in openings detected in CHM_{DAP} and CHM_{Hybrid} for all three techniques, with openings detected using the Hybrid approach consistently providing the lowest values. It strikes as interesting that the average vegetation height in openings detected by the ALS and the Hybrid approach using the CHM_{ALS} are close to the previously defined fixed threshold of 1.30 m (1.42 and 1.32m), whereas DAP_VAR produced an average value of 2.15 m.

Table 10 Mean vegetation height within openings > 4m² derived from all opening maps and each based on every data set.

Openings located by	CHM used for height measurement		
	ALS	DAP	Hybrid
Fixed Height Approach			
ALS	0.28	1.96	1.90
DAP	0.27	0.67	0.56
Hybrid	0.30	0.72	0.61
Variable Height Approach			
ALS	1.42	3.20	3.26
DAP	2.15	2.16	2.75
Hybrid	1.32	1.91	1.85

6.3.3 Overlap and agreement of classifications

Spatial overlap analysis between all produced opening maps resulted in a raster of agreement (fig. 36). This figure shows that most opening maps agree on big openings, and thus displays high values (around 5 and 6) on roads, clear cuts, seismic lines and water bodies, indicating that at least 5 approaches agree on the classification of these pixels as opening. Higher values of disagreement are found further away from seismic lines and point to the areas in which the fixed height approach identifies many small individual openings and the variable height approach classifies larger, contiguous areas as openings.

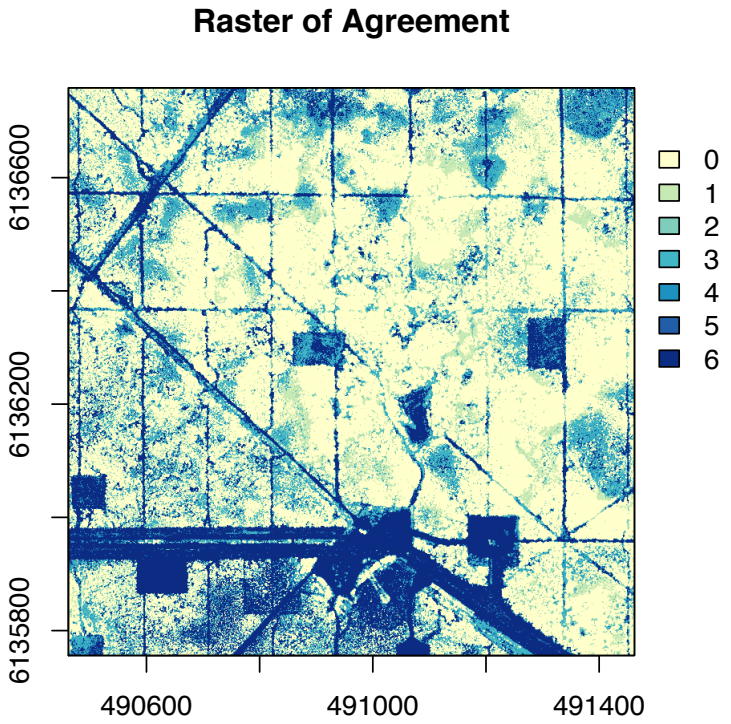

Figure 36 Raster of agreement for all six opening detection approaches. The legend shows the number of opening maps agreeing on the classification of a pixel as opening. Pixels with the value "0" are not classified as opening by any approach.

Furthermore, the calculation of the decision tree shown in figure 28, which makes a distinction between different kind of matches for spatial overlap (quasi 1:1 matches, good

matches and poor matches) produced the results presented in table 11. ALS_VAR was chosen as the reference map, as it produced the highest overall accuracy (table 5). In this step, the area of overlap was categorized by match (case 1 being a quasi 1:1 fit and case 4 being a poor match). Interestingly, the fixed height approach did not produce any case 3 matches at all (cases in which multiple RP match with one larger TMP) and the variable height approaches produced lower values for case 2 than the fixed height approaches. Areas of overlap vary markedly among the different approaches, with the variable height approaches producing the highest amount of area in case 1 matches, and DAP_FIX and HYB_FIX producing the lowest. ALS_FIX has less amount of case 1 area than the DAP_VAR and HYB_VAR, but more than the other two fixed height approaches. By far the highest amount of case 4 area is produced by ALS_FIX, which produced many singular, small openings.

Table 11 Total area of overlap [m^2] by individual overlap cases, presented for each Target Map with the Reference Map ALS_ VAR.

	Case 1	Case 2	Case 3	Case 4
ALS_FIX	5066	219152	0	21704
DAP_FIX	112	154307	0	6799
Hyb_FIX	128	164172	0	7093
DAP_VAR	227595	1155	4486	4829
HYB_VAR	224043	45	232	46

Table 12 presents the mean size of the overlapping area in m^2. It is apparent that the variable height approach produces maps that overlap with ALS_VAR mainly in the bigger polygons, such as seismic lines, roads and large areas of connected openings which would be classified as a many small openings by the fixed height approach. The fixed height approach shows a 10 to 20 times bigger average overlap size for case 2 overlaps than the variable height approach.

Table 12 Mean area of overlaps for each approach [m^2].

	C1	C2	C3
ALS_FIX	13.3	100.3	NA
DAP_FIX	22.4	107.0	NA
Hyb_FIX	25.6	120.8	NA
DAP_VAR	2616.0	12.2	15,0
HYB_VAR	3069.1	5.0	13,6

In table 13, the proportions of the sum of all overlaps in cases 1 – 3 relative to the total area identified as opening by the reference map and the target map, respectively, is presented. Notably in all cases, the proportion of overlaps relative to the target maps is larger than the proportions relative to the reference map. While the variable height approaches produce maps with the largest areas of case 1 matches (table 12), ALS_FIX produces an equal proportion of overlaps relative to the reference map, while DAP_FIX and Hyb_FIX produce values below that. Thus, a maximum of 52% – 54% of the reference map are detected by the target maps. The proportion values relative to the target map are higher for the fixed height approaches, which signifies that larger areas of the openings detected by the target maps using the fixed

height approach have a counterpart in the reference map than those identified by the variable height approach.

Table 13 Proportions of overlapping areas relative to the total area of Reference Polygons and Target Map Polygons.

	Reference Map	Target Maps
ALS_FIX	0.52	0.91
DAP_FIX	0.36	0.95
Hyb_FIX	0.38	0.95
DAP_VAR	0.54	0.61
HYB_VAR	0.52	0.65

6.4 Landscape condition

As suggested by the Provincial Woodland Caribou Range Plan (2017), metrics on the condition of the landscape were evaluated. This provincial plan contains three metrics on landscape condition. These will be presented in the following.

6.4.1 Footprint

Footprint is defined as "*the area of anthropogenic disturbance features, classified by originating activity*" (Alberta Government, 2017, p. 72). While the classification based on originating activity is not possible on the base of remote sensing data alone, the area of anthropogenic disturbance features, including clear cuts, roads and seismic lines (fig. 23), was determined to amount to 185,590 m^2, which constitutes 19 % of the AoI. This assessment is based on the first stratification level which was conducted by visual analysis of the CHM_{ALS} as well as the LeafOn orthomosaic.

6.4.2 Natural Disturbance

Natural disturbance, defined as *"the area of disturbed and undisturbed habitat affected by natural disturbance"* (Alberta Government, 2017, p. 72) was assessed on the base of the ALS_VAR opening map, excluding all areas discussed in 6.4.1, as the sum of the remaining openings detected in the areas unaffected by human disturbance. These openings amount to 254,431 m^2, which constitutes 25 % of the AoI.

6.4.3 Linear Features

In the AoI, 26 seismic lines were detected. The majority (9 seismic lines) are North/South oriented (average length: 919 m), 3 Northeast/Southwest oriented, 2 Northwest/Southeast oriented (average length of diagonal features: 587 m), and 2 West/East oriented (average length: 1000 m). The most regular ones, stretching in a longitudinal fashion, were spaced 115 m apart from each other. In contrast, the diagonal lines did not follow any regularity. The total length of all linear features amounts to 13,206 m, which results in a linear feature density of 13,206 m/km^2. In addition to the linear features, 10 clear cuts were detected, which showed an average size 5,900 m^2.

7 Discussion

In the following, the previously presented results shall be discussed and their meaning defined precisely. To get a sense of how the results and differences in findings relative to each approach can be explained, table 14 serves to visualize the systematic differences in the outcomes produced by ALS, DAP and the Hybrid data sets.

7.1 Performance of opening detection procedures

The following chapters present the accuracies for opening detection approaches. It gives a visual impression for the differences in gap classification and concludes with a comparison of the different approaches.

7.1.1 Normalized Vegetation Index

This study has demonstrated that the NDVI is not a reliable solution for the purpose of mapping and quantifying anthropogenic disturbances like seismic lines in the boreal forest. The overall accuracies are the lowest of all approaches conducted, and with 50% OvA, the NDVI results are certainly not very reliable in the classification of openings and non-openings. There are several explanations for these results. First, one has to consider the naturally low photosynthetic efficiency of high latitude conifers which is a result of their low demand for carbohydrates, which would lead to low NDVI values where the vegetation is in fact healthy (Jönsson et al., 2010). In addition to this phenomenon, the high content of coarse woody is likely to have further lowered the NDVI within intact tree stands (fig. 8), leading to the omission of "non-opening" areas. Most importantly, errors of commission in the same class can be linked to an overestimation of biological activity within seismic lines due to grass growth. As an estimator of green-ness, the NDVI finds green vegetation everywhere, in the forest and in the openings. A similar phenomenon was previously discussed by Chen & Cihlar (2000) and Zhirin et al. (2016). The understory vegetation, mostly consisting of Labrador tea, sphagnum moss and grass, leads to high NDVI values within anthropogenically disturbed areas. The differences between the LeafOff and LeafOn data can be explained by different amounts of biological activity and possibly different soil moisture contents, given that the boggy soils of the study area can drastically influence the NDVI's values by absorbing large amounts of NIR radiation. If the soil moisture content was not the same at both acquisition dates (which is to be expected) the differences in outcomes can be easily explained.

The use of multispectral images, either retrieved via airborne or spaceborne sensors, has been very popular and successfully used in a variety of research studies for decades. This has been due to easy access (especially since the institution of open data platforms for Landsat or Sentinel), low costs and easy to execute procedures like calculating the NDVI. Further, products like the NDVI are comprehensible for the broader public and non-scientific stakeholders. Additional advantages include a high temporal resolution which allows for dense time series analysis.

However, due to their inability to penetrate the canopy cover (Wulder, 1998), spectral indices are susceptible for a variety of disruptive factors, such as atmospheric perturbations, shadowing effects due to the stark spatial differences in forest structure, solar zenith angle and

soil reflectance and interference (McDonald et al., 1998). Particularly in higher latitudes, low solar zenith angles and large quantities of snow can have significant negative effects on the accuracy of winter values (Jönsson et al., 2010). As a mere indicator of greenness, this approach is thus not suitable in the context of this study.

7.1.2 ALS, DAP and Hybrid data sets

The first research question presented in chapter 1 asks for the accuracies of opening detection for ALS and DAP data. While the overall accuracies of the DAP and Hybrid approach are quite similar (63% and 64% for the fixed height approach and 82% for the variable height approach), table 14 shows that DAP_VAR performs especially poorly in high density areas, where openings are strongly overestimated. This is attributed to the underestimation of vegetation height when using a DTM_{DAP}, which in turn can be attributed to the overestimation of ground points, where vegetation is very dense and the ground cannot be seen by the sensor above. This effect can be ameliorated by using a LiDAR derived DTM, as can be seen from the corresponding image by Hybrid_VAR in table 14. DAP and Hybrid data resulted in underestimation of gap area when applying the fixed height approach especially in low to medium density areas. Overall accuracies indicated that there lies a significant advantage in using ALS derived products over the DAP or Hybrid data sets. Especially accuracies determined for DAP_FIX and Hybrid_FIX produce accuracies (63% and 64%) that are worse than the ones produced by the normalized vegetation index presented in the introduction (50% and 71%). In contrast to this, ALS_FIX and ALS_VAR were found to have overall accuracies of 90% and 93%, respectively. The findings of this study correspond to the value range of OvA found by White et al. (2018), but disagree with their results, in that the variable height approach produced a marked improvement of OvA for DAP and Hybrid data sets in this study, whereas it resulted in a lower OvA relative to using the fixed height approach in the study of White et al. (2018). This might be attributed to different thresholds applied in this study (25%) and White et al. (2018; 64%), different sizes of the moving window (100 m and 11 m respectively) and different physiological vegetation structures.

This study showed that ALS and DAP/Hybrid data sets show significant differences in the number and size of the detected openings. Using the fixed height approach especially, the number of openings < 4 m^2 detected by ALS is more than twice the number detected by DAP and Hybrid. The difference becomes less stark using the variable height approach, but ALS_VAR still detects 20% more openings than DAP_VAR or Hybrid_VAR. The same trend is observed for the number of openings > 4 m^2, with the differences being less pronounced for these bigger openings (table 7). However, ALS continuously produces the highest number of openings in all approaches. Table 8 shows that a bigger fraction of openings is classified as class 3 and 4 openings by DAP and Hybrid data sets when using the variable height approach and as class 4 openings when using the fixed height approach. It is remarkable that ALS_FIX produced the highest number of openings, and ALS_VAR produced the largest total area classified as opening. The DAP and Hybrid data sets must therefore omit a significant number of openings covering a significant area of land. This can be seen in the raster of agreement (fig. 36), which shows that most opening maps agree on the classification of seismic lines and other human disturbances, and reports higher disagreement in parts of the AoI off of the main grid of linear features and clear cuts. Here, only 2 – 3 maps detect openings in what is classified as "natural" in the first stratification level. This explanation is corroborated by the strikingly high

errors of omission for the DAP and Hybrid datasets presented in table 5. It becomes apparent in table 5 that commission errors for openings and omission errors for non-openings are relative homogenous among the different approaches. Omission errors for openings and commission errors for non-openings show remarkable differences. DAP and Hybrid show omission errors of 46% for the fixed height approach compared to 10% by ALS_FIX and 16% and 17% respectively by DAP_VAR and Hybrid_VAR compared to 2% by ALS_VAR. This can be detailed further by figure 33. DAP and Hybrid fail to detect class 1 – 3 openings with relatively small differences in their detection rates when using the fixed height approach. These errors of omission explain the main source for differences in overall accuracy between ALS and DAP and the lower number of openings detected by DAP and Hybrid data sets.

A previous study by White et al. (2018) showed similar patterns. Comparing ALS and DAP for characterizing canopy openings in the temperate rain forest of British Columbia, they found significant differences in opening sizes and numbers, as well as large differences in the overall accuracies of the detection methods. In their study, errors of omission for DAP exceeded the 80% mark in both the fixed and the variable height approach. These large errors of commission further commensurate with results produced by Zielweska-Büttner et al. (2016). Using fixed height thresholds of 1 m and 2 m for low ($<$ 8 m) and tall ($>$ 8 m) growth forests in southern Germany to detect canopy openings using DAP data, they found errors of omission to be 48% in tall growth forests in 2012. Zielewska-Büttner et al. (2016) and White et al. (2018) ascribe these values to the significant impacts shadows and occlusions can have on photogrammetric approaches. These effects are especially pronounced in tall growth forests. Particularly small openings can be completely "covered" by shadows or occluded by tall trees at certain viewing angles, so that DAP and the Hybrid data set perform very poorly in the detection of small openings. Especially using the fixed height approach, only class 4 openings can reliable be detected using DAP/Hybrid (table 6). Class 1 – 3 openings are omitted by ratios of 67 - 93%. The variable height approach performs better, however, here, too, errors of omission for opening classes 1 – 3 lie between 27% (class 3) and 38% (class 1). Table 14 serves to provide a sense of the different opening detection outcomes. It is clearly visible that the variable height approach produces more area classified as opening than the fixed height approach. This, however, comes at a cost of omitting small growth trees and results in a greater error of omission of non-opening areas. Figure 33 shows that non-opening areas are more poorly classified by the variable height threshold approach, which is due to small trees being classified as openings.

Average opening size differs markedly between the approaches, with ALS producing the smaller average openings size values. ALS_FIX by far produced the smallest opening size. This corresponds with the highest total number of openings detected by any approach. DAP and Hybrid, neglecting small trees and failing to detect small openings, show higher average opening sizes. This is amplified by using the variable height approach, which may lower the cut off height value so that even more small growth trees may by disregarded (table 14). This effect stands in contrast to the expectation that the variable height approach will perform better in the low density lowland areas. Table 9 shows that using the fixed and the variable height approach, these two data sets produce larger average openings sizes, with the Hybrid data set resulting in the largest average opening size.

Table 14 Matrix of opening classification results in low, medium and high vegetation density segments of the AoI for each approach.

	Low density	Medium density	High density
ALS_FIX	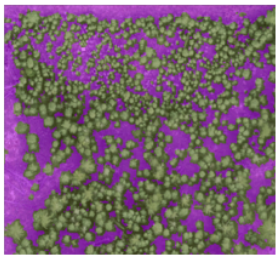	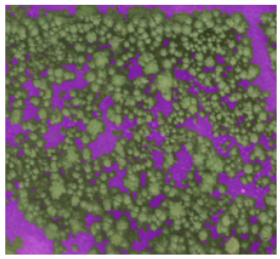	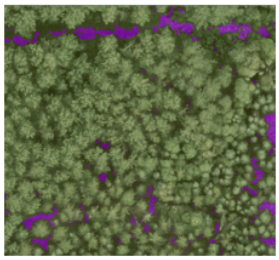
DAP_FIX	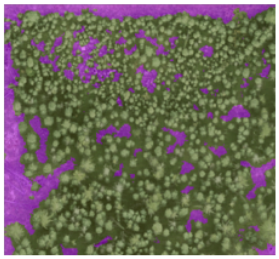	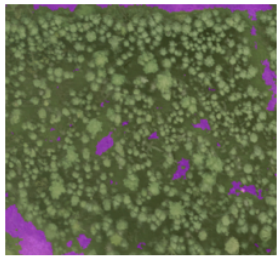	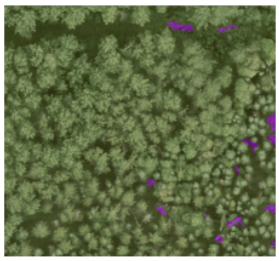
Hybrid_FIX	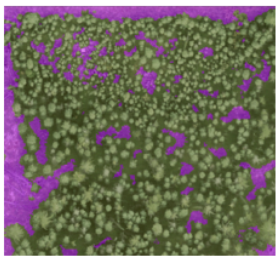	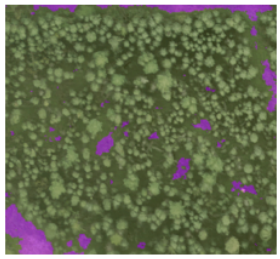	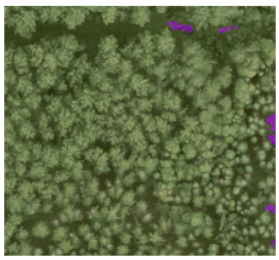
ALS_VAR	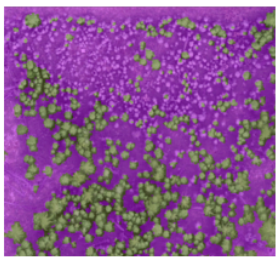	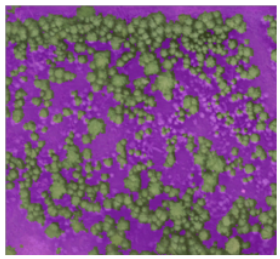	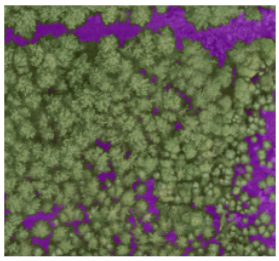
DAP_VAR	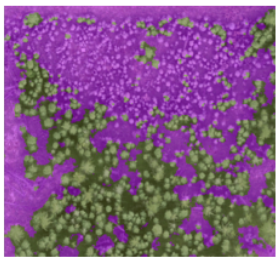	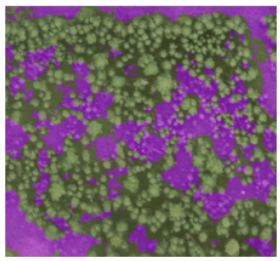	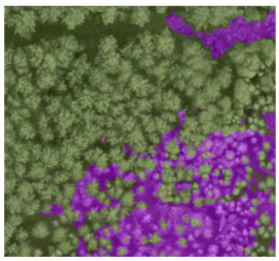
Hybrid_VAR	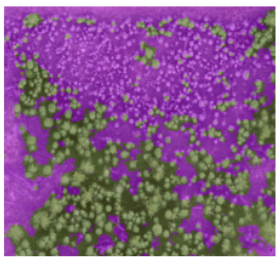	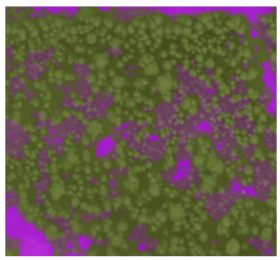	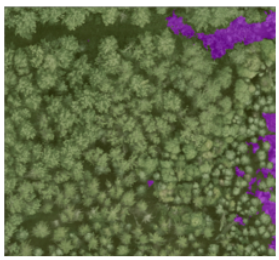

The evaluation of overlaps helps to analyze the similarity between the opening detection maps further. The raster of agreement shows that most maps agree on the detection of large openings, like the network of linear features, roads and clear cuts. However, table 12 details that DAP and Hybrid data sets, when using the fixed height approach, overlap with ALS_VAR by a quasi 1:1 match in a very small amount total area (112 and 128 m^2 respectively). Only small detected openings with an average size of 22.4 m^2 and 25.6 m^2 respectively meet openings detected by ALS_VAR in a case 1 match. The bulk of opening area detected by DAP and Hybrid are overlapping ALS_VAR in case 2 matches, which means that multiple DAP/Hybrid openings together match one reference map polygon. The number for case 2 matches is only higher for ALS_FIX. However, the overlap shows stronger patters between the fixed height and variable height approaches than between ALS and DAP/Hybrid data sets.

Opening size distributions have previously been examined for tropical forests (Asner et al., 2013; Kellner & Asner, 2009; Lloyd et al., 2009) and the temperate rain forest (White et al., 2018), but not yet for the boreal forest. Lobo & Dalling (2014) and White et al. (2018) conclude that the scaling parameter λ is strongly dependent on the height threshold applied in the opening detection process. Lobo & Dalling (2014) report that when the minimum fixed height was raised from 2 m to 10 m, λ was reduced from 2.4 to 1.8, which indicated a greater abundance of large openings. This tendency is also visible in the present study's results. The variable height approach continuously produces lower scaling parameter values than the fixed height approach (fig. 35), indicating a higher percentage of large openings among the total number of openings. This is due to the variable height approach occasionally dipping below the 1.3 m fixed height threshold and thereby classifying larger areas containing small trees as contiguous openings. Considering the large number of small openings in the AoI (table 7), linear features exert a noticeable effect on the opening size distribution, lowering the scaling parameter below 2.0. Given that a λ value of < 2.0 characterizes a given forested area as dominated by larger openings, this is true for this study's AoI according to the scaling parameters derived from each approach (fig. 35).

This study is based on a very high density DAP point cloud (table 2). Since a 0.2 m resolution is maintained throughout the CHM derivation process, the omission of small openings is expected to be due to confounding optical factors, such as occlusions and shadows, as well as physical tree sway, all of which lower the quality of the DSM_{DAP}. These factors, having no impact on the data collection process of ALS, do not affect the ability of ALS to detect very small openings, even though the point density is lower for the ALS point cloud. A visual impression of these differences can be gained by figure 29, depicting the different CHMs with visible differences in detail.

7.2 Is it possible to produce a reliable CHM from DAP data?

Financially, photogrammetry is an attractive alternative solution for opening detection and mapping. While the exact pricing depends on the individual situation at hand (such as required hardware, location of the AoI, accessibility etc.), costs for DAP imagery acquisition is estimated to be around one half to one third of the costs of ALS data (S. Chen et al., 2017; White et al., 2013). In addition to lower expenses, photogrammetry data can easily be collected by using a consumer grade optical digital camera and UAV (Rahman et al., 2017), therefore avoiding the need for special equipment like an ALS scanner. Easier and more affordable data acquisition

in areas that demand stringent monitoring of endangered habitat could potentially facilitate more frequent inventory cycles (White et al., 2013). For example, if the DAP approach proves to be an appropriate means of opening detection and mapping, the monitoring could be conducted without any ALS data acquisition, which is expensive and requires more coordination with third party aircraft companies. If the DAP approach is not appropriate, but the Hybrid approach proves to reliably detect and map openings in the AoI, a DTM_{ALS} could be acquired once and then be used for the derivation of a CHM_{Hybrid}, using a topical DSM_{DAP} after given time increments for time series analysis.

As discussed in chapter 7.1, there are significant differences in the performance of DAP and Hybrid models compared to ALS derived models. The overall accuracies of DAP and Hybrid products do not differ strongly from each other. This corresponds with results produced by Lovitt et al. (2017). In their study, they characterize microtopographic variability in peatlands of north-western Alberta, using photogrammetry data and enhancing their data set with an ALS point cloud. They did not find a significant improvement when using ALS data in combination with DAP data.

Using the fixed height approach, DAP and Hybrid OvA (63% and 64%, respectively) lie more than 25% below the OvA achieved by ALS_FIX (90%). Using the variable height approach, DAP and Hybrid achieve an OvA of 82%, compared to 93% produced by ALS_VAR. These results compare to 59.50% for HYB_FIX and 50.00% for HYB_VAR as presented as overall accuracies by White et al. (2018). In their study, they concluded that a hybrid dataset, utilizing a DTM_{ALS} and a DSM_{DAP} does not provide a sufficiently reliable CHM to detect canopy openings. There are several aspects to this decision, which, given the slightly elevated OvA values in this study, must be considered.

Photogrammetry is a completely optical method and as such, is susceptible to a series of interference factors which are harmless to the active remote sensing method that is LiDAR. The most common ones are occlusions and shadows (White et al., 2013, 2018). With the right viewing angle, occlusions can conceal openings small enough to disappear behind tall trees. These openings will not appear in the DSM generated, nor in the derived CHM. Shadows can further confuse the matching software. If the centre of an opening is dark enough so that the software is unable to detect an appropriate matching pair, the dip in canopy height will go unseen and not appear in the DSM, nor in the CHM. These factors are exacerbated by object movement: even moderate breezes can lead to tree tops swaying more than one meter or more, which causes significant matching problems, especially if the tree sway is in different directions between flight lines. This can create false parallax (White et al., 2013). These phenomena explain the high errors of omission using the DAP/Hybrid datasets, affecting especially the smaller openings.

Using photogrammetry data to generate the DSM and combining it with a DTM_{ALS} will not result in significant improvements to the overall accuracy, as can be seen in table 5. This finding is supported by the results of Lovitt et al. (2017) and Kukkonen et al. (2017), who compared two image matching procedures and ALS data for forest inventory characterization in a typical managed boreal forest environment in southern Finland. If the DSM is derived from DAP data, it will be affected by the optical shortcomings described before. Substituting the DTM_{DAP} with a DTM_{ALS} will thus not result in a noticeable improvement. Interestingly, applying a DTM_{DAP} did not result in a worsening of OvA of the CHM_{DAP} compared to

CHM_{Hybrid} as could be expected, given the very limited applicability for DTM generation from DAP data.

The clear majority of structural openings in the AoI fall into the category of size class 1 (table 7) and even when excluding this size class from analysis, size class 2 openings (functional openings) make up 70% – 80% of all openings detected. It is thus of the utmost importance for a tool that is applied in this setting to reliably detect and map very small openings in the canopy cover. Monitoring purposes demand the ability to provide regrowth vegetation measurements within openings and a reliable number of disturbances. CHM height within openings delineated by ALS approaches are continuously higher for CHM_{DAP} and CHM_{Hybrid}, indicating that a large proportion of these areas are not identified as openings in the DAP/Hybrid CHMs. Regrowth vegetation height within openings are significantly different. This finding is in line with the study by Vastaranta et al. (2013), which found that lower height percentiles are greater when using DAP and that predictions regarding height, basal area and stem volume from ALS are more accurate than those from DAP. The DAP and Hybrid data sets thus fail to provide this criterion. Table 14 provides a visual impression of this shortcoming. Especially in medium and high vegetation density parts of the AoI, DAP and Hybrid miss a plethora of openings. In the high-density column, it becomes apparent that even whole linear features, such as seismic lines delineated by tall, densely growing trees, can go unnoticed by the DSM_{DAP}.

Using DAP data could potentially cut data acquisition costs in half. However, while DAP_VAR and Hybrid_VAR provide an acceptable overall accuracy and overview of the state of a forest at hand, DAP_FIX and Hybrid_FIX show overall accuracies that are lower than the ones produced by the NDVI, and, with 63% and 64% respectively, cannot be considered as equal counterparts to the same approach applied to an ALS data set. Thus, using DAP data with the fixed height approach, regardless whether combined with a DTM_{ALS} or not, is not recommended for a reliable detection and mapping of structural openings and/or regrowth vegetation, especially of small openings, in the forest canopy of the boreal forest of Alberta. Therefore, the claim by White et al. (2018), that stereo-image matching does not consistently capture small openings, is supported by the results in this study.

7.3 Are ALS and DAP appropriate means for the quantification of human disturbances?

Human disturbances in the AoI follow systematic patterns, be it the regular, grid shaped network of seismic lines or symmetrical, rectangular or circle shaped clear cuts distributed all across the AoI. They are also usually of considerable size, and except for linear features which are generating strong regrowth vegetation, can be made out easily via visual interpretation. These disturbances are easier to detect and map than small, naturally caused openings. For one, occlusions play almost no role, since the majority of the opening is still visible, even when a small part of it close to the opening edge might be occluded by tall trees. Further, within large openings, DAP software is more likely to detect an appropriate amount of matching pairs and can therefore classify the opening more reliably. Due to the absence of trees within large openings, tree sway and falsification of matching pairs can be avoided, too. These limiting factors have no impact on ALS. Large openings are equally as easy to detect for ALS as they are for DAP (fig. 33).

If one aims at solely assessing the number of and area affected by large scale openings, ALS and even DAP are appropriate means. However, as soon as the research shifts towards identifying structural openings of all sizes in the forest at hand, DAP data quickly becomes obsolete. As table 14 shows, even seismic lines, which have almost become overgrown but are still distinguishable for ALS data sets, were not identified by the DAP and Hybrid data sets, neither using the fixed height nor the variable height approach. This poses an important limitation for the usage of DAP data. While clear cuts and big roads can be identified, narrow parts of linear features are already being missed in high vegetation density areas. This study shows that ALS outperforms DAP in both the fixed and the variable height approach, even when DAP is enhanced by a DTM_{ALS}. This finding is corroborated by the results produced by Kukkonen et al. (Kukkonen et al., 2017) and White et al. (2018), who state that ALS is more capable of a detailed description of the canopy surface than DAP.

However, it is important to note that both ALS as well as DAP pose a radically different approach to opening detection compared to normalized differential indices. By taking into consideration vegetation height, two advantages arise. First, greenness does not play a role in the detection of openings anymore, which enables a reliable opening detection process regardless of the season and/or light conditions. And even DAP produces data sets, which, by including the height component of the vegetation, and in combination with a reliable DTM, can lead to good results in coarser scale applications. Thus, by moving away from spectral signals and towards the actual measurement of vegetation height, opening detection further approaches the reality found on ground. Second, vegetation height within openings is an important ecological factor which should be considered in the monitoring process of a given forested area (White et al., 2015). It allows conclusions to be drawn about the state of vegetation regeneration within openings. This is of special importance in areas where regrowth generation has been encouraged by ecological measurements such as the planting of seedlings or saplings (Wu et al., in prep.). This essential step cannot be reliably fulfilled by DAP data sets. As table 10 shows, vegetation height is continuously overestimated by the DAP and even the Hybrid data sets, which would lead to an overly positive evaluation of the regrowth vegetation height, possibly a reduction in political and/or technical support of plant regrowth and overall a misrepresentation of the state of the boreal forest in general. Regarding shape index, no significant difference is detected, which leads to the conclusion that for the assessments of edge effects, both ALS, and DAP and Hybrid data sets might be appropriate means.

While ALS generally fulfills all requirements to accurately characterize the disturbance patterns of the forest at hand, the ecosystem of the AoI is further disrupted by human interference which is not as apparent from either ALS and/or DAP data sets. These include effects the oil sand mining activities have on the boreal forest, such as toxicity levels in local streams and rivers, which have been shown to be elevated near oil sands fields in Alberta for 13 priority pollutants (PPE) by Kelly et al. (2010). Another impact human disturbance might exert on the boreal forest is a change in species composition and changes in biodiversities, both alpha biodiversity within openings, as well as beta biodiversity between openings and forested areas. Correspondingly, species population shifts have been noticed in the study area, such that within linear features, deer and bear population raise markedly (Hebblewhite, 2017).

In conclusion, ALS is an appropriate means of characterizing human disturbance in the study area, as well as naturally cause openings. DAP and Hybrid datasets show more limited possibilities of application. Using these approaches, a majority of human disturbance, but not

all of its impacts, can be detected. The greatest shortcomings lie in densely vegetated areas, where even long stretches of linear features can go unnoticed by a DSM_{DAP}. In order to not only detect and map disturbances, but characterize the impacts they have on the ecosystem, further research is needed into how the aforementioned effects of human interference might correlate with opening characteristics available from ALS and DAP products. Links might be found between biodiversity and, among others, factors such as vegetation structure, underlying substrate, opening size.

7.4 Can ALS or DAP help fulfill the goals stated by the Provincial Woodland Caribou Range Plan?

The PWCRP intends for a detailed monitoring process of the woodland caribou habitat, which coincides with the AoI (Alberta Government, 2017). ALS_VAR was able to help answer all three demands posed by the PWCRP in order to define landscape condition. The area of anthropogenic disturbance features was classified, albeit manually, with the visual support of opening classification using ALS_VAR. Research on an automated approach to delineate linear features in the study has been undertaken by Cole et al. (2016) and showed promising results. However, identifying pixels with sub-meter accuracy to be affected by an opening or not is heavily supported by 3D data such as ALS data sets.

The area affected by natural disturbance was reliably identified by ALS_VAR. ALS_VAR showed the greatest overall accuracy, and, most importantly for the detection of small scale, naturally caused disturbances, showed the highest accuracies for class 1 and 2 openings, where the DAP and Hybrid data sets showed errors of omission of up to 93%. This step could hardly be undertaken without the help of ALS data. The need for manual opening detection or the last resort solution of applying a differential vegetation index was avoided by using 3D data which allowed small scale opening classification with accuracies of 96% in identifying class 1-2 openings as such.

The amount and density of linear features was manually derived from the finished opening map produced on the basis of ALS_VAR. Linear features were clearly discernible from undisturbed forest areas and could therefore be counted and measured with high precision. Should this be applied to larger scale AoIs, an automated procedure, such as proposed by Cole et al. (2016) or a deep learning artificial intelligence (AI) would be appropriate.

The current study found that ALS_VAR was of significant assistance in the process of answering the PWCRP's monitoring goals to a large extent. However, some questions remain to be answered: first, how can areas of anthropogenic disturbance features be classified (automatically) by originating activity, and, second, how can the ALS products used in a more automated procedure in this undertaking.

7.5 Potential sources of error and room for improvement

Promising results were produced by ALS data, but DAP was only partially able to catch up with accuracies produced by ALS. This study has shown that there is still abundant room for further progress in this matter. Trying to improve the performance of DAP would prove to be a worthwhile investment promoting affordable and easy environmental monitoring. First,

potential sources of error shall be discussed, followed of a suggestion of further research questions.

The RTK GPS, while highly accurate in most cases, can suffer from noticeable errors when the connection between the rover and the satellite, or between the base station and the satellite is obstructed by a dense vegetation cover. This may affect the accuracy of the coordinates of ground sample points and thereby distort the accuracies of the opening detection procedures (Rahman et al., 2017). Since there was no way around sampling coordinates under dense canopy cover, these errors were reduced by waiting for the rover to receive a signal good enough for at least a 10 cm accuracy.

Furthermore, field classification was designed to perfectly sample the fixed height approach. This was done by determining whether sky was visible at breast height (1.3 m). Thus, the variable height approach was evaluated by a validation data set which was not specifically designed for this approach. To reduce impacts on the validation process, sample points previously collected in-situ were verified via visual image interpretation after the field campaign.

Another factor influencing the accuracies of the variable height approach is the technical derivation of the opening classification. In this study, this was done following the process presented by Gaulton & Malthus (2010) with altered threshold values. The biggest source of improvement is likely the choice of the value for the moving window. In the two aforementioned studies, the maximum value within the moving window was chosen as the new pixel value. Instead of the maximum value, standard deviation was also applied in this study, but it was discarded after accuracies and especially errors of omission increased further using a standard deviation instead of a maximum value moving window. Before analysis, the point clouds were cleaned of outliers and error points clearly above the canopy cover, but remaining single tall trees might still have noticeable impacts on the value of the moving window pixels. Alternatively, a 99 or 98 percentile applied to the ToC derivation before applying a moving window could get rid of very tall trees. However, since canopy height is relatively homogenous in the AoI, this might only yield a minor positive effect. In addition, a different approach than a moving window, such as an object based approach, might return even more reliable results.

Finally, even though there was no significant difference in accuracies between the DAP and Hybrid approaches, there is room for improvement in the production of a DAP derived DTM. For example, the patches of very large offset in figure 31 could be masked and interpolated with surrounding DTM values. This would provide a very coarse scale DTM, however, it would reduce the overestimation of ground values. Alternatively, the original point cloud could be thinned further to only contain the lowest points within 20 x 20 m or even 50 x 50 m grid squares. This way, the interpolation would again result in a very coarse resolution DTM, however, it would eliminate patches of high divergence from the DTM_{ALS}, which might produce a more realistic DTM overall.

This study, for the first time, compared ALS and DAP data sets for the detection and mapping of openings in the canopy cover of the boreal forest in northwestern Canada. While opening detection has been performed in tropical and temperate rain forests before (White et al., 2018), this is the first attempt at defining structural vs. functional openings, as was necessary in the AoI, given the highly variable forest structure between lowlands and highlands. The results found in this study are in line with findings from previous studies on the subject

matter of comparing ALS and DAP for characterizing forest structure. New additions, such as multi-image matching, the examination of class 1 structural openings and the improvement of the DSM_{DAP} by using a spike-free DSM triangulation approach, resulted in higher OvA values than those found by previous studies.

8 Conclusions and Outlook

This study set out to define canopy openings in the boreal forest of Alberta, Canada and to determine the capabilities of ALS and DAP to detect and map structural openings in said AoI. The investigation of opening detection accuracies has shown that DAP derived products, with and without the enhancement of using a DTM_{ALS}, did not produce the reliability and accuracy in detailed mapping of openings required to be considered a viable alternative to ALS data sets. While results for DAP and Hybrid techniques were better for the variable height approach, using the fixed height approach on these data sets resulted in worse OvA than when using a simple differential vegetation index. This study discussed the reasons for the lower OvA using DAP/Hybrid data sets: occlusions, shadows and tree sway make the detection of small openings especially hard and sometimes impossible to achieve using the optical method that is aerial photogrammetry.

The resulting marked differences in opening sizes, number of detected openings and limited spatial overlap indicate that DAP should not be used to detect and map small openings and even linear features in high density areas. The characterization of the boreal forest of Alberta was conducted with the highest OvA using ALS_VAR (93%), though ALS_FIX had an OvA of 90%. Both approaches applied to ALS produced reliable results in all size classes. The results of this study suggest thus that the perfect approach would consist of a combination of ALS_VAR and ALS_FIX, with the opening detection rate of ALS_VAR and the lower error of omission of small trees of ALS_FIX.

The investigation of CHM_{DAP} and CHM_{Hybrid} has shown that there is no significant improvement when using a DTM_{ALS} to enhance the CHM_{DAP}, and, conversely, there is no significant shortcoming of using a CHM_{DAP}. However, neither should be used when mapping small scale openings in the boreal forest of Alberta, since many factors can worsen the quality of a DSM derived from an optical data source, which leads to the omission of a marked number of small openings.

The evidence from this study suggests that ALS is an appropriate means to quantify human impact in the study area, as well as small scale structural openings of less than 4 m^2. The CHM_{DAP} and CHM_{Hybrid}, when used with the variable height threshold approach, suffice to map large human disturbances on a coarse scale, however, they do not fulfill the criteria for reliable detection of small scale human and natural disturbances in the AoI.

ALS_VAR facilitated in answering the questions stated by the PWCRP regarding the monitoring of the woodland caribou habitat. In combination with further in-situ and optical analysis, these findings can be further improved.

Taken together, these results suggest that ALS is an invaluable means for characterizing forest structure going beyond the mere detection and mapping of canopy openings. ALS point clouds can facilitate the monitoring of the current states of habitats, not just that of the woodland caribou. The characteristics of a disturbed vs. a pristine habitat are certainly species-specific, however, the results derived from ALS data sets can be applied to a wide range of ecological research questions. The next step inevitable is utilizing the produced results in a variety of modeling procedures, either to derive forest attributes straight from ALS point clouds, such as stem number, basal area, diameter, height and volume, or to implement them in bigger models. For example, an ALS derived DTM can be used for advanced local and regional hydrological

modeling, and impacts of increased solar radiation reaching the ground on biodiversity could be modeled based on a CHM_{ALS}. The final step is then to employ the resulting findings in appropriate management plans, policies and practices applied by the government, forestry professionals and possibly even oil exploitations companies themselves, such as spatial and temporal limitations of oil exploration campaigns and the usage of heavy machinery, afforestation, and continued progress supervision.

Given that DAP is an attractive, affordable and easily accessible data source, further research into the derivation of detailed CHMs from either DAP or Hybrid data sets is recommended. This would lead to a facilitation of monitoring, modeling and ultimately, management of vulnerable ecosystems like the Canadian boreal forest. At the current state, DAP is not able to produce the accuracies needed for reliable and helpful ecological inventory assessment, however, the results produced in this and other studies justify optimism that with further software and hardware development, 3D modeling of forest ecosystems will become more and more reliable and affordable

References

Abdullah, H., Darvishzadeh, R., Skidmore, A. K., Groen, T. A., & Heurich, M. (2018). European spruce bark beetle (Ips typographus, L.) green attack affects foliar reflectance and biochemical properties. *Int J Appl Earth Obs Geoinformation*, *64*, 199–209. https://doi.org/10.1016/j.jag.2017.09.009

Alberta Government. (2017). *DRAFT Provincial Woodland Caribou Range Plan.*

Allen, C. D., Macalady, A. K., Chenchouni, H., Bachelet, D., McDowell, N., Vennetier, M., et al. (2010). A global overview of drought and heat-induced tree mortality reveals emerging climate change risks for forests. *Forest Ecology and Management, 259*(4), 660-684. https://doi.org/10.1016/j.foreco.2009.09.001

Asner, G. P., Kellner, J. R., Kennedy-Bowdoin, T., Knapp, D. E., Anderson, C., & Martin, R. E. (2013). Forest Canopy Gap Distributions in the Southern Peruvian Amazon. *PLoS ONE*, *8*(4), 1-10. https://doi.org/10.1371/journal.pone.0060875

Athabasca Landscape Team. (2009). *Management Options. Athabasca Caribou Landscape Management Options Report.*

Barrette, M., Bélanger, L., De Grandpré, L., & Royo, A. A. (2017). Demographic disequilibrium caused by canopy gap expansion and recruitment failure triggers forest cover loss. *Forest Ecology and Management*, *401*, 117–124. https://doi.org/10.1016/j.foreco.2017.07.012

Bartels, S. F., Chen, H. Y. H., Wulder, M. A., & White, J. C. (2016). Trends in post-disturbance recovery rates of Canada's forests following wildfire and harvest. *Forest Ecology and Management*, *361*, 194–207. https://doi.org/10.1016/j.foreco.2015.11.015

Blumberg, S. (2018): May the forest be with you: GEDI moves toward launch to space station. URL: https://www.nasa.gov/feature/goddard/2018/may-the-forest-be-with-you-gedi-to-launch-to-iss. Accessed on September 6, 2018.

Bone, R. M. (2011): The Regional Geography of Canada. Fifth Edition. Oxford University Press.

Bonnet, S., Gaulton, R., Lehaire, F., & Lejeune, P. (2015). Canopy gap mapping from airborne laser scanning: An assessment of the positional and geometrical accuracy. *Remote Sensing*, *7*(9), 11267–11294. https://doi.org/10.3390/rs70911267

Brokaw, N. V. L. (1982). The Definition of Treefall Gap and Its Effect on Measures of Forest Dynamics. *Biotropica*, *14*(2), 158–160.

Brokaw, N. V. L. (1985). Gap-Phase Regeneration in a Tropical Forest. *Ecology*, *66*(3), 682–687.

Brokaw, N. V. L., & Scheiner, S. M. (1989). Species composition in gaps and structure of a tropical forest. *Ecology*, *70*(3), 538–541.

Burton, P. J., Parisien, M. A., Hicke, J. A., Hall, R. J., & Freeburn, J. T. (2008). Large fires as agents of ecological diversity in the North American boreal forest. *International Journal of Wildland Fire*, *17*(6), 754–767. https://doi.org/10.1071/WF07149

Busing, R. T., & White, P. S. (1997). Species Diversity and Small-Scale Disturbance in an Old-Growth Temperate Forest: A Consideration of Gap Partitioning Concepts. *OIKOS*, *78*(3), 562–568.

Canham, C. D., Denslow, J. S., Platt, W. J., Runkle, J. R., Spies, T. A., & White, P. S. (1990). Light regimes beneath closed canopies and tree-fall gaps in temperate and tropical forests. *Canadian Journal of Forest Research*, *20*, 620–631.

Caron, M.-N., Kneeshaw, D. D., De Grandpré, L., Kauhanen, H., & Kuuluvainen, T. (2009). Canopy Gap Characteristics and Disturbance Dynamics in Old-Growth Picea abies Stands in Northern Fennoscandia: Is the Forest in Quasi-Equilibrium? *Annales Botanici Fennici*, *46*(4), 251–262. https://doi.org/10.5735/085.046.0402

Cenovus (2018): Christina Lake. An oil sands project. URL: https://www.cenovus.com/operations/oilsands/christina-lake.html. Accessed on September 5, 2018.

Chen, J. M., & Cihlar, J. (2000). Retrieving Leaf Area Index of Boreal Conifer Forests Using Landsat TM Images. *Remote Sensing of Environment*, *162*, 153–162. https://doi.org/10.1016/0034-4257(95)00195-6

Chen, S., McDermid, G. J., Castilla, G., & Linke, J. (2017). Measuring vegetation height in linear disturbances in the boreal forest with UAV photogrammetry. *Remote Sensing*, *9*(12). https://doi.org/10.3390/rs9121257

Christensen, N. L., & Franklin, J. F. (1987). Small scale disturbance in forest ecosystems. *Bulleting of Ecological Society of America*, *68*, 51–60.

Coates, K. D. (2000). Conifer seedling response to northern temperate forest gaps. *Forest Ecology and Management, 127*, 249–269.

Cole, S., McDermid, G., Cranston, J., Palmer, M., Tigner, J., Hall-Beyer, Mryka (2016): A workflow for the semi-automated detection and attribution of linear features in a forested environment. Poster presentations at the BERA stakeholder engagement workshop 2016, Edmonton, AB. URL: http://www.bera-project.org/wp-content/uploads/2016/12/SCole_BERAposter.pdf (accessed Oct. 31, 2018).

Coppin, P. R., & Bauer, M. E. (1996). Digital Change Detection in Forest Ecosystems with Remote Sensing Imagery. *Remote Sensing Reviews*, *13*(3), 207–234.

Cumming, S. G., Schmiegelow, F. K. A., & Burton, P. J. (2000). Gap dynamics in boreal aspen stands: is the forest older than we think? *Ecological Applications*, *10*(3), 744–759.

Dabros, A., Pyper, M., & Castilla, G. (2018). Seismic lines in the boreal and arctic ecosystems of North America: environmental impacts, challenges, and opportunities. *Environmental Reviews*, *16*, 1–16. https://doi.org/10.1139/er-2017-0080

Dai, X. (1996). Influence of light conditions in canopy gaps on forest regeneration: A new gap light index and its application in a boreal forest in east-central Sweden. *Forest Ecology and Management*, *84*(1–3), 187–197. https://doi.org/10.1016/0378-1127(96)03734-6

Downing, D. J., & Pettapiece, W. W. (2006). *Natural Regions and Subregions of Alberta. Government of Alberta.*

Duncan, R. P., Buckley, H. L., Urlich, S. C., Stewart, G. H., & Geritzlehner, J. (1998). Small-Scale Species Richness in Forest Canopy Gaps : The Role of Niche Limitation versus the Size of the Species Pool. *Journal of Vegetation Science*, *9*(3), 455–460.

EMR. (2006). Yukon Oil and Gas Best Management Practices. *Yukon Government, Energy Mines and Resources, Oil and Gas Management Branch, Whitehorse, Y.T.*

Environment Canada. (2012). Recovery Strategy for the Woodland Caribou (Rangifer tarandus caribou), Boreal population, in Canada. *Species at Risk Act Recovery Strategy Series.* https://doi.org/10.2307/3796292

Erdody, T. L., & Moskal, L. M. (2010). Fusion of LiDAR and imagery for estimating forest canopy fuels. *Remote Sensing of Environment*, *114*(4), 725–737. https://doi.org/10.1016/j.rse.2009.11.002

Feldmann, E., Drößler, L., Hauck, M., Kucbel, S., Pichler, V., & Leuschner, C. (2018). Forest ecology and management canopy gap dynamics and tree understory release in a virgin beech forest, Slovakian Carpathians. *Forest Ecology and Management*, *415–416*, 38–46. https://doi.org/10.1016/j.foreco.2018.02.022

Ferreira De Lima, R. A. (2005). Gap size measurement: The proposal of a new field method. *Forest Ecology and Management*, *214*(1–3), 413–419. https://doi.org/10.1016/j.foreco.2005.04.011

Fox, T. J., Knutson, M. G., & Hines, R. K. (2000). Mapping forest canopy gaps using ground interpretation surveys. *Wildlife Society Bulletin*, *28*(4), 882–889.

Gaulton, R., & Malthus, T. J. (2010). LiDAR mapping of canopy gaps in continuous cover forests: A comparison of canopy height model and point cloud based techniques. *International Journal of Remote Sensing*, *31*(5), 1193–1211. https://doi.org/10.1080/01431160903380565

Government of Canada (2018): Environmental and Natural Resources. Historical Data. URL:

http://climate.weather.gc.ca/historical_data/search_historic_data_e.html. Accessed May 17, 2018.

Gray, A. N., & Spies, T. A. (1996). Gap Size, Within-Gap Position and Canopy Structure Effects on Conifer Seedling Establishment. *The Journal of Ecology*, *84*(5), 635. https://doi.org/10.2307/2261327

Gray, A. N., & Spies, T. A. (1997). Microsite Controls on Tree Seedling Establishment in Conifer Forest Canopy Gaps. *Ecology*, *78*(8), 2458–2473.

Hanel, R., Corominas-Murtra, B., Liu, B., & Thurner, S. (2017). Fitting power-laws in empirical data with estimators that work for all exponents. *PLoS ONE*, *12*(2), 1–15. https://doi.org/10.1371/journal.pone.0170920

Hardy, W.G. (1967): Alberta. A Natural History. Hurtig.

Hebblewhite, M. (2017). Billion dollar boreal woodland caribou and the biodiversity impacts of the global oil and gas industry. *Biological Conservation*, *206*, 102–111. https://doi.org/10.1016/j.biocon.2016.12.014

Hendl, M., Liedtke, H. (1997): Lehrbuch der Allgemeinen Physischen Geographie. Justus Perthes Verlag Gotha.

Hess, D., Tasa, D. (2014): McKnight's Physical Geography – A Landscape Appreciation. Eleventh Edition. Pearson Education Ltd.

Holopainen, M., Vastaranta, M., Karjalainen, M., Karila, K., Kaasalainen, S., Honkavaara, E., & Hyyppä, J. (2015). Forest Inventory Attribute Estimation Using Airborne Laser Scanning, Aerial Stereo Imagery, Radargrammetry and Interferometry–Finnish Experiences of the 3D Techniques. *ISPRS Annals of Photogrammetry, Remote Sensing and Spatial Information Sciences*, *II-3/W4*(March), 63–69. https://doi.org/10.5194/isprsannals-II-3-W4-63-2015

Hörnberg, G., Ohlson, M., & Zackrisson, O. (2011). Stand dynamics, regeneration patterns and long-term continuity in boreal old-growth Picea abies swamp-forests. *Journal of Vegetation Science*, *6*(2), 291–298.

Isenburg (2016): rapidlasso GmbH – Generating spike free digital surface models from LiDAR. URL: https://rapidlasso.com/2016/02/03/generating-spike-free-digital-surface-models-from-lidar/. Accessed October 11, 2018.

Isenburg (2018): rapidlasso GmbH – LAStools. URL: https://rapidlasso.com/lastools/. Accessed October 2, 2018.

Järnstedt, J., Pekkarinen, A., Tuominen, S., Ginzler, C., Holopainen, M., & Viitala, R. (2012). Forest variable estimation using a high-resolution digital surface model. *ISPRS Journal of Photogrammetry and Remote Sensing*, *74*, 78–84.

https://doi.org/10.1016/j.isprsjprs.2012.08.006

Jet Propulsion Laboratory (2018): Shuttle Radar Topography Mission. URL: https://www2.jpl.nasa.gov/srtm/. Accessed on August 29, 2018.

Jönsson, A. M., Eklundh, L., Hellström, M., Bärring, L., & Jönsson, P. (2010). Annual changes in MODIS vegetation indices of Swedish coniferous forests in relation to snow dynamics and tree phenology. *Remote Sensing of Environment*, *114*, 2719–2730. https://doi.org/10.1016/j.rse.2010.06.005

Kellner, J. R., & Asner, G. P. (2009). Convergent structural responses of tropical forests to diverse disturbance regimes. *Ecology Letters*, *12*(9), 887–897. https://doi.org/10.1111/j.1461-0248.2009.01345.x

Kelly, E. N., Schindler, D. W., Hodson, P. V, Short, J. W., Radmanovich, R., & Nielsen, C. C. (2010). Oil sands development contributes elements toxic at low concentrations to the Athabasca River and its tributaries. *PNAS*, *107*(37), 16178–16183. https://doi.org/10.1073/pnas.1008754107

Kershaw, J.A., Ducey, Jr. M. J., Beers, T.W., Husch, B. (2016): Forest Mensuration. Fifth Edition. John Wiley & Sons.

Kneeshaw, D. D., & Bergeron, Y. (1998). Canopy Gap Characteristics and Tree Replacement in the Southeastern Boreal Forest. *Ecology*, *79*(3), 783–794.

Kottek, M., Grieser, J., Beck, C., Rudolf, B., & Rubel, F. (2006). World map of the Köppen-Geiger climate classification updated. *Meteorologische Zeitschrift*, *15*(3), 259–263. https://doi.org/10.1127/0941-2948/2006/0130

Kubota, Y. (1995). Effects of disturbance and size structure on the regeneration process in a sub-boreal coniferous forest, northern Japan. *Ecological Research*, *10*(2), 135–142. https://doi.org/10.1007/BF02347935

Kukkonen, M., Maltamo, M., & Packalen, P. (2017). Image matching as a data source for forest inventory – Comparison of Semi-Global Matching and Next-Generation Automatic Terrain Extraction algorithms in a typical managed boreal forest environment. *International Journal of Applied Earth Observation and Geoinformation*, *60*, 11–21. https://doi.org/10.1016/j.jag.2017.03.012

Lawton, R., & Putz, F. E. (1988). Natural Disturbance and Gap-Phase Regeneration in a Wind-Exposed Tropical Cloud Forest. *Ecology*, *69*(3), 764–777.

Leberl, F., Irschara, A., Pock, T., Meixner, P., Gruber, M., Scholz, S., & Wiechert, A. (2010). Point Clouds: Lidar versus 3D Vision. *Photogrammetric Engineering & Remote Sensing*, *76*(10), 1123–1134. https://doi.org/0099-1112/10/7610–1123

Leemans, R. (1991). Canopy gaps and establishment patterns of spruce (Picea abies (L.) Karst.)

in two old-growth coniferous forests in central Sweden. *Vegetatio*, *93*(2), 157–165.

Lefsky, M. A., Cohen, W. B., & Spies, T. A. (2001). An evaluation of alternate remote sensing products for forest inventory, monitoring, and mapping of Douglas-fir forests in western Oregon. *Canadian Journal of Forest Research*, *31*(1), 78–87. https://doi.org/10.1139/x00-142

Lefsky, M. A., Cohen, W. B., Parker, G. G., & Harding, D. J. (2002). Lidar Remote Sensing for Ecosystem Studies. *BioScience*, *52*(1), 19–30.

Lertzman, K. P., Sutherland, G. D., Inselberg, A., & Saunders, S. C. (1996). Canopy Gaps and the Landscape Mosaic in a Coastal Temperate Rain Forest. *Ecology Ecology*, *77*(4), 1254–1270. https://doi.org/10.2307/2265594

Lillesand, T.M., Kiefer, R.W., Chipman, J.W. (2015): Remote Sensing and Image Interpretation. Seventh Edition. Wiley

Linke, J., Fortin, M.-J., Courtenay, S., & Cormier, R. (2017). High-resolution globalmaps of 21st-century annual forest loss: Independent accuracy assessment and application in a temperate forest region of Atlantic Canada. *Remote Sensing of Environment*, *188*, 164–176.

Lloyd, J., Gloor, E. U., & Lewis, S. L. (2009). Are the dynamics of tropical forests dominated by large and rare disturbance events? *Ecology Letters*, *12*(12), 19–21. https://doi.org/10.1111/j.1461-0248.2009.01326.x

Lobo, E., & Dalling, J. W. (2014). Spatial scale and sampling resolution affect measures of gap disturbance in a lowland tropical forest: Implications for understanding forest regeneration and carbon storage. *Proceedings of the Royal Society B: Biological Sciences*, *281*(1778). https://doi.org/10.1098/rspb.2013.3218

Lovitt, J., Rahman, M. M., & McDermid, G. J. (2017). Assessing the value of UAV photogrammetry for characterizing terrain in complex peatlands. *Remote Sensing*, *9*(7), 1–13. https://doi.org/10.3390/rs9070715

Lovitt, J., Rahman, M. M., Saraswati, S., McDermid, G. J., Strack, M., & Xu, B. (2018). UAV remote sensing can reveal the effects of low-impact seismic lines on surface morphology, hydrology, and methane (CH4) release in a boreal treed bog. *Journal of Geophysical Research: Biogeosciences*.

Mccarthy, J. (2001). Gap dynamics of forest trees: A review with particular attention to boreal forests. *Environ. Rev*, *9*, 1–59.

McDonald, A. J., Gemmell, F. M., & Lewis, P. E. (1998). Investigation of the Utility of Spectral Vegetation Indices for Determining Information on Coniferous Forests. *Remote Sensing of Environment*, *66*, 250–272.

McGarigal, K., & Marks, B. (1995). FRAGSTATS: Spatial pattern analysis program for quantifying landscape structure. *United States Department of Agriculture, Pacific Northwest Research Station.*, (August), 120 pages. https://doi.org/10.1061/(ASCE)0733-9437(2005)131:1(94) CE

Muscolo, A., Bagnato, S., Sidari, M., & Mercurio, R. (2014). A review of the roles of forest canopy gaps. *Journal of Forestry Research*, *25*(4), 725–736. https://doi.org/10.1007/s11676-014-0521-7

Næsset, E. (2015). Vertical height errors in digital terrain models derived from airborne laser scanner data in a boreal-alpine ecotone in Norway. *Remote Sensing*, *7*(4), 4702–4725. https://doi.org/10.3390/rs70404702

Nagel, T. A., Svoboda, M., Rugani, T., & Diaci, J. (2010). Gap regeneration and replacement patterns in an old-growth Fagus-Abies forest of Bosnia-Herzegovina. *Plant Ecology*, *208*(2), 307–318. https://doi.org/10.1007/s11258-009-9707-z

Nakashizuka, T. (1987). Regeneration dynamics of beech forests in Japan. *Vegetatio*, *69*, 169–175.

Poage, N. J., & Peart, D. R. (1993). The Radial Growth Response of American Beech (Fagus grandifolia) to Small Canopy Gaps in a Northern Hardwood Forest. *Bulletin of the Torrey Botanical Club*, *120*(1), 45–48.

Rahman, M. M., McDermid, G. J., Strack, M., & Lovitt, J. (2017). A new method to map groundwater table in peatlands using unmanned aerial vehicles. *Remote Sensing*, *9*(10), 1–14. https://doi.org/10.3390/rs9101057

Remondino, F., Spera, M. G., Nocerino, E., Menna, F., & Nex, F. (2014). State of the art in high density image matching. *The Photogrammetric Record*, *29*(146), 144–166. https://doi.org/10.1111/phor.12063

Van Rensen, C. K., Nielsen, S. E., White, B., Vinge, T., & Lieffers, V. J. (2015). Natural regeneration of forest vegetation on legacy seismic lines in boreal habitats in Alberta's oil sands region. *Biological Conservation*, *184*, 127–135. https://doi.org/10.1016/j.biocon.2015.01.020

Riva, F., Acorn, J. H., & Nielsen, S. E. (2018). Localized disturbances from oil sands developments increase butterfly diversity and abundance in Alberta's boreal forests. *Biological Conservation*, *217*(April 2017), 173–180. https://doi.org/10.1016/j.biocon.2017.10.022

Runkle, J. R. (1982). Patterns of disturbance in some old-growth mesic forests of eastern North America. *Ecology*, *63*(5), 1533–1546.

Runkle, J. R. (1992). Guidelines and Sample Protocol for Sampling Forest Gaps. *Portland: US Department of Agriculture, Forest Service, Pacific Northwest Research Station* (Vol. 283).

https://doi.org/10.1029/2010WR009341

Sachs, L. & Hedderich, J. (2009): Angewandte Statistik. Methodensammlung mit R. Springer

Safranyik, L., Carroll, A. L., Régnière, J., Langor, D. W., Riel, W. G., Shore, T. L., et al. (2010). Potential for range expansion of mountain pine beetle into the boreal forest of North America. *Canadian Entomologist*, *142*(5), 415–442. https://doi.org/10.4039/n08-CPA01

Schnitzer, S. A., & Carson, W. P. (2001). Treefall gaps and the maintenance of species diversity in a tropical forest. *Ecology*, *82*(4), 913–919.

Senf, C., Seidl, R., & Hostert, P. (2017). Remote sensing of forest insect disturbances: Current state and future directions. *Int J Appl Earth Obs Geoinformation*, *60*, 49–60. https://doi.org/10.1016/j.jag.2017.04.004

Severson-Baker, C. (2004). *Seismic Exploration. Environment & Energy in the North*. Retrieved from http://www.pembina.org/pub/168

Stan, A. B., & Daniels, L. D. (2018). Growth releases of three shade-tolerant species following canopy gap formation in old- growth forests. *Journal of Vegetation Science*, *21*(1), 74–87. https://doi.org/10.1 lll/j.1654-1 103.2009.01 120.x

Stewart, G. H., Rose, A. B., & Veblen, T. T. (1991). Forest Development in Canopy Gaps in Old-Growth Beech (Nothofagus) Forests, New-Zealand. *Journal of Vegetation Science*, *2*(5), 679–690. https://doi.org/10.2307/3236178

Timoney, K. P. (2003). The changing disturbance regime of the boreal forest of the Canadian Prairie Provinces. *Forestry Chronicle*, *79*(3), 502–516. https://doi.org/10.5558/tfc79502-3

Vastaranta, M., Wulder, M. A., White, J. C., Pekkarinen, A., Tuominen, S., Ginzler, C., et al. (2013). Airborne laser scanning and digital stereo imagery measures of forest structure: Comparative results and implications to forest mapping and inventory update. *Canadian Journal of Remote Sensing*, *39*(5), 382–395. https://doi.org/10.5589/m13-046

Veblen, T. T. (1985). Forest development in tree-fall gaps in the temperate rain forest of Chile. *National Geographic Research*, (Spring), 162–183.

Vehmas, M., Packalén, P., Maltamo, M., & Eerikäinen, K. (2011). Using airborne laser scanning data for detecting canopy gaps and their understory type in mature boreal forest. *Annals of Forest Science*, *68*(4), 825–833. https://doi.org/10.1007/s13595-011-0079-x

Vepakomma, U., St-Onge, B., & Kneeshaw, D. (2008). Spatially explicit characterization of boreal forest gap dynamics using multi-temporal lidar data. *Remote Sensing of Environment*, *112*(5), 2326–2340. https://doi.org/10.1016/j.rse.2007.10.001

Vepakomma, U., Kneeshaw, D., & St-Onge, B. (2010). Interactions of multiple disturbances in shaping boreal forest dynamics: A spatially explicit analysis using multi-temporal lidar data and high-resolution imagery. *Journal of Ecology*, *98*(3), 526–539. https://doi.org/10.1111/j.1365-2745.2010.01643.x

Vepakomma, U., St-onge, B., & Kneeshaw, D. (2011). Response of a boreal forest to canopy opening: assessing vertical and lateral tree growth with multi-temporal lidar data. *Ecological Applications*, *21*(1), 99–121.

Vepakomma, U., Kneeshaw, D., & Fortin, M. J. (2012). Spatial contiguity and continuity of canopy gaps in mixed wood boreal forests: Persistence, expansion, shrinkage and displacement. *Journal of Ecology*, *100*(5), 1257–1268. https://doi.org/10.1111/j.1365-2745.2012.01996.x

White, J. C., Wulder, M. A., Vastaranta, M., Coops, N. C., Pitt, D., & Woods, M. (2013). The utility of image-based point clouds for forest inventory: A comparison with airborne laser scanning. *Forests*, *4*(3), 518–536. https://doi.org/10.3390/f4030518

White, J. C., Stepper, C., Tompalski, P., Coops, N. C., & Wulder, M. A. (2015). Comparing ALS and image-based point cloud metrics and modelled forest inventory attributes in a complex coastal forest environment. *Forests*, *6*(10), 3704–3732. https://doi.org/10.3390/f6103704

White, J. C., Tompalski, P., Coops, N. C., & Wulder, M. A. (2018). Comparison of airborne laser scanning and digital stereo imagery for characterizing forest canopy gaps in coastal temperate rainforests. *Remote Sensing of Environment*, *208*, 1–14. https://doi.org/10.1016/j.rse.2018.02.002

Whitmore, T. C. (1989). Canopy gaps and the two major groups of forest trees. *Ecology*, *70*(3), 536–538.

Wu, M.F., Rahman, M.M., McDermid, G., Castilla, G. (in preparation). Remote sensing tools for conifer stocking assessment. Automated object-based analysis. Poster presentations at the BERA stakeholder engagement workshop 2018, Edmonton, AB.

Wulder, M. (1998). Progress in Physical Geography parameters Optical remote-sensing techniques for the assessment of forest inventory and biophysical parameters. *Progress in Physical Geography*, *22*(4), 449–476. https://doi.org/10.1177/030913339802200402

Zhang, K. (2008). Identification of gaps in mangrove forests with airborne LIDAR. *Remote Sensing of Environment*, *112*(5), 2309–2325. https://doi.org/10.1016/j.rse.2007.10.003

Zhirin, V. M., Knyazeva, S. V, & Eydlina, S. P. (2016). Long-Term Dynamics of Vegetation Indices in Dark Coniferous Forest after Siberian Moth Disturbance. *Contemporary Problems of Ecology*, *9*(7), 834–843. https://doi.org/10.1134/S1995425516070118

Zielewska-Büttner, K., Adler, P., Ehmann, M., & Braunisch, V. (2016). Automated detection

of forest gaps in spruce dominated stands using canopy height models derived from stereo aerial Imagery. *Remote Sensing*, *8*(5), 1–21. https://doi.org/10.3390/rs9050471

Zieli, K. M., Kiedrzy, M., & Chmura, D. (2018). Anthropogenic linear gaps in managed forests – Plant traits are associated with the structure and function of a gap. *Forest Ecology and Management, 413*, 76–89. https://doi.org/10.1016/j.foreco.2018.02.001

Zolkos, S. G., Goetz, S. J., & Dubayah, R. (2013). A meta-analysis of terrestrial aboveground biomass estimation using lidar remote sensing. *Remote Sensing of Environment*, *128*, 289–298. https://doi.org/10.1016/j.rse.2012.10.017

Eigenständigkeitserklärung (German)

Ich versichere, dass ich die vorliegende Arbeit selbständig verfasst habe, keine anderen als die angegebenen Quellen oder Hilfsmittel benutzt, sowie Zitate als solche gekennzeichnet habe.

Ort, Datum	Unterschrift
	Annette Dietmaier

Appendix

Appendix A: Digital Terrain Models from ALS and DAP

Appendix B: Batch scripts for the processing of ALS and DAP points clouds

Appendix C: Field Plan

Appendix D: Confusion matrices

Appendix A: Visualization of Digital Terrain Models derived from ALS and DAP. Values are m above sea level.

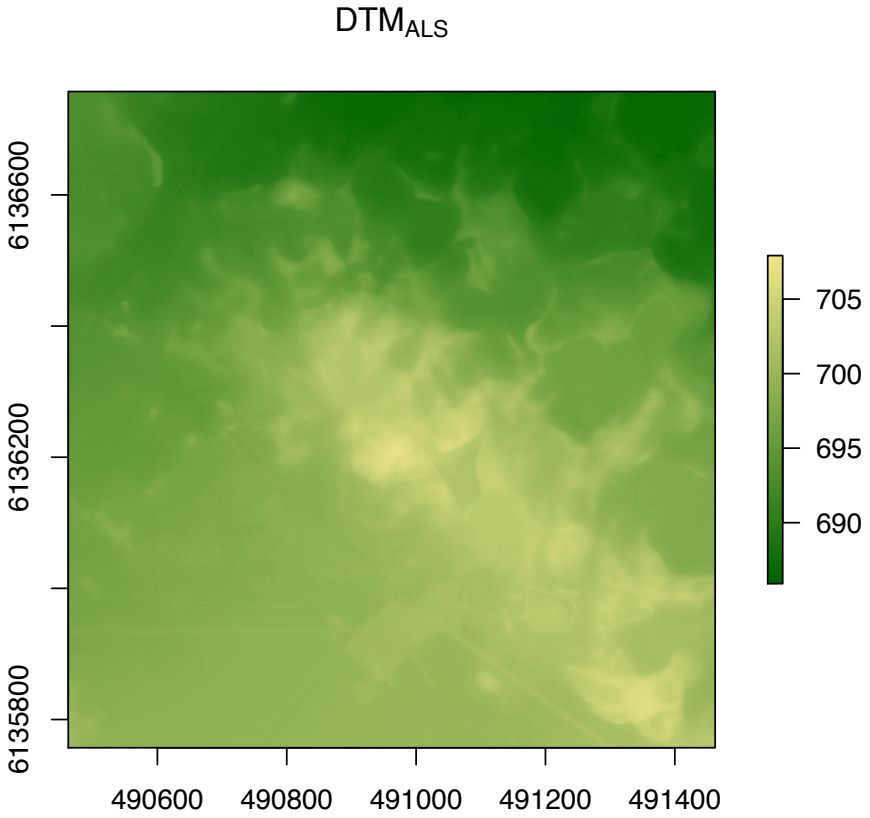

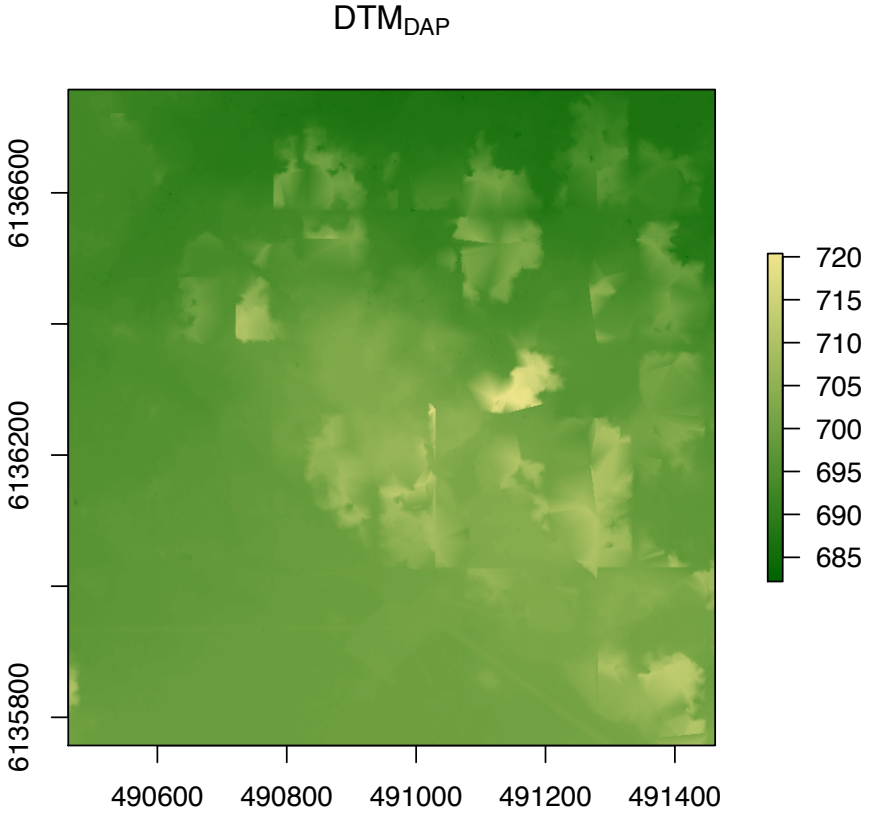

Appendix B: Batch scripts for 3D points clouds

The following batch scripts derive DTMs, DSMs and CHMs. First, the batch script processing ALS data is presented. The following two batch scripts process DAP data. The detailed purpose of each batch script is specified in the first line.

Appendix B 1: Batch script for ALS data

```
:: Batch script for the processing of LiDAR data into DEM, DSM and
CHM
:: Author: Annette Dietmaier
:: Calgary, August 2018


:::::::::::::::
:: Set paths ::
:::::::::::::::

:: sets Path to the folder that stores las binary files
SET PATH=%PATH%;E:\Annette\LAStools\bin;

:: set path to the folder that will contain the results and the raw
file
SET FILES=E:\Annette\ALS

:: sets path to raw lidar file
set RAW_LIDAR=%FILES%\*.laz

:: sets path to normalized file with subcircles
set SUBCIRCLE_NORMALIZED=%FILES%\subcircle_normalized\*.laz

:: make temporary storage folder for partial CHMS
set TEMP_CHM_DIR=%Files%\Products\CHM


:::::::::::::::::::::::::
::  Check Input Files  ::
:::::::::::::::::::::::::

:: check if file conforms to the ASPRS LAS 1.0 to 1.4 specifications
lasvalidate -i %RAW_LIDAR% ^
           -o %FILES%\validate_report.xml

start %FILES%\validate_report.xml


::::::::::::::::::::
:: Set parameters ::
::::::::::::::::::::
```

```
set STEP=0.2
set SPIKE=0.3
SET CORES=5
set KILL=0.45
set SUBCIRC=0.2

ECHO Start computing


::::::::::::::::::::
:: START COMPUTING ::
::::::::::::::::::::

:: 1. Visualize

lasview -i %RAW_LIDAR%

:: 2. Make data manageable by creating files that are easier to
compute

lastile -i %RAW_LIDAR% ^
           -tile_size 250 ^
           -buffer 10 ^
           -cores %CORES% ^
           -odir %FILES%\tiles ^
           -olaz

:: 3. Classify noise

lasnoise -i %FILES%\tiles\*.laz ^
           -cores %CORES% ^
           -odir %FILES%\noise ^
           -olaz

:: 4. Classify ground

lasground_new -i %FILES%\noise\*.laz ^
           -compute_height ^
           -ignore_class 7 ^
           -spike %SPIKE% ^
           -wilderness ^
           -cores %CORES%% ^
           -odir %FILES%\ground ^
           -olaz

:: 5 Classification
:: 5.1 Classify vegetation, buildings etc. (requires height to be
computed in step 4)
```

```
lasclassify -i %FILES%\ground\*.laz ^
           -small_trees ^
           -small_buildings ^
           -drop_classification 7 ^
           -cores %CORES% ^
           -odir %FILES%\classified ^
           -olaz

:: 5.2 Manual classification of noise etc.


::::::::::::::::::::
:: Derive Products ::
::::::::::::::::::::

:: 6 Rasterize DEM

las2dem -i %FILES%\classified\*.laz ^
           -keep_classification 2 ^
           -elevation ^
           -use_tile_bb ^
           -step %STEP% ^
           -cores %CORES% ^
           -odir %FILES%\Products\DEM ^
           -obil

:: 7 Rasterize DSM

lasthin -i %FILES%\classified\*.laz ^
           -subcircle %SUBCIRC% ^
           -step %STEP% ^
           -ignore_class 7 ^
           -highest ^
           -cores %CORES% ^
           -odir %FILES%\subcircle ^
           -olaz

las2dem -i %FILES%\subcircle\*.laz ^
           -elevation ^
           -use_tile_bb ^
           -step %STEP% ^
           -cores %CORES% ^
           -odir %FILES%\Products\DSM ^
           -obil

:: 9.Rasterize CHM
:: 9.1 Normalize Image for CHM (should have been in done step 4,
this step is just for reinssurance) and lose points classified as
anything else but ground and vegetation
```

```
lasheight -i %FILES%\classified\*.laz ^
          -replace_z ^
          -drop_below 0 ^
          -cores %CORES% ^
          -drop_classification 7 ^
          -drop_classification 6 ^
          -odir %FILES%\normalized ^
          -olaz

:: 9.2 Thin data set to include highest points only, and duplicate
each point in a certain perimeter to represent width of laser beam

lasthin -i %FILES%\normalized\*.laz ^
 -subcircle %SUBCIRC% ^
 -step %STEP% ^
 -highest ^
 -drop_classification 6 ^
 -drop_classification 7 ^
 -odir %FILES%\subcircle_normalized ^
 -olaz

:: 9.3 Five sets of blast2dem to detect highest points only,
starting at different minimum heights. This will create a spike-free
CHM

blast2dem -i %SUBCIRCLE_NORMALIZED% ^
 -step %STEP% ^
 -cores %CORES% ^
 -drop_classification 6 ^
 -drop_classification 7 ^
 -use_tile_bb ^
 -odir %TEMP_CHM_DIR% -odix _00 -obil

blast2dem -i %SUBCIRCLE_NORMALIZED% ^
 -drop_z_below 5 ^
 -step %STEP% -kill %KILL% ^
 -cores %CORES% ^
 -use_tile_bb ^
 -drop_classification 6 ^
 -drop_classification 7 ^
 -odir %TEMP_CHM_DIR% -odix _05 -obil

blast2dem -i %SUBCIRCLE_NORMALIZED% ^
 -drop_z_below 10 ^
 -step %STEP% -kill %KILL% ^
 -cores %CORES% ^
 -use_tile_bb ^
 -drop_classification 6 ^
 -drop_classification 7 ^
 -odir %TEMP_CHM_DIR% -odix _10 -obil
```

```
blast2dem -i %SUBCIRCLE_NORMALIZED% ^
 -drop_z_below  15 ^
 -step %STEP% -kill %KILL% ^
 -cores %CORES% ^
 -use_tile_bb ^
 -drop_classification 6 ^
 -drop_classification 7 ^
 -odir %TEMP_CHM_DIR% -odix _15 -obil

blast2dem -i %SUBCIRCLE_NORMALIZED% ^
 -drop_z_below 20 ^
 -step %STEP% -kill %KILL% ^
 -cores %CORES% ^
 -use_tile_bb ^
 -drop_classification 6 ^
 -drop_classification 7 ^
 -odir %TEMP_CHM_DIR% -odix _20 -obil

PAUSE
```

Appendix B 2: Batch script for DAP data (DTM derivation)

```
:: Batchscript for the processing of DAP data into DTM
:: Author: Annette Dietmaier
:: Munich, May 2018


:::::::::::::::
:: Set paths ::
:::::::::::::::

:: Sets Path to the folder that stores las binary files
SET PATH=%PATH%;D:\Annette\LAStools\bin;

:: set path to the folder that will contain the results and the raw
file
SET FILES=D:\Annette\DAP_LeafOff

:: sets path to raw DAP file
SET RAW_DAP=%FILES%\KirbySmallGridLeafOff2017.laz


:::::::::::::::::::::::::
::  Check Input Files  ::
:::::::::::::::::::::::::

:: check spatial resolution ("spacing") for input in spikefree
parameter
lasinfo -i %RAW_DAP% ^
           -last_only ^
           -compute_density


::::::::::::::::::::
:: Sets parameters ::
::::::::::::::::::::

set STEP=0.2
set CORES=11
set KILL=100

ECHO Start computing
```

```
::::::::::::::::::::
:: START COMPUTING ::
::::::::::::::::::::

:: 1. Visualize

lasview -i %RAW_DAP%

:: 2. Make data manageable by creating files that are easier to
compute

lastile -i %RAW_DAP% ^
           -tile_size 250 ^
           -buffer 30 ^
           -cores %CORES% ^
           -odir %FILES%\tiles ^
           -olaz

:: 3. Classify noise

lasnoise -i %FILES%\tiles\*.laz ^
           -cores %CORES% ^
           -odir %FILES%\noise ^
           -olaz

:: 4. Classify ground

lasthin -i %FILES%\tiles\*.laz ^
           -step 1 ^
           -lowest ^
           -cores %CORES% ^
           -odir %FILES%\thinned ^
           -odix _thinned ^
           -olaz

lasground_new -i %FILES%\thinned\*.laz ^
           -step 10 ^
           -bulge 0.5 ^
           -spike 0.1 ^
           -offset 0.1 ^
           -all_returns ^
           -drop_classification 7 ^
           -extra_coarse ^
           -compute_height ^
           -olaz ^
           -cores %CORES% ^
           -odir %FILES%\ground ^

:: 5. Manually classify noise in lasview
```

```
::::::::::::::::::::::::
:::: Derive Products ::::
::::::::::::::::::::::::

:: 6. Rasterize DTM

las2dem -i %FILES%\ground\*.laz ^
          -keep_classification 2 ^
          -elevation ^
          -kill %KiLL% ^
          -step %STEP% ^
          -cores %CORES% ^
          -odir %FILES%\DTM_tiles ^
          -obil
PAUSE
```

Appendix B 3: Batch script for DAP data (DSM derivation)

```
:: Batchscript for the processing of DAP data into DSM
:: Author: Annette Dietmaier
:: Munich, June 2018


:::::::::::::::
:: Set paths  ::
:::::::::::::::

:: Sets Path to the folder that stores las binary files
SET PATH=%PATH%;D:\Annette_forreal\LAStools\bin;

:: set path to the folder that will contain the results and the raw
file
SET FILES=D:\Annette\DAP_LeafOn

:: sets path to raw DAP file
SET RAW_DAP=%FILES%\KirbySmallGridLeafOn2017.laz

:: sets path to de-noised file with subcircles
set SUBCIRCLE="%FILES%\subcircle\*.laz


:::::::::::::::::::::::::
::  Check Input Files  ::
:::::::::::::::::::::::::

:: Check spatial resolution ("spacing") for input in spikefree
parameter
lasinfo -i %RAW_DAP% ^
           -last_only ^
           -compute_density


::::::::::::::::::::
:: Set parameters ::
::::::::::::::::::::

set STEP=0.1
set CORES=11
set SUBCIRC=0.1

ECHO Start computing
```

```
::::::::::::::::::::
:: START COMPUTING ::
::::::::::::::::::::

:: 1. Visualize

lasview -i %RAW_DAP%

:: 2. Make data manageable by creating files that are easier to
compute

lastile -i %RAW_DAP% ^
           -tile_size 250 ^
           -buffer 30 ^
           -cores %CORES% ^
           -odir %FILES%\tiles ^
           -olaz

:: 3 Classification
:: 3.1 Classify noise

lasnoise -i %FILES%\tiles\*.laz ^
           -cores %CORES% ^
           -odir %FILES%\noise ^
           -olaz

:: 3.2 Manual noise classification in lasview

PAUSE


:::::::::::::::::::::::::
:::: Derive Products ::::
:::::::::::::::::::::::::

:: 4. Thin data set to include highest points only, and duplicate
each point in a certain perimeter to represent width of laser beam

lasthin -i %FILES%\noise\*.laz ^
           -subcircle %SUBCIRC% ^
           -drop_classification 14 ^
           -drop_classification 6 ^
           -drop_classification 7 ^
           -step %STEP% ^
           -highest ^
           -cores %CORES% ^
           -odir %FILES%\subcircle ^
           -olaz
```

```
:: 6. Rasterize DSM

las2dem -i %FILES%\subcircle\*.laz ^
          -elevation ^
          -drop_classification 7 ^
          -use_tile_bb ^
          -step %STEP% ^
          -cores %CORES% ^
          -odir %FILES%\DSM_tiles ^
          -obil

PAUSE
```

Appendix C: Field Plan

Quantifying the effects of industrial disturbance on Boreal Forest Canopy Openings

Field Plan Summer 2018

Annette Dietmaier
MSc Student
Department of Geography, University of Calgary

Calgary, AB
June 2018

1 Introduction

In this study, we aim at quantifying the impact of human disturbance on Boreal Forests in Northern Alberta, Canada. The Boreal Forest of Alberta is not only home to wildlife species like the woodland caribou, wolves, moose and deer, but the same area covers the world's third largest oil bitumen deposit. While some of the boreal forest's species are endangered and require special protection in the shape of national and/or provincial wildlife conservancy legislation, oil sand in Alberta has been exploited for decades. To locate oil sand deposits, oil companies have cut down parts of the forest in linear features or seismic lines, which allow for the scanning of the soil beneath for bitumen. These seismic lines create a network of clear cut alleys spanning across vast areas of Alberta. Among their effects on the environment are direct and indirect negative impacts on wildlife like caribou and wolf populations (Hebblewhite, 2017).

To detect openings in the boreal forest, we are using four approaches: a LiDAR based Canopy Height Model (CHM), a CHM based on photogrammetric surface data and LiDAR terrain data, a Digital Aerial Photogrammetry (DAP) based approach and a traditional vegetation index based on a multispectral (RGB-N) image of the study site. We will compare their overall accuracies and their relative accuracies compared to the LiDAR based approach.

Many studies have been conducted on the generation and effects of openings in forest canopies, predominately focusing on both temporally and spatially discrete events. The majority of the literature studied temperate forests and rain forests, with only a handful of authors examining the forests of higher latitudes (Vepakomma et al., 2008). Ground based surveys are lengthy and costly and produce questionable results which are often affected by an error of omission of around 25% (White et al., 2018). The latest comparison of relative performances between LiDAR and DAP data in this application was done by White et al. (2018) who compare a LiDAR based CHM with a CHM for which the Surface Model was derived from DAP data.

Our study site is characterized by a higher variety in tree phenology, especially in height, than regions of interest in previous studies. Tree height in temperate and rain forests is usually homogenous, whereas the boreal forest of northern Alberta exhibits a wide range of tree height, with small trees growing in the bogs and fens of the lowlands, and pine trees reaching up to 35 m in height in the uplands. Given that 3D approaches are much more precise than ground based surveys (White et al., 2018), it is necessary to test previous approaches of 3D canopy detection for their applicability in the Canadian boreal forest. Furthermore, opening detection based on only DAP data will be tested and its relative performance compared to the LiDAR based approach will be determined.

We hypothesize that it is possible to generate a CHM with sufficient accuracy to detect openings that require treatment according to the Alberta wild life conservancy policies, using a solely DAP based approach, which would make mapping of canopy openings in areas affected by the oil sand industry more accessible and affordable and therefore more effective for wildlife protection than previous mapping techniques.

To test this hypothesis, we validate our digital models using ground truth data collected in our study site. This field plan details the methods applied to gather this information. Our variables

are *vegetation structure across the vertical scale (types A-F)*, which will be used to characterize results from the Variable Height Approach, and the *presence of an opening in the continuous canopy cover (Opening, No-Opening)*, which will be used to validate both the results from the Variable Height and Fixed Height Approaches. Conducting a GPS RTK survey when taking the measurements will provide the exact geolocation of each field site to enable synchronization of the ground truth data with the CHM models.

2 Study Area

2.1 Overview

The study site (fig. 1) is located near Conklin, AB. This part of the boreal forest is characterized by a mixture of uplands and lowlands, dispersed across gently undulating terrain (Natural Regions Committee, 2006). A significant share of the low-lying regions are treed bogs and fens, with black spruce and tamarack being the dominating tree species. Considering the bogs and fens of the low lands with the interspersing dry upland ridges (which are dominated by jack pine), the study area comprises a considerable variety of forest and tree phenology. The entire study site is affected by a multitude of seismic lines and some deactivated oil exploration infrastructure (Queiroz, 2018).

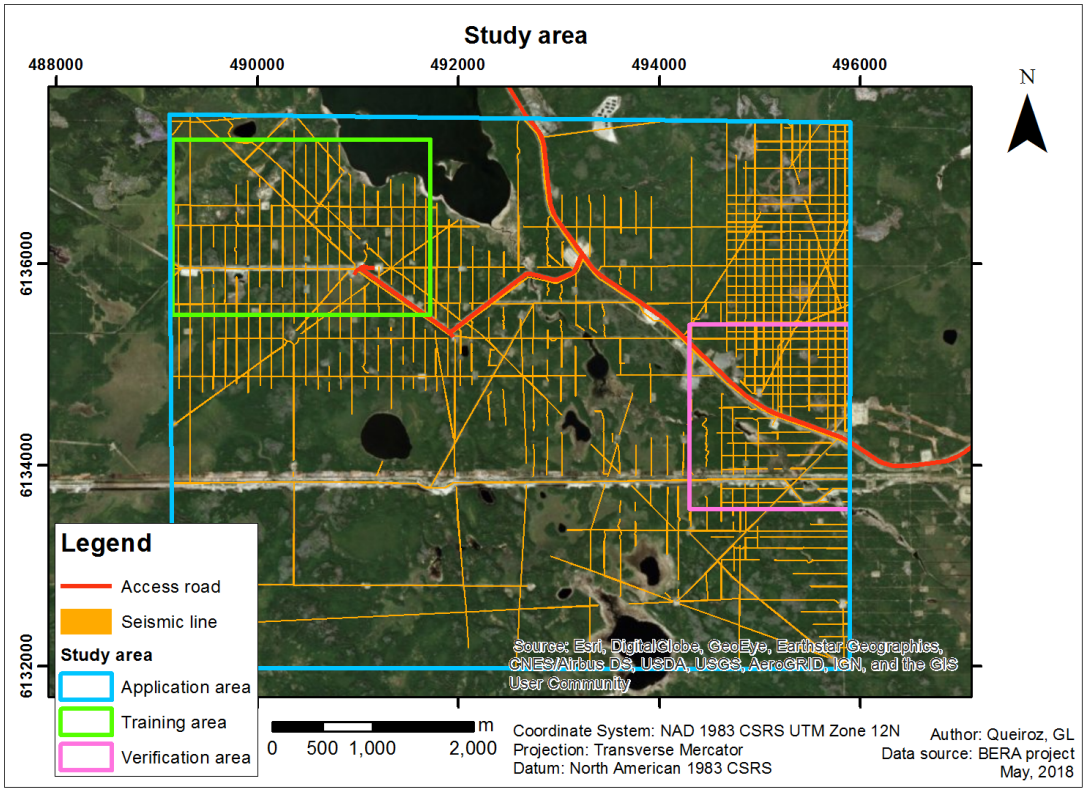

Figure 1 Area of Interest: Kirby South (application area), study area (training area), access roads and seismic lines.

2.2 Study sites

To assess opening detection capabilities regarding human disturbances vs. natural disturbances, and depending on opening size, the sampling points have been selected using a stratified sampling technique, using two strata:

1) Altered vs. natural areas in the study area

   a. Altered areas are defined as altered by human influence such as clear cuts, seismic lines, roads etc.

   b. Natural areas are defined as the inverse areas of the altered areas stratum

2) Opening class

   a. Opening class 0: No Opening

   b. Opening class 1: 0 – 4 m^2

   c. Opening class 2: 4 – 20 m^2

   d. Opening class 3: 20 – 200 m^2

   e. Opening class 4: > 200 m^2

Random points were selected within each stratum, the number of points depending on the size variability of openings within each opening size class. The list of coordinates to be sampled will be printed and readily available to surveyors.

3 Field Measurements

3.1 Sampling vertical vegetation structure

Upon arrival at a sample point, the surveyor will characterize the vertical vegetation structure at the sample point based on six schematic categories (fig. 2):

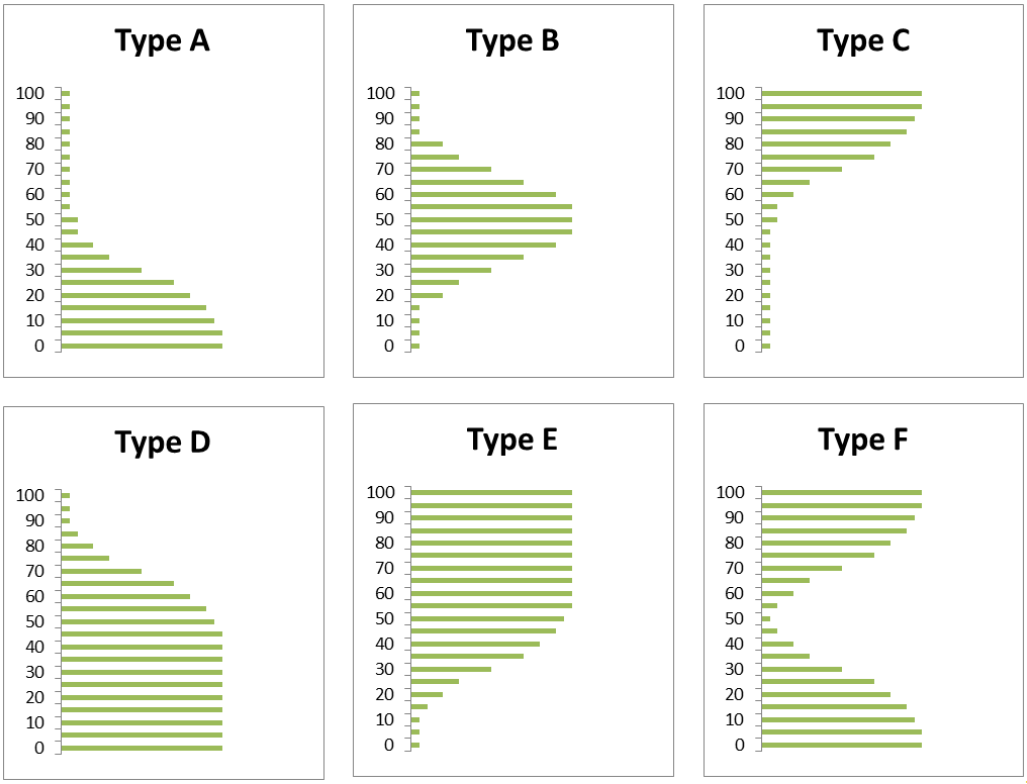

Figure 2 Types of vertical vegetation structure for ground sampling. This is a schematic classification of vegetation and should be used with discretion.

On the y-axis, 100 represents the top of the canopy. For example, if the bulk of the vegetation at the coordinate is growing in the lower vertical third, it is to be classified as Type A. If there

is a thick canopy layer in the upper third and dense understory vegetation, it will be classified as Type F. This information might be of use when assessing error patterns in the evaluation stage of this study.

3.2 Sampling crown closure

Crown closure will be determined based on the visibility of sky through the canopy cover. The surveyor will take a picture looking straight up, placing the camera at breast height (1.30 m).

* If the point sampled is exposed to the sky by an opening between two trees and not by openings within the canopy of one tree, it will be characterized as “opening”. The size class will have to be estimated by the surveyor.

* If the crown closure is not complete and allows for the sky to be visible on the ground, but there is no opening created by distance to another tree (e.g. thin and porous but homogenous canopies with little openings between the leaves or branches of the same tree), the point will be characterized as “no-opening”.

* If the sky overhead is not visible on the ground, the point will be characterized as “no-opening”

4 Field Protocol

1. Set up GPS RTK system
    a. projection: UTM 12 N, NAD 83
    b. measure antenna height
2. Approach site and note Point ID
3. Note GPS coordinates and time of acquisition
4. Take picture at 1.30 m looking straight up
5. Define “opening” or “no-opening” on the classification sheet
6. Classify vegetation according to the understory vegetation type classification sheet

5 Equipment list & Classification Sheets

- Navigation:
    - handheld GPS
    - orthophotos
    - site maps with sample points
    - compass
- Site sampling:
    - digital camera
    - field sheet (attached to this field plan)
    - pencils
    - eraser
    - clipboard
- Office:
    - Computer
    - ArcMap
    - Excel
    - LAStools
    - R

Canopy Closure and Understory Vegetation Point Classification Field Sheet	
Site Number:	Date:
Crew Members:	Start Time:
	End Time:

GPS Data	GPS Base Antenna Height:			Base Signal Strength:		
	Projection:			Datum:		
	Base X:		Base Y:		Base Z:	

Vertical vegetation structure	Opening size classification	Opening size
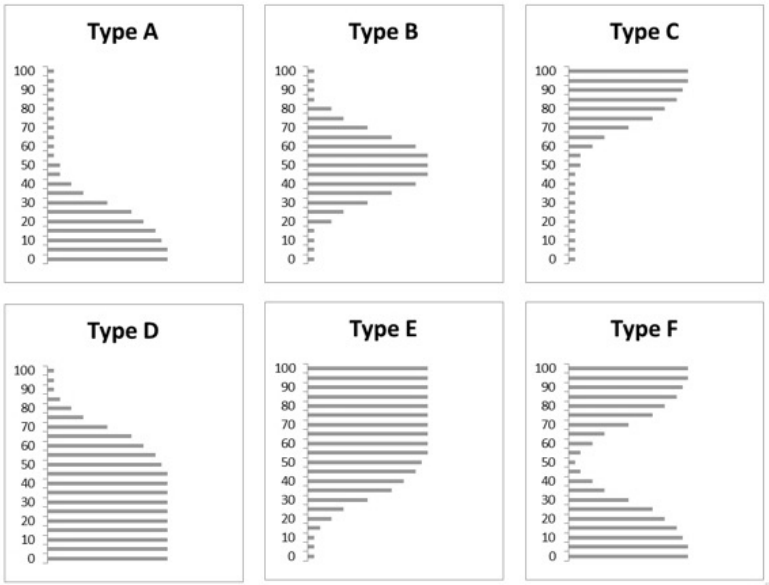	1	< 4 m^2
	2	4-20 m^2
	3	20 – 200 m^2
	4	> 200 m^2
	999	No opening
	Confidence in classification	
	1	Very confident (clearly the right size, clearly an opening/no opening)
	2	Somewhat confident (probably the right size, probably an opening/no opening)
	3	Not at all confident (size of opening uncertain)

Point ID	Coordinates		Picture Numbers		Opening Size Class	Confidence in Classification	Vegetation Structure
(Site #/ Consec. #)	X	Y	Up	Around	Class 1 - 4, 999		(Type A-F)

Appendix D: Confusion Matrices

In the following, the raw confusion matrices of the accuracy assessment are presented. They provide the data behind tables 5 and 6. First, binary assessment results will be shown (tables 15 – 20), followed by the assessment relative to opening size class (tables 21 – 26).

Table 15 Confusion matrix for ALS_FIX, binary opening detection.

ALS_FIX	Reference 0	Reference 1
Classified 0	336	147
Classified 1	28	1324

Table 16 Confusion matrix for DAP_FIX, binary opening detection.

DAP_FIX	Reference 0	Reference 1
Classified 0	357	680
Classified 1	7	791

Table 17 Confusion matrix for Hybrid_FIX, binary opening detection.

Hybrid_FIX	Reference 0	Reference 1
Classified 0	357	654
Classified 1	7	817

Table 18 Confusion matrix for ALS_VAR, binary opening detection.

ALS_VAR	Reference 0	Reference 1
Classified 0	258	22
Classified 1	106	1449

Table 19 Confusion matrix for DAP_VAR, binary opening detection.

DAP_VAR	Reference 0	Reference 1
Classified 0	265	230
Classified 1	99	1241

Table 20 Confusion matrix for Hybrid_VAR, binary opening detection.

Hybrid_VAR	Reference 0	Reference 1
Classified 0	278	245
Classified 1	86	1226

Table 21 Confusion matrix for ALS_FIX, relative to reference by opening size class.

	Reference Opening Size Class				
ALS_FIX	1	2	3	4	No Opening
Opening	154	101	182	887	29
No Opening	47	20	22	57	336

Table 22 Confusion matrix for DAP_FIX, relative to reference by opening size class.

	Reference Opening Size Class				
DAP_FIX	1	2	3	4	No Opening
Opening	14	10	61	706	8
No Opening	187	111	143	238	357

Table 23 Confusion matrix for Hybrid_FIX, relative to reference by opening size class.

	Reference Opening Size Class				
Hybrid_FIX	1	2	3	4	No Opening
Opening	14	10	68	725	8
No Opening	187	111	136	219	357

Table 24 Confusion matrix for ALS_VAR, relative to reference by opening size class

	Reference Opening Size Class				
ALS_VAR	1	2	3	4	No Opening
Opening	193	119	202	935	107
No Opening	8	2	2	9	258

Table 25 Confusion matrix for DAP_VAR, relative to reference by opening size class.

	Reference Opening Size Class				
DAP_VAR	1	2	3	4	No Opening
Opening	130	84	148	879	100
No Opening	71	37	56	65	265

Table 26 Confusion matrix for Hybrid_VAR, relative to reference by opening size class.

	Reference Opening Size Class				
Hybrid_VAR	1	2	3	4	No Opening
Opening	124	73	148	881	87
No Opening	77	48	56	63	278